Lentes gravitacionales en astrofísica y cosmología

Martín Makler
CBPF & ICAS/IFICI/CONICET-UNSAM

MINISTRY OF SCIENCE, TECHNOLOGY AND INNOVATION
BRAZILIAN GOVERNMENT
BRASIL
UNITING AND REBUILDING

CBPF

Instituto de Ciencias Físicas
ICIFI-ECYT_UNSAM-CONICET
CONICET

universidad de buenos aires - exactas
departamento de física
Juan José Giambiagi

EXACTAS UBA

Estructura general de la materia

Parte I: Introducción, visión general y microlentes gravitacionales

[GR, SL][lentes puntuales, astrofísica, materia oscura]

- [x] Introducción a las lentes gravitacionales y sus aplicaciones actuales
- [x] Deflexión de la luz y ecuación de la lente
- [x] Lentes puntuales
- [x] Mapeo de lentes, magnificación, cáusticas y curvas críticas
- [x] Lentes binárias
- [x] Curvas de luz de microlentes y microlentes por astrometria
- [x] Mas allá de la lente puntual y movimientos uniformes (efectos de segunda orden)
- [ ] Estadística de lentes

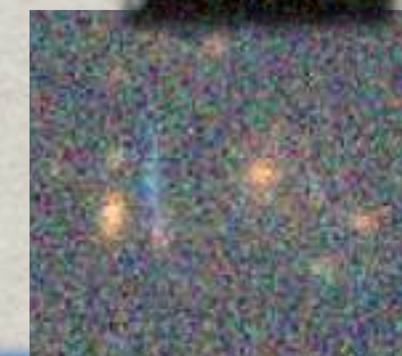

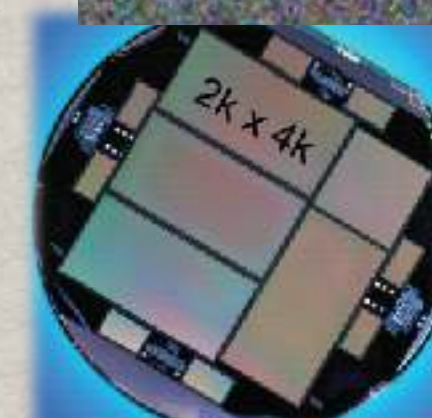

Estructura general de la materia

Parte II: lentes por galáxias y cúmulos de galáxias

[cosmología, *weak & strong*][objetos astrofísicos + cosmología]

- Ecuación de la lente en un universo en expansión
- Modelos de lentes extensas
- Retraso temporal

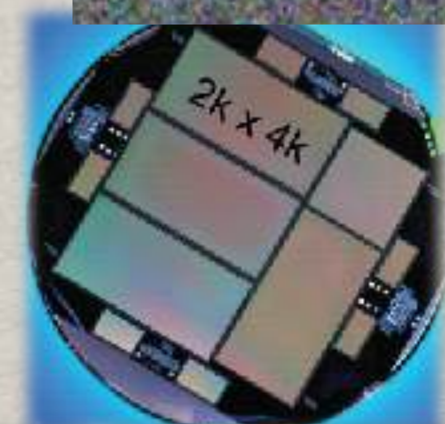

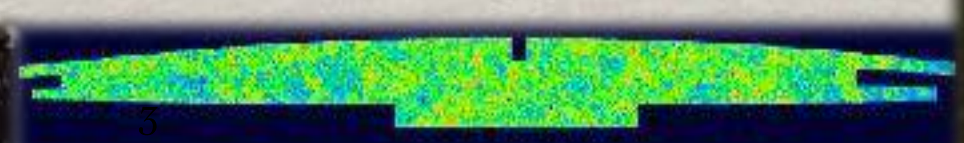

Estructura general de la materia

Parte III: lensing a nivel cosmológico y tópicos avanzados

[perturbaciones, *week lensing*][gravedad fuerte, ondas gravitacionales, Maxwell]

- ❑ Efecto débil de lentes (fundamentos de *weak lensing*, regímenes y métodos)
- ❑ Mas allá del plano único: lentes y estructura en gran escala
- ❑ *Lensing* de la radiación cósmica de fondo
- ❑ Lentes en gravedad modificada
- ❑ *Lensing* de ondas gravitacionales
- ❑ Lentes en la óptica ondulatória

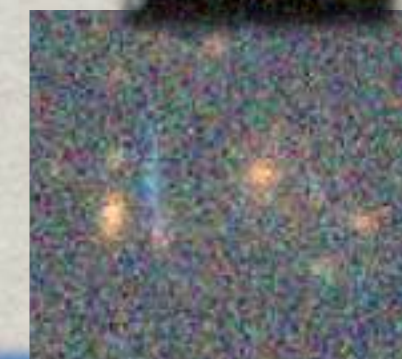

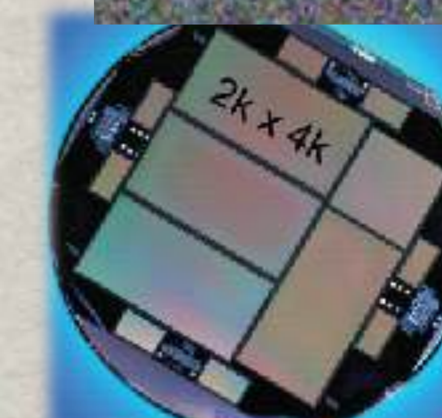

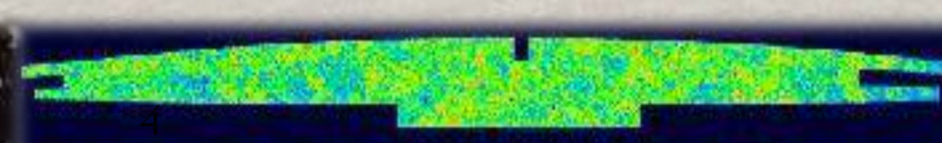

La ecuación de la lente

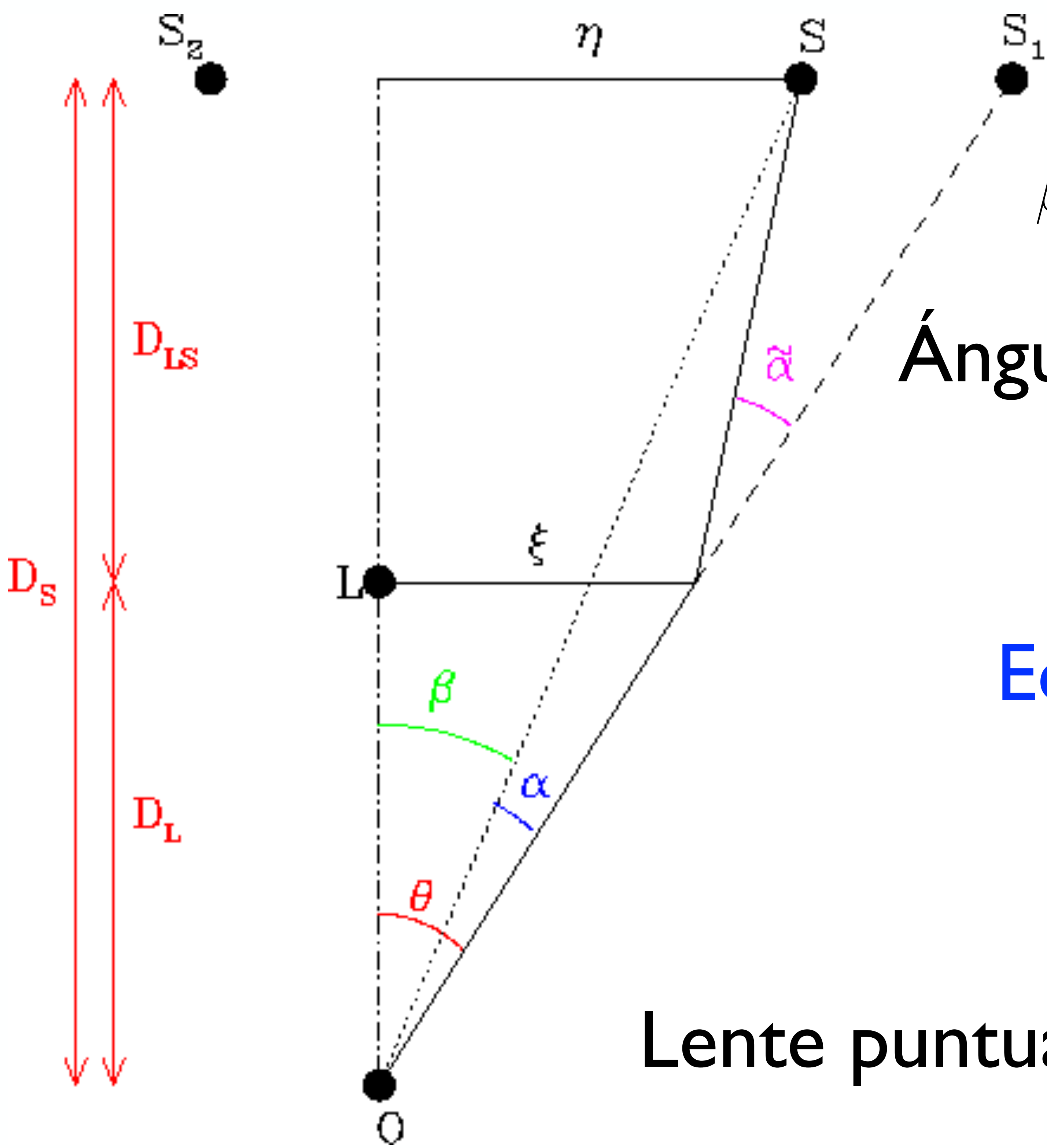

$$\vec{\beta} D_{OS} = \vec{\theta} D_{OS} - \hat{\vec{\alpha}} D_{LS} \left(\vec{\theta}\right)$$

Ángulo de deflexión reducido

$$\vec{\alpha} = \hat{\vec{\alpha}} \frac{D_{LS}}{D_{OS}}$$

Ecuación de la lente

$$\vec{\beta} = \vec{\theta} - \vec{\alpha}\left(\vec{\theta}\right)$$

Lente puntual $\vec{\alpha} = \frac{D_{LS}}{D_{OS} D_{OL}} \frac{4GM}{c^2 \theta} \hat{\theta}$

La curva de luz más simple

Magnificación de lente puntual:

$$\mu = \frac{u^2+2}{u\sqrt{u^2+4}}$$

Trayectoria relativa lente-fuente:

$$\vec{u}(t) = \frac{\vec{\beta}(t)}{\theta_E}$$

Radio (angular) de Einstein:

$$\theta_E = \sqrt{\frac{D_{LS}}{D_{OS}D_{OL}}\frac{4GM}{c^2}}$$

$\omega_\perp$: velocidad angular entre lente y fuente (relativa al observador)

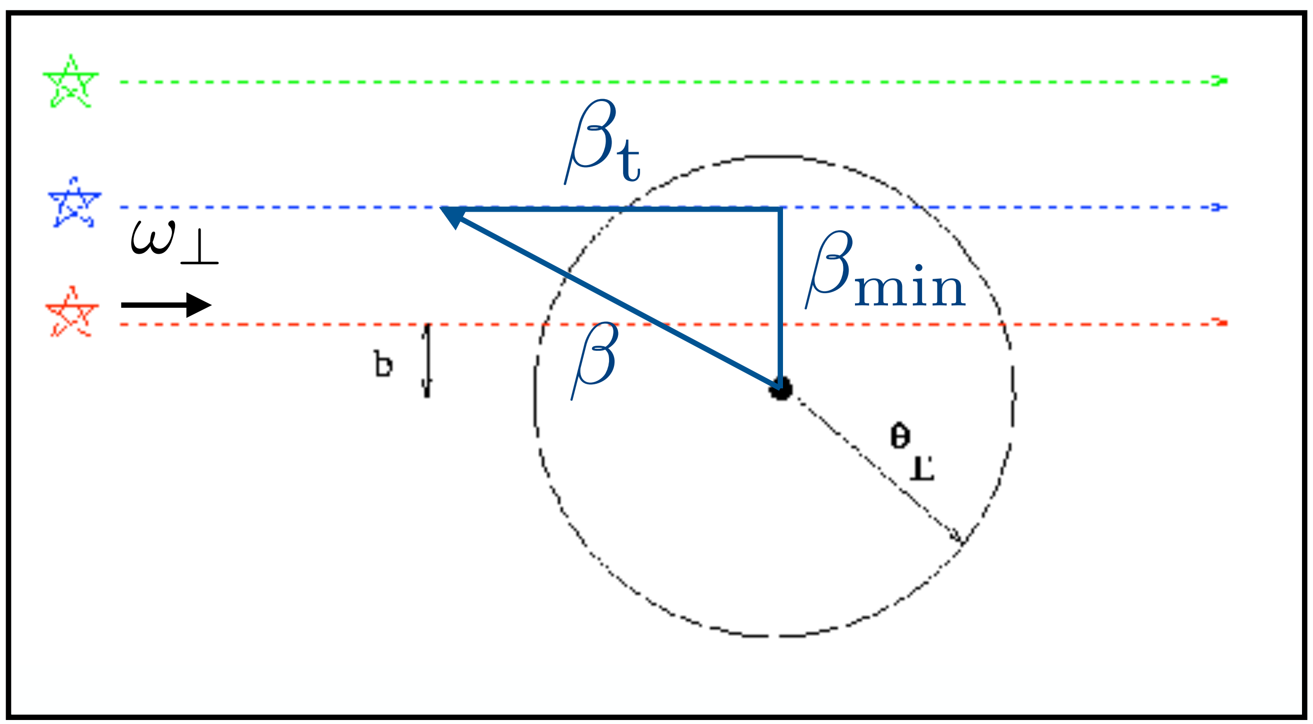

Plano de las fuentes

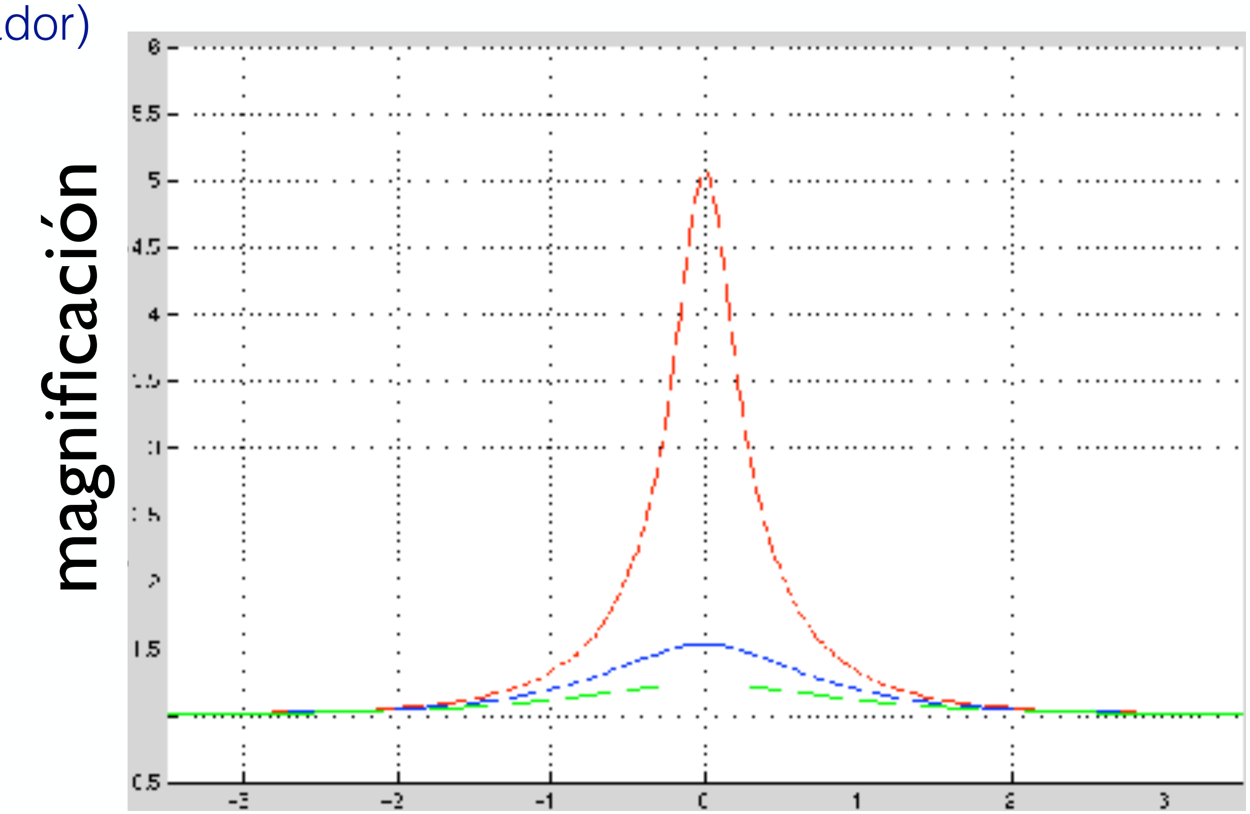

Tiempo en unidades del tiempo de Einstein

Movimiento rectilíneo uniforme:

$$\beta_t = \omega_\perp t = \frac{v_\perp}{D_{OL}} t$$

$$u(t) = \sqrt{u_{min}^2 + \left(\frac{v_\perp t}{\theta_E D_{OL}}\right)^2} = \sqrt{u_{min}^2 + \left(\frac{t}{t_E}\right)^2}$$

$$\boxed{t_E = \frac{\theta_E D_{OL}}{v_\perp}}$$

Para un tiempo con origen arbitrária $t \rightarrow (t - t_0)$

Aplicaciones de microlentes

Ejemplos: descubierta de planetas y agujeros negros, búsqueda de materia oscura, caracterización de la distribución de objetos compactos…

- Eventos individuales
  - Informaciones adicionales: efectos de orden más alta (fuente finita, paralaje), desvío astrométrico, informaciones externas (movimiento propio, distancias, dimensiones)
  - Eventos de lentes binárias y múltiples (incluso exoplanetas y QSO *microlensing*)
- Estadística
  - Materia oscura, poblaciones

Nuestra galaxia

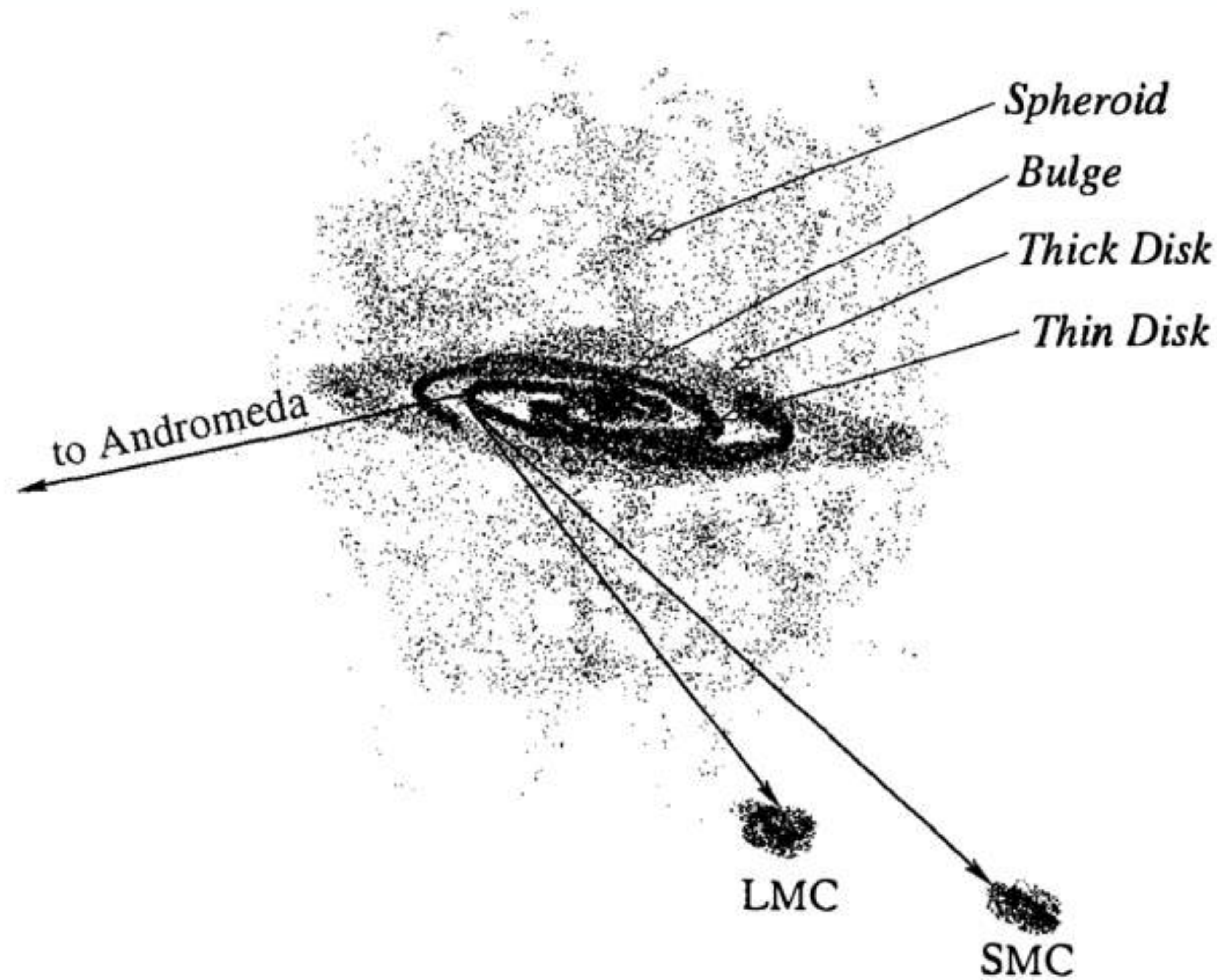

Estadística de microlentes y materia oscura

Sección eficaz

- área en el plano de las fuentes en que se genera un evento detectable
- hipótesis/modelo: magnificación superior a un umbral μ_T
- Recordando $\mu = \dfrac{u^2+2}{u\sqrt{u^2+4}}$
- Condición $\mu > \mu_T \ \rightarrow \ u < u_T$
- Ejemplo $\mu_T = 1,34 \ \rightarrow \ u_T = 1$
- Pregunta: ¿mejor definición práctica de detectabilidad?

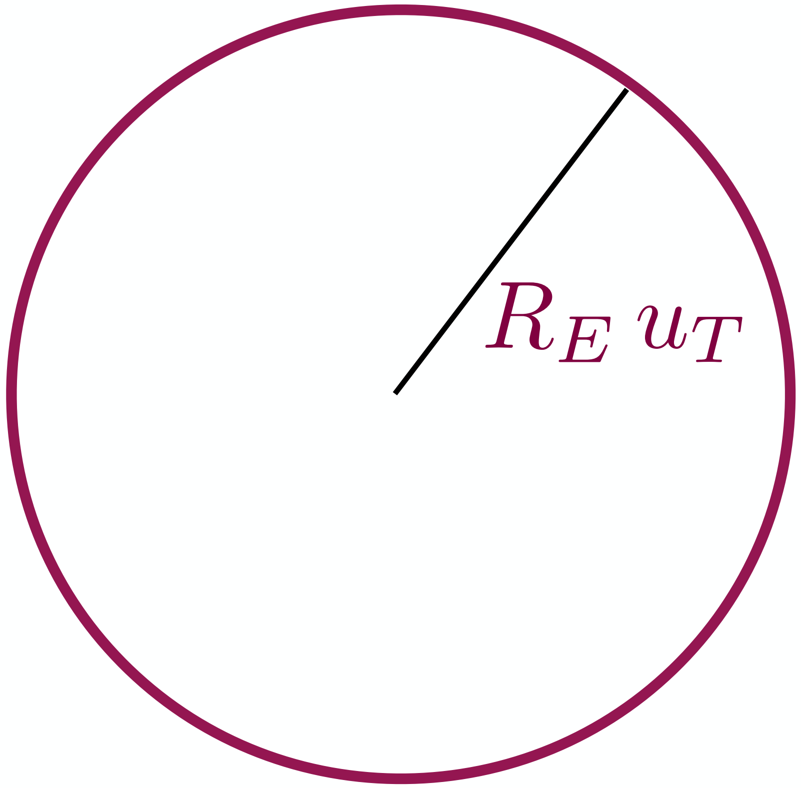

Tasa de eventos

- Calcularmos la profundidad óptica.
  Y la duración de los eventos, no tiene un papel?
- Hay que considerar la **tasa** de eventos
- Número de eventos de *microlensing* por unidad de tiempo por unidad de masa de las lentes

densidad de lentes
(número por unidad de volumen)
por unidad de masa

probabilidad de la
velocidad relativa

$$\frac{d\Gamma}{dm} = \frac{dn}{dm} \underbrace{v_r \cos\theta}_{v_r} \overline{f(\vec{v}_r) d^2 v_r} \, dV$$

volumen del
"tubo de microlensing"

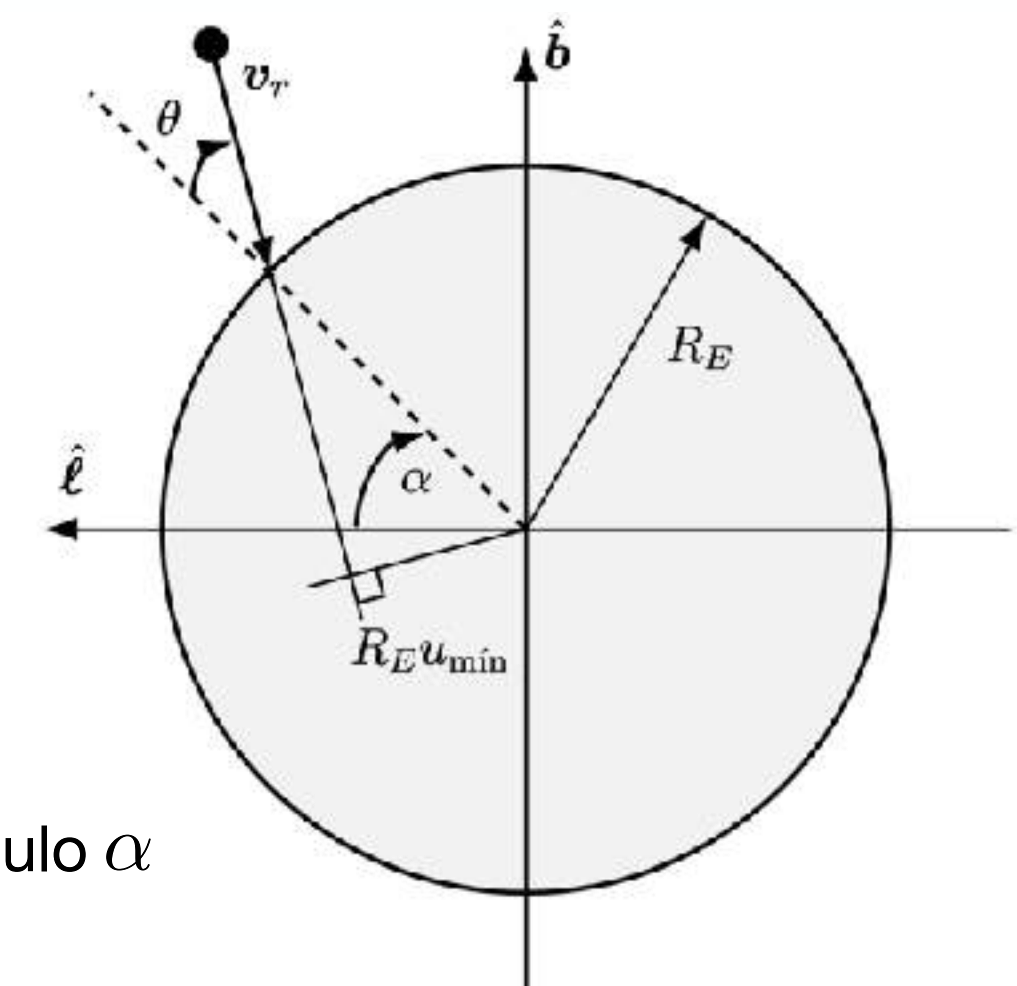

Tasa en que cruza una porción del cilindro de angulo α

Tasa de eventos

Monocromaticidad
(única masa)

$$\frac{dn}{dm} = \frac{\rho(x)}{m}\delta(m - M)$$

Elemento de volumen del
"tubo de microlensing"

$$dV = u_T R_E \, d\alpha \, dD_{OL}$$

Isotropia de la distribución
de velocidades

$$d^2 v_r = v_r \; d\theta \, dv_r$$

densidad de lentes
(número por unidad de volumen)
por unidad de masa

probabilidad de la
velocidad relativa

$$\frac{d\Gamma}{dm} = \frac{dn}{dm} \underbrace{v_r \cos\theta}_{v_r} \overbrace{f(\vec{v}_r) d^2 v_r}\; dV$$

volumen del
"tubo de microlensing"

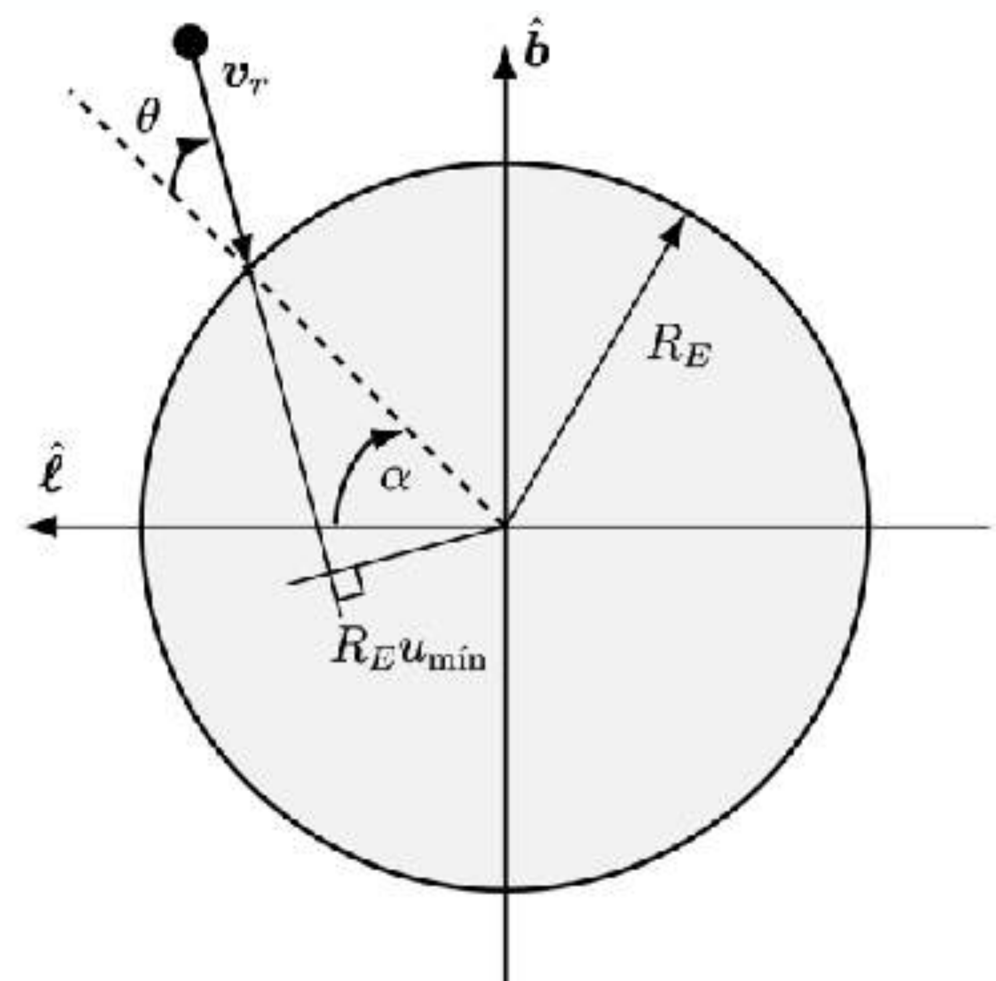

Tasa de eventos

Monocromaticidad
(única masa)

$$\frac{dn}{dm} = \frac{\rho(x)}{m}\delta(m - M)$$

Elemento de volumen del
"tubo de microlensing"

$$dV = u_T R_E \, d\alpha \, dD_{OL}$$

Isotropia de la distribución
de velocidades

$$d^2 v_r = v_r \; d\theta \, dv_r$$

$$\frac{d\Gamma}{dm} = \frac{dn}{dm} v_r \cos\theta \, f(\vec{v}_r) d^2 v_r \; dV$$

$$\boxed{d\Gamma = \frac{\rho(x)}{M} v_r^2 u_T R_E \cos\theta \, f(v_r) \, d\theta \, dv_r \, d\alpha \, dD_{OL}}$$

Distribución maxwelliana de velocidades: $f(v_r) = \exp\left(-\frac{v_r^2}{v_c^2}\right)$

Esta y próximas filminas adaptadas de Anibal Varela, tesis de licenciatura, UBA (2022)

Tasa de eventos

$$d\Gamma = \frac{\rho(x)}{M} v_r^2 u_T R_E \cos\theta\, f(v_r)\, d\theta\, dv_r\, d\alpha\, dD_{OL}$$

Distribución maxwelliana de velocidades: $f(v_r) = \exp\left(-\frac{v_r^2}{v_c^2}\right)$

- Como introducir la duración de los eventos?
- Tiempo para cruzar la sección eficaz

$$\hat{t} = \frac{2 R_E u_T \cos(\theta)}{v_r}$$

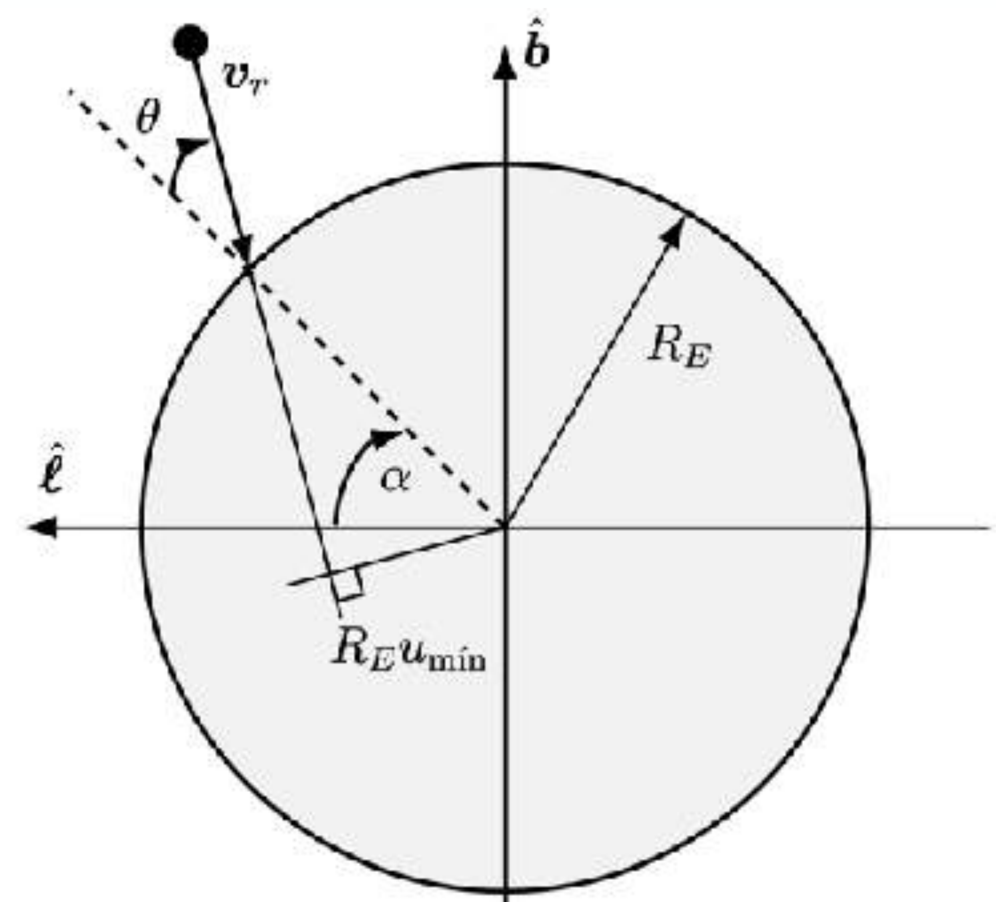

Observación: a veces se llama a esa cantidad de “Einstein crossing time”. No confundir con el tiempo de Einstein como estamos definiendo en este curso.

Tasa de eventos

$$\boxed{d\Gamma = \frac{\rho(x)}{M} v_r^2 u_T R_E \cos\theta f(v_r)\, d\theta\, dv_r\, d\alpha\, dD_{OL}}$$

Distribución maxwelliana de velocidades: $f(v_r) = \exp\left(-\frac{v_r^2}{v_c^2}\right)$

$$\hat{t} = \frac{2R_E u_T \cos(\theta)}{v_r}$$

- Finalmente, la tasa de eventos será dada por

$$\frac{d\Gamma}{d\hat{t}} = \int_0^\infty dv_r \int_0^{2\pi} d\alpha \int_0^{D_S} dD_{OL} \int_{-\pi/2}^{\pi/2} d\theta\, \frac{\rho(D_{OL})}{M} v_r^2 \cos\theta\, u_T R_E\, e^{\left(-\frac{v_r^2}{v_c^2}\right)} \delta\left(\hat{t} - \frac{2R_E u_T \cos(\theta)}{v_r}\right)$$

- Modelos de la distribución de materia oscura

Esfera isotérmica suavizada

$$\rho_{isot}(R) = \rho_\odot \frac{R_{Sol}^2 + R_C^2}{R_C^2 + R^2}$$

Navarro-Frenk-White

$$\rho_{NFW}(R) = \frac{\rho_0}{\frac{R}{R_s}\left(1 + \frac{R}{R_s}\right)^2}$$

Tasa de eventos

$$\frac{d\Gamma}{d\hat{t}} = \int_0^{\infty} dv_r \int_0^{2\pi} d\alpha \int_0^{D_S} dD_{OL} \int_{-\pi/2}^{\pi/2} d\theta \; \frac{\rho(D_{OL})}{M} v_r^2 \cos\theta u_T R_E \, e^{\left(-\frac{v_r^2}{v_c^2}\right)} \delta\left(\hat{t} - \frac{2R_E u_T \cos(\theta)}{v_r}\right)$$

$[d\Gamma/d\hat{t}]$=[eventos/día/día]

$$\frac{d\Gamma}{d\hat{t}} = \int_0^{D_S} dD_{OL} \int_{-\pi/2}^{\pi/2} d\theta \; \frac{\rho(D_{OL})}{M} v_r^4 \cos\theta u_T R_E \exp\left(-\frac{v_r^2}{v_c^2}\right)$$

- Cambiando de variables

$$u_{\text{mín}} = u_T \sin(\theta) \qquad d\theta = \frac{du_{\text{mín}}}{\sqrt{u_T^2 - u_{\text{mín}}^2}}$$

$$\boxed{\frac{d\Gamma}{d\hat{t}} = \int_0^{D_S} dD_{OL} \int_0^{u_T} \frac{du_{\text{mín}}}{\sqrt{u_T^2 - u_{\text{mín}}^2}} \frac{\rho(D_{OL})}{M} v_r^4 \exp\left(-\frac{v_r^2}{v_c^2}\right)}$$

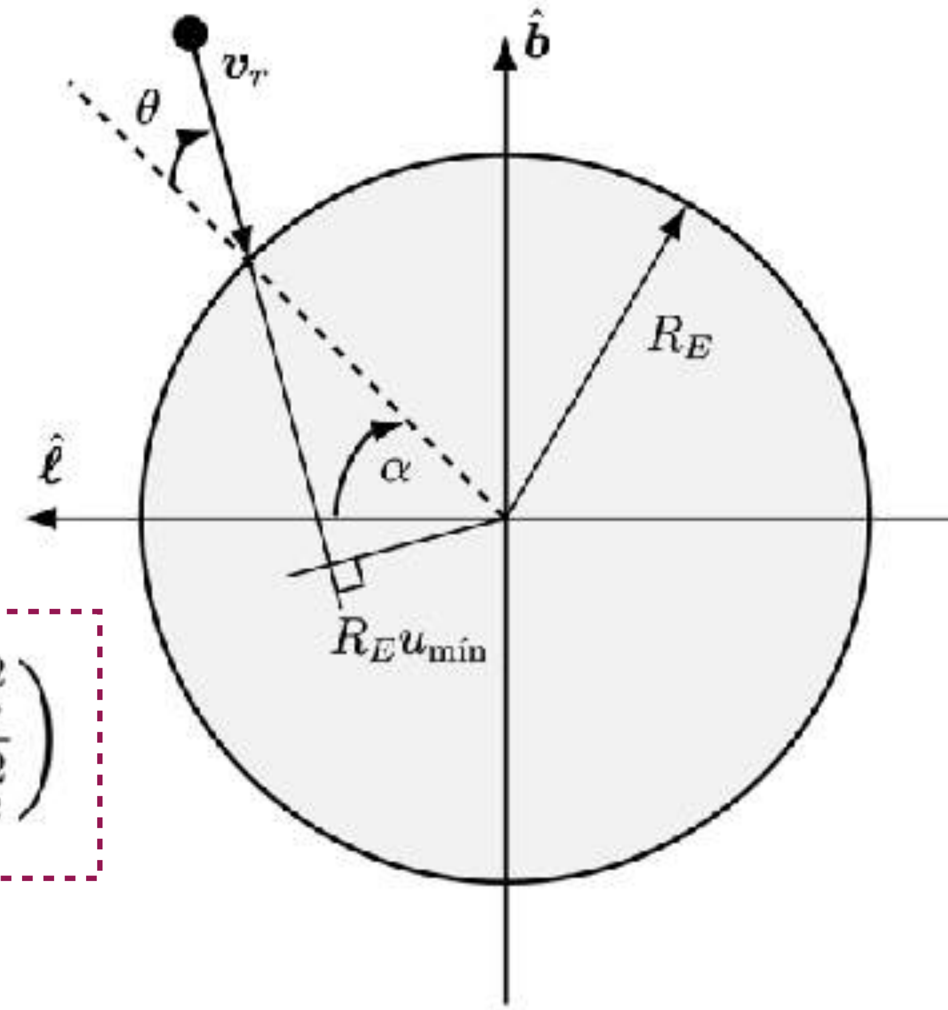

Tasa de eventos

$$\frac{d\Gamma}{d\hat{t}} = \int_0^{D_S} dD_{OL} \int_0^{u_T} \frac{du_{\text{mín}}}{\sqrt{u_T^2 - u_{\text{mín}}^2}} \frac{\rho(D_{OL})}{M} v_r^4 \exp\left(-\frac{v_r^2}{v_c^2}\right)$$

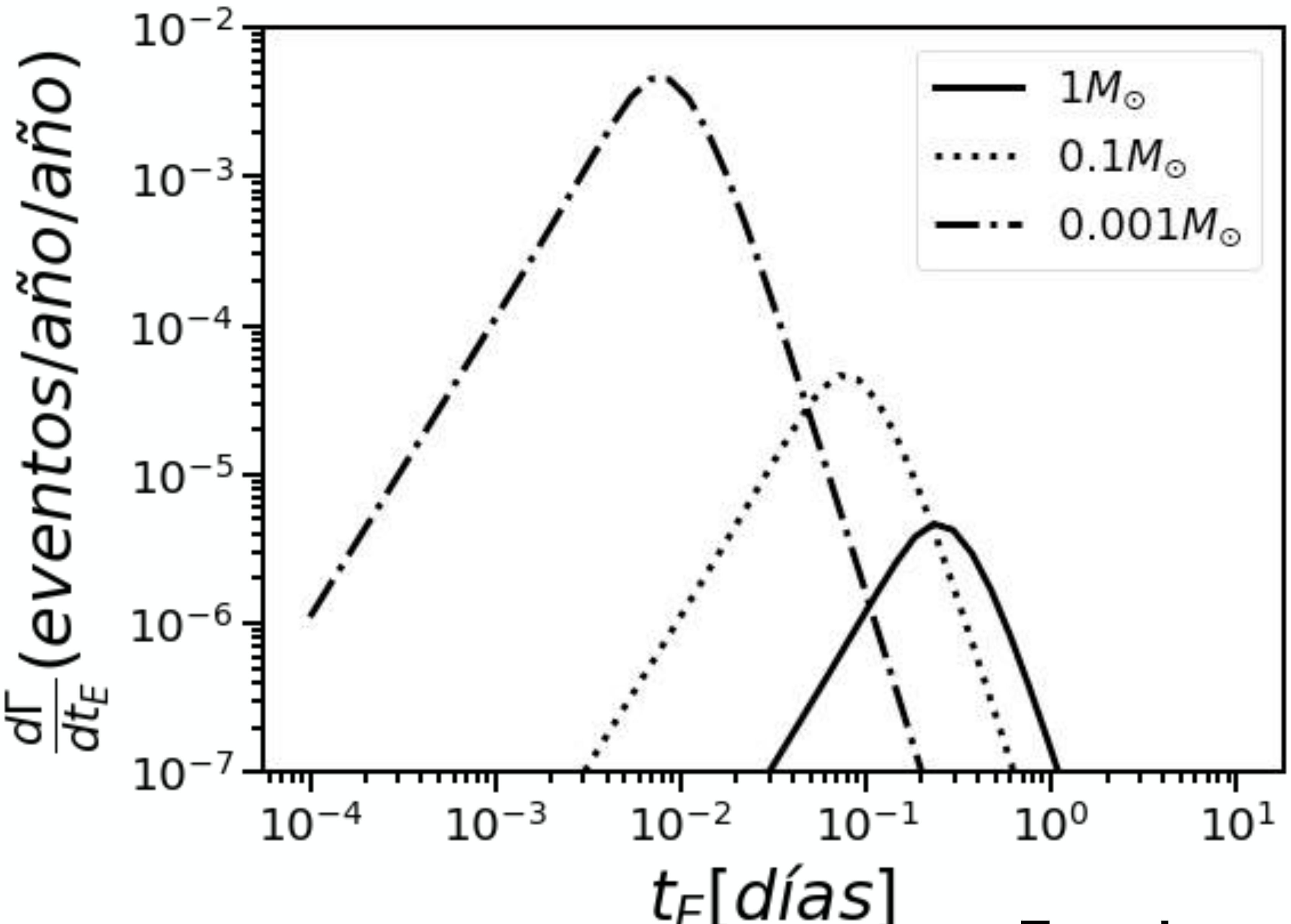

Tasa de eventos para LMC

Tasa de eventos
LMC x M31

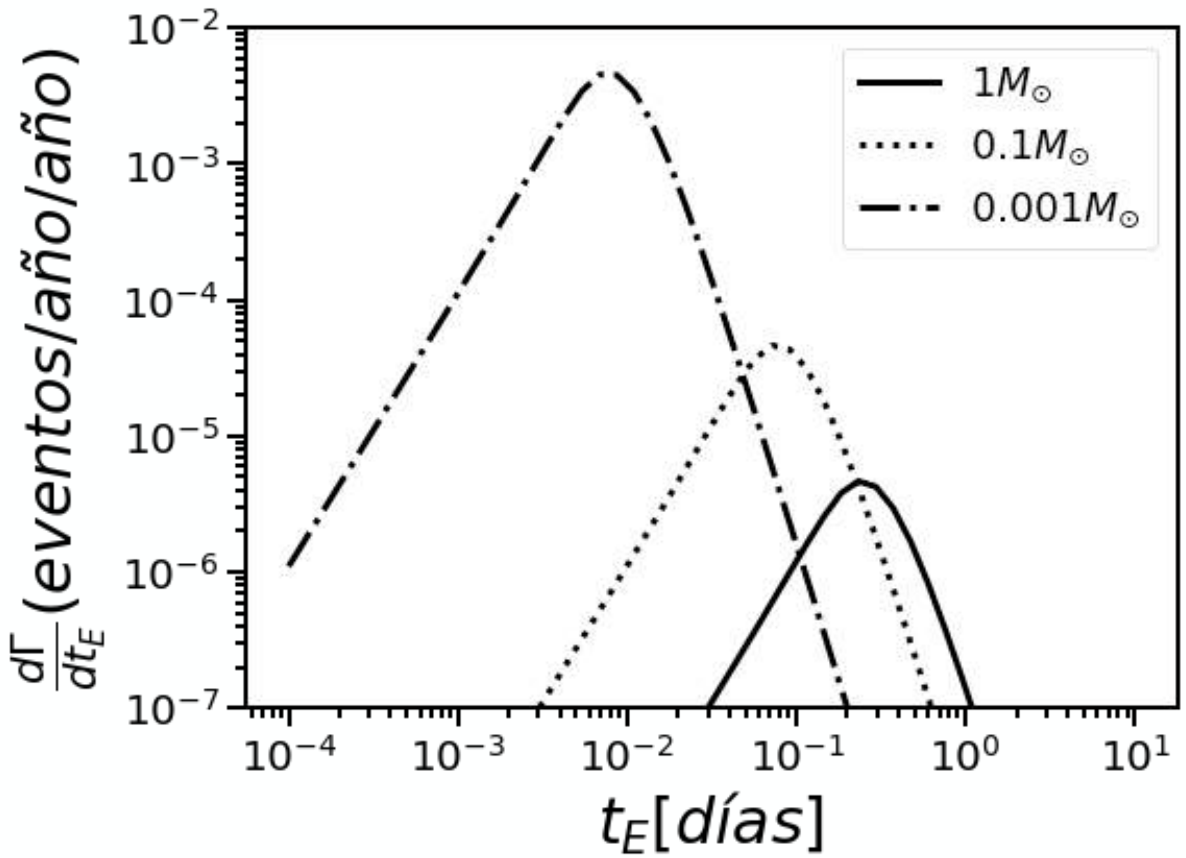

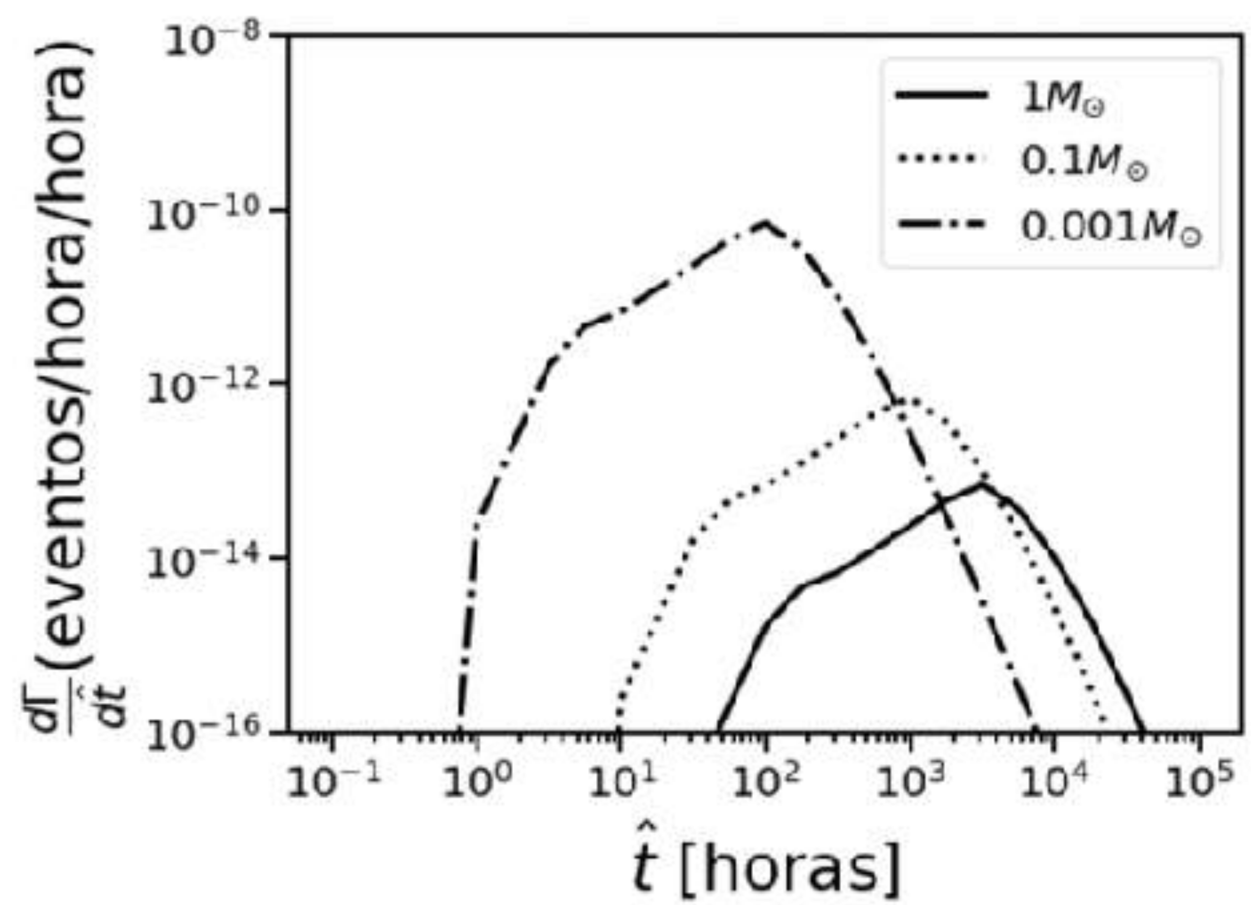

Tasa de eventos hacia M31

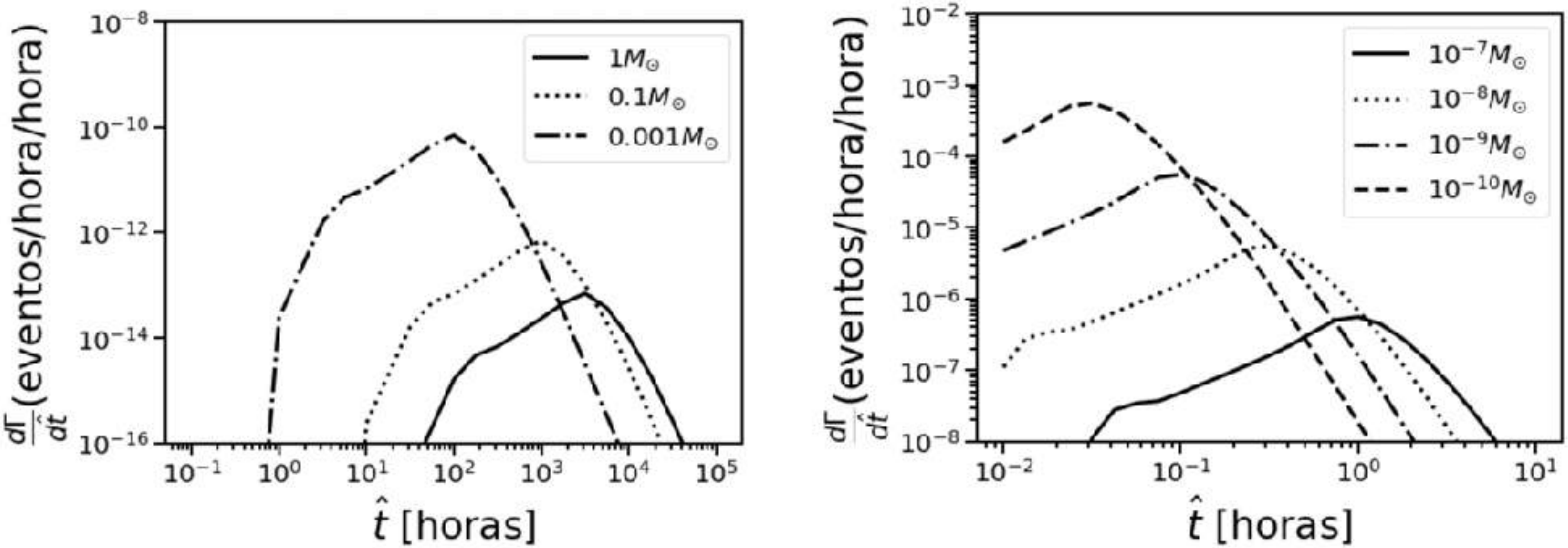

Número esperado de eventos

$$N_{exp} = E \int_0^\infty \frac{d\Gamma}{d\hat{t}} d\hat{t} \qquad E = N_{\text{estrellas}} \times T_{\text{observación}}$$

Ejemplos: $E_{LMC} = 10^7$ estrellas-años $\qquad E_{HSC} = 7{,}0 \times 10^4$ estrellas-años

- Eficiencia: fracción que se detecta para cada tiempo característico

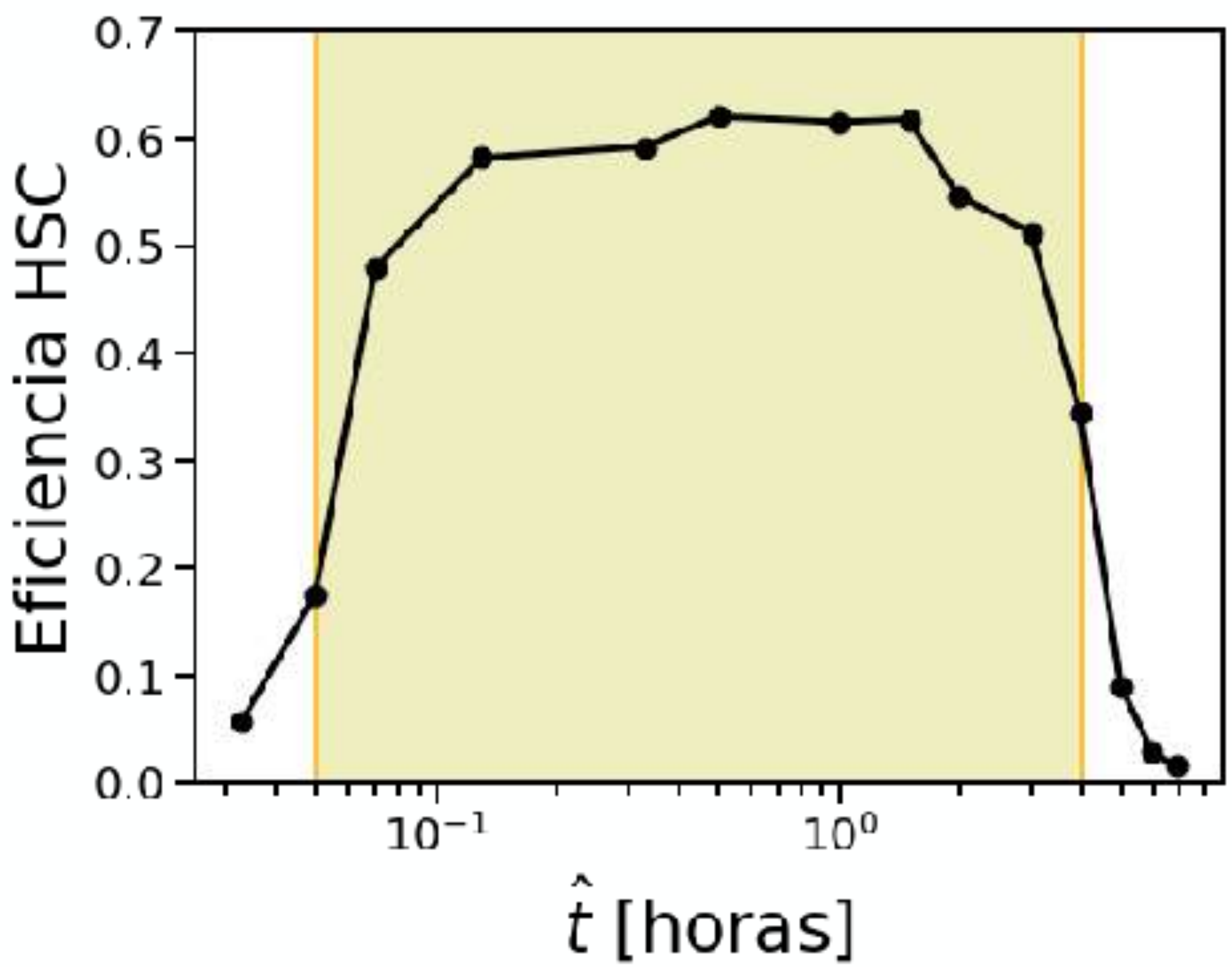

Número esperado de eventos

$$N_{exp} = E\int_0^{\infty} \frac{d\Gamma}{d\hat{t}}\,d\hat{t} \qquad E = N_{\text{estrellas}} \times T_{\text{observación}}$$

Ejemplos: $E_{LMC} = 10^7$ estrellas-años $\qquad E_{HSC} = 7{,}0 \times 10^4$ estrellas-años

- Eficiencia: fracción que se detecta para cada tiempo característico

$$N_{exp} = E\int_0^{\infty} \mathcal{E}(\hat{t})\frac{d\Gamma}{d\hat{t}}\,d\hat{t}$$

Aquí, para simplificar, consideramos que la eficiencia de detección no depende de la magnitud de la fuente. ¿Cómo quedaría la expresión de N_{exp} si tomamos en cuenta que la eficiencia depende de la magnitud de las fuentes m_s?

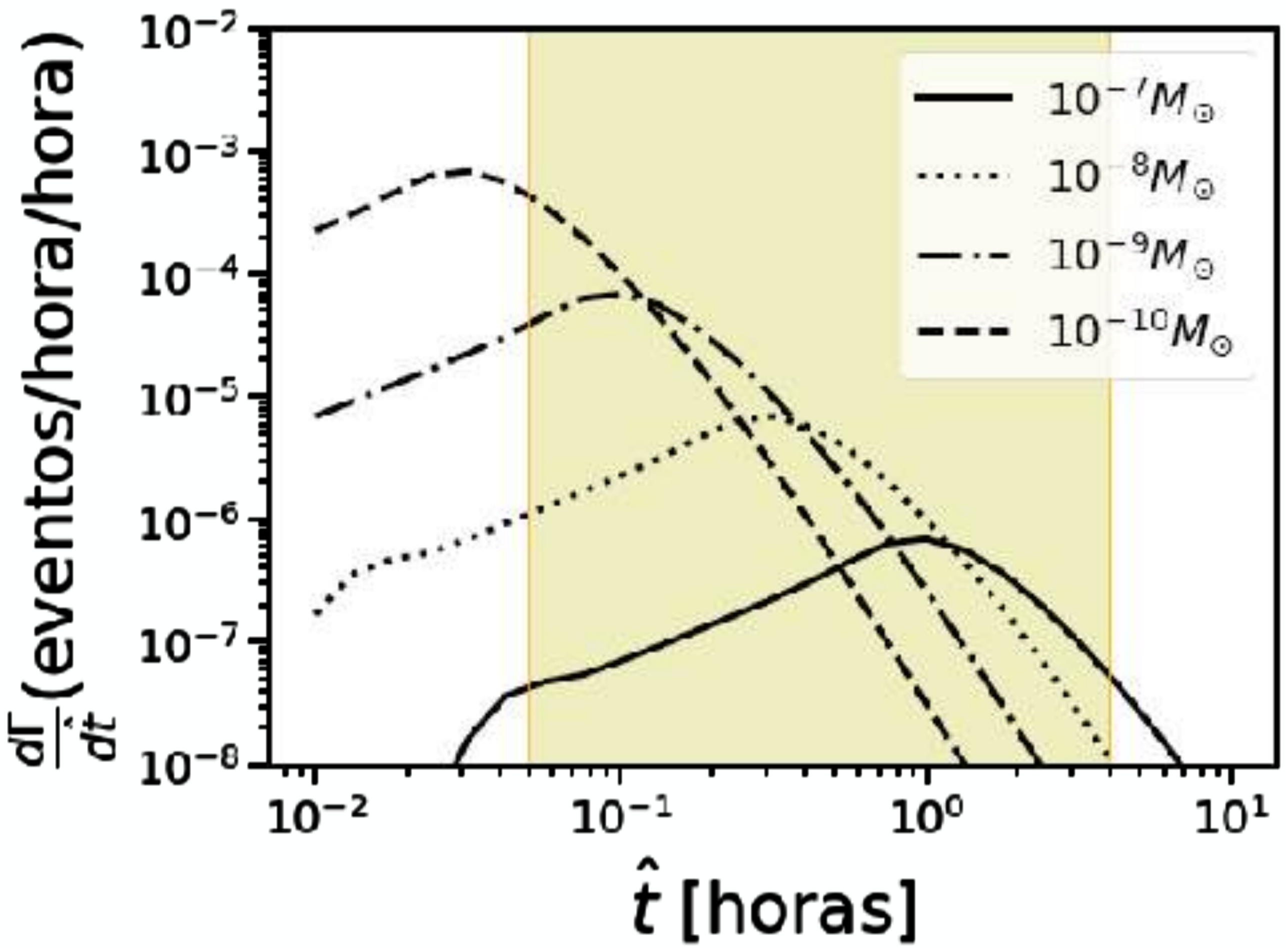

Número esperado de eventos

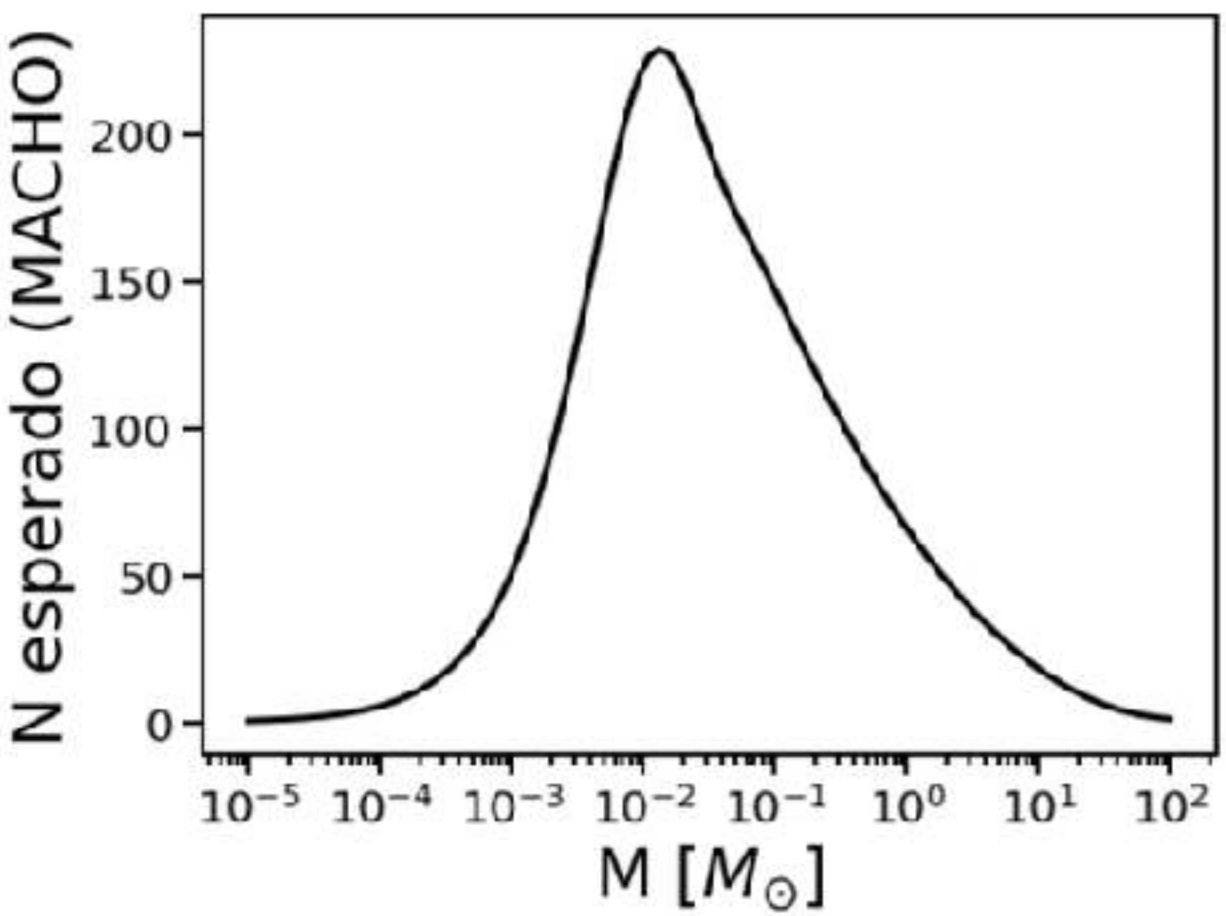

(a) Número esperado de eventos de la colaboración MACHO, con su eficiencia y la exposición asociada al primer año de observaciones.

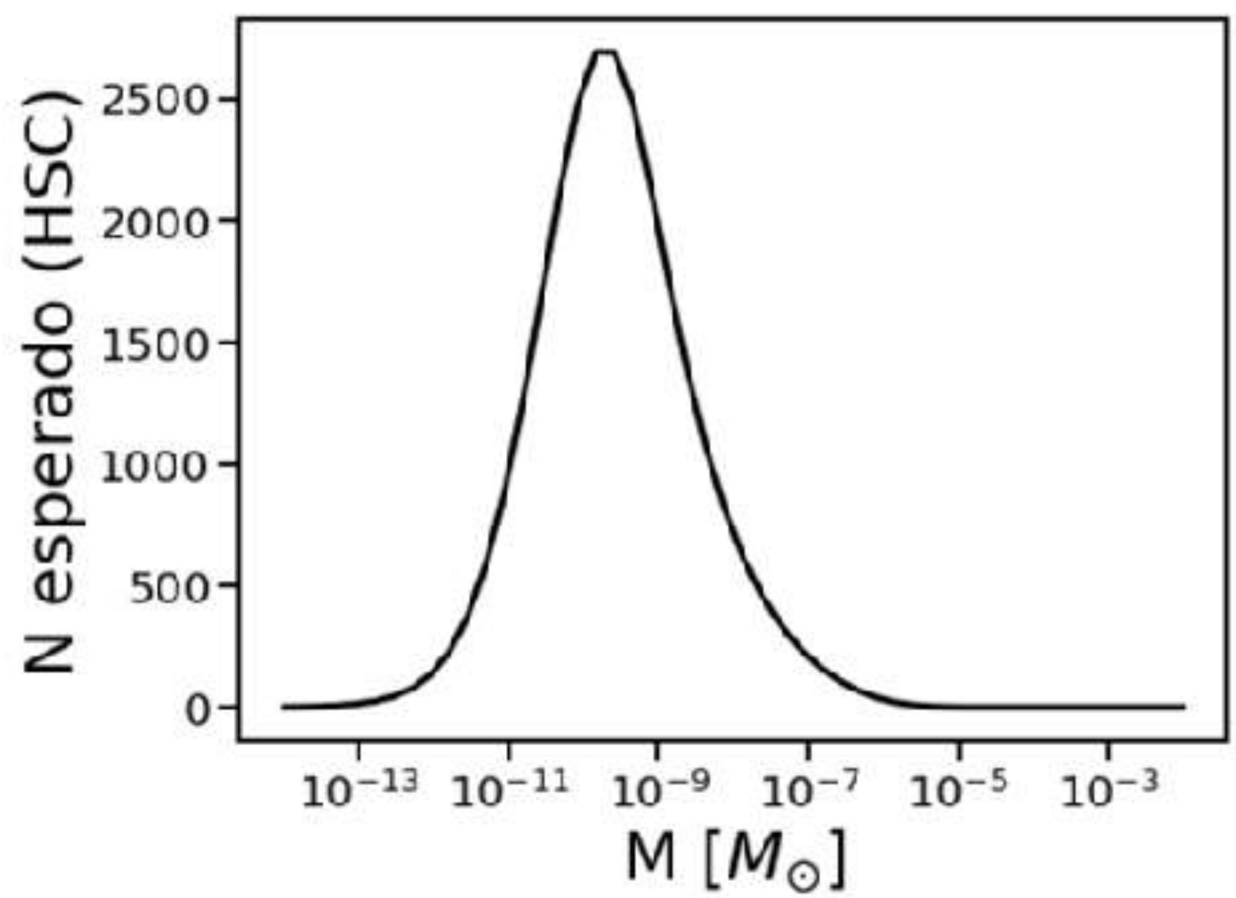

(b) Número esperado de eventos para M31, con la eficiencia y la exposición de HSC.

Expectativa x observación

- Conteo de eventos sigue estadística de Poisson

$$P(N_{obs}|N_{exp}) = \frac{(N_{exp})^{N_{obs}}}{N_{obs}!}e^{-N_{exp}}$$

- Dados *N* eventos observados, ¿en qué rango limito mi modelo dentro de una cierta probabilidad?

- Ejemplo 95% de nivel de confianza

$$\sum_{k=0}^{N_{obs}} P(k|N_{exp}) < 0{,}05$$

Expectativa x observación

- ¿Y si el número es significativamente menor al esperado?

$$N_{exp} = f_{DM} N_{exp}^{TOTAL} \qquad f_{DM} = \frac{\Omega_{DCO}}{\Omega_{DM}}$$

- Ningún evento observado

$$P(0|N_{exp}) = e^{-f_{DM} N_{exp}^{TOTAL}}$$

- Excluye $N_{exp} > 3$ en 95% C.L

$$f_{95CL} = \frac{-\ln(0{,}05)}{N_{exp}^{TOTAL}} \approx \frac{3{,}0}{N_{exp}^{TOTAL}}$$

Resumen

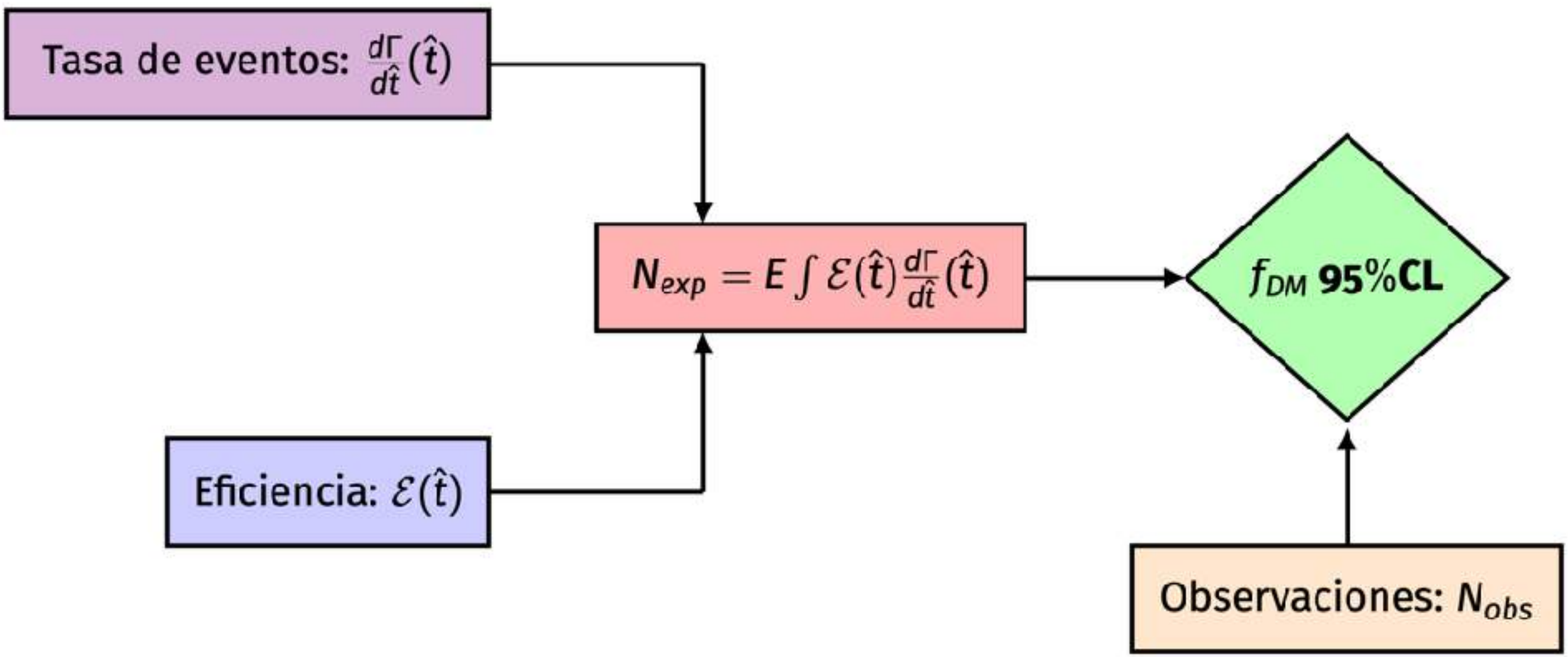

Tasa de eventos: $\frac{d\Gamma}{d\hat{t}}(\hat{t})$
$N_{exp} = E \int \mathcal{E}(\hat{t}) \frac{d\Gamma}{d\hat{t}}(\hat{t})$
f_{DM} **95%CL**
Eficiencia: $\mathcal{E}(\hat{t})$
Observaciones: N_{obs}

Límites en la abundancia de Materia Oscura

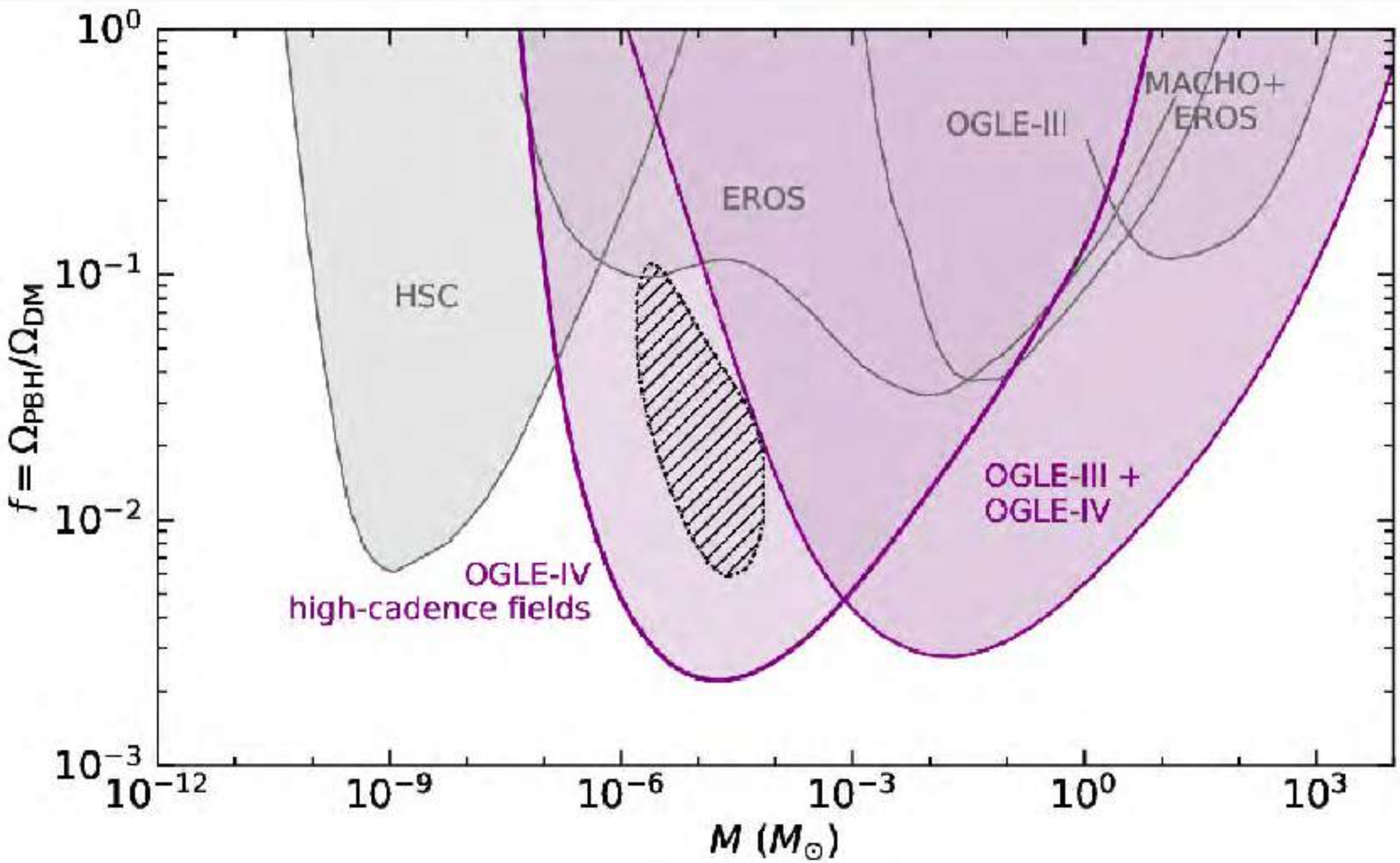

EROS combined results in dark matter

(1) Galactic halo: all data + combine EROS+MACHO toward LMC

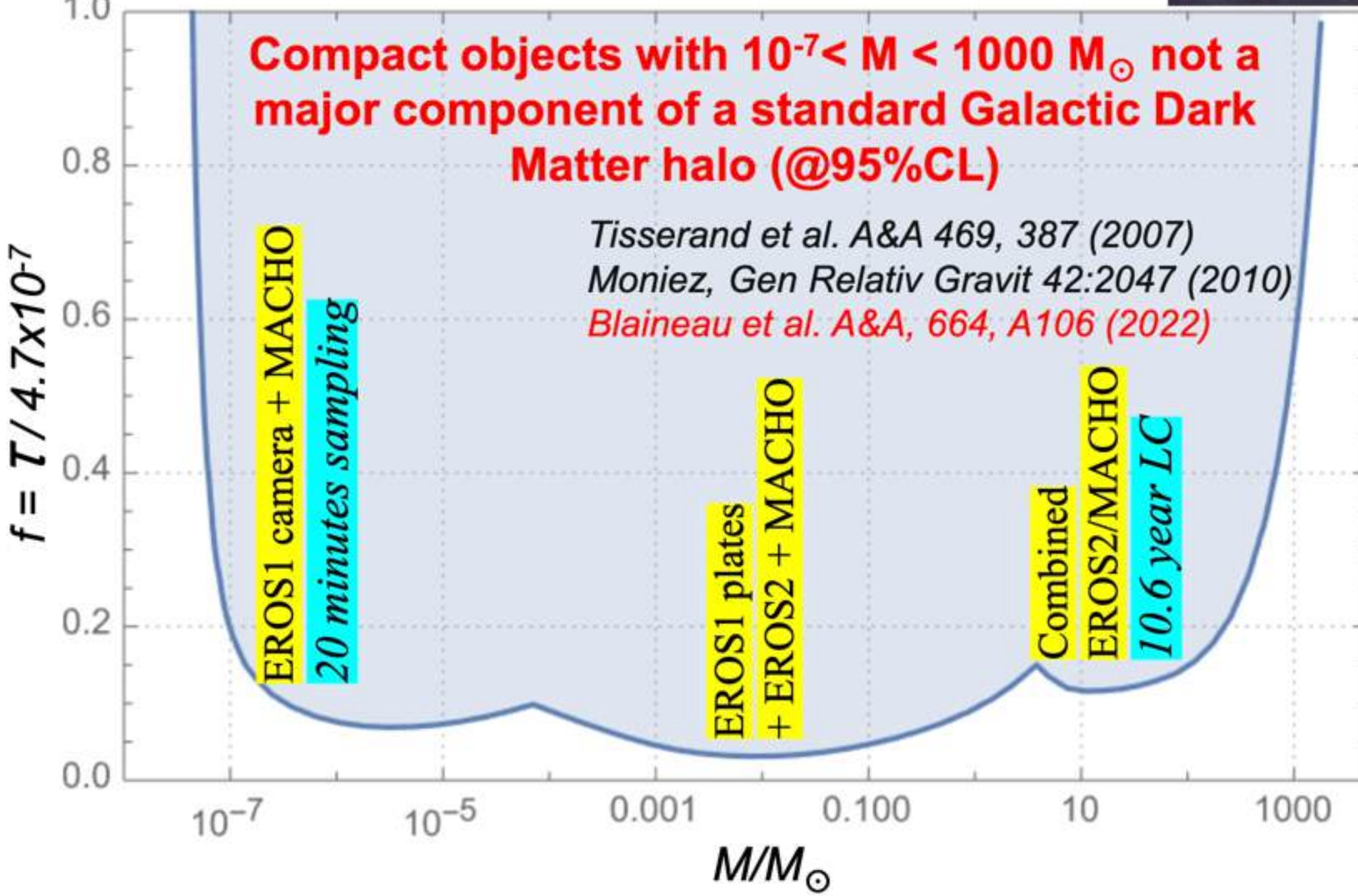

Límites actuales

No massive black holes in the Milky Way halo

Nature **volume 632**, pages 749–751 (2024), https://www.nature.com/articles/s41586-024-07704-6

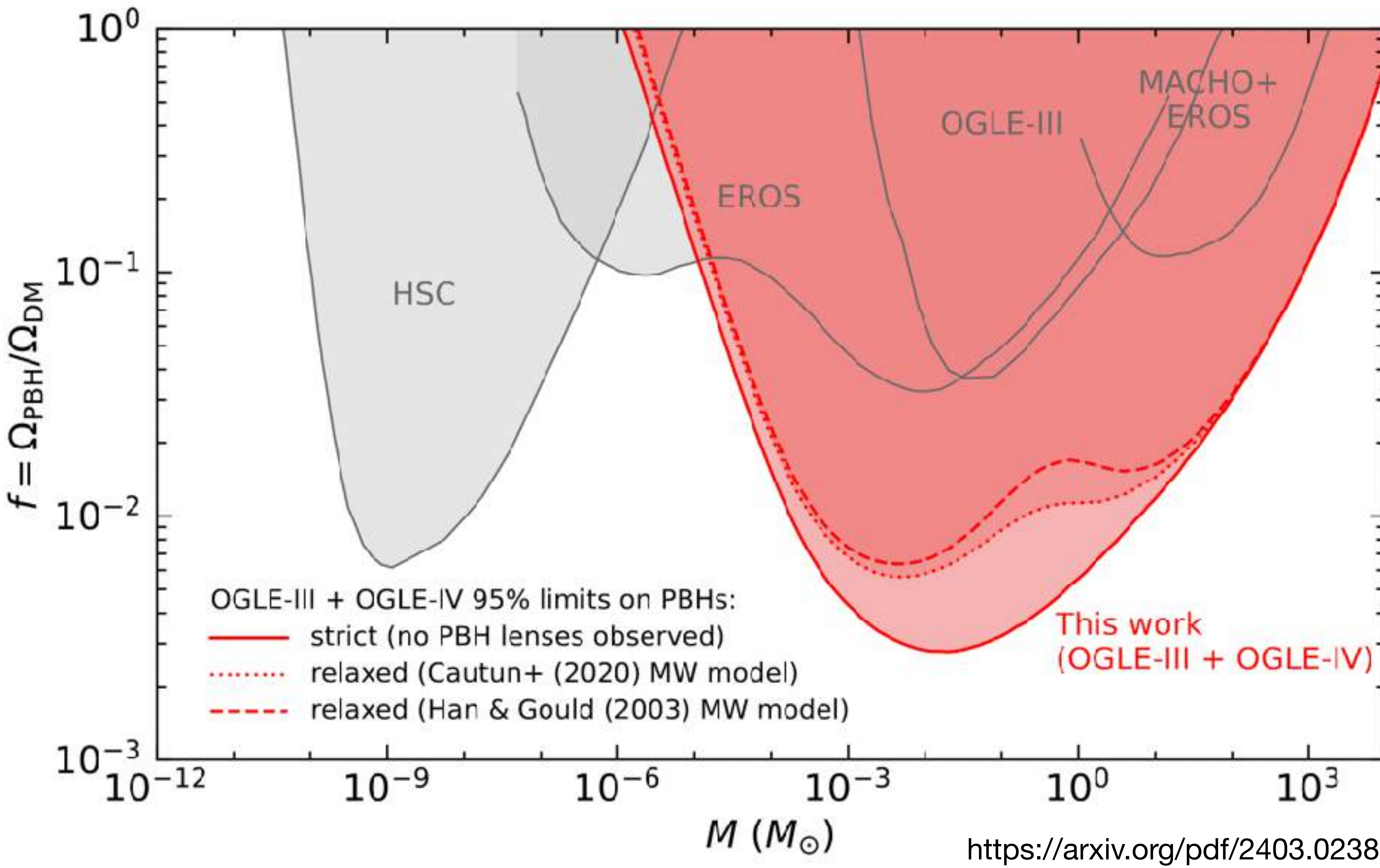

https://arxiv.org/pdf/2403.02386

arXiv: 2403.02398 https://iopscience.iop.org/article/10.3847/1538-4365/ad452e/pdf

The Astrophysical Journal Supplement Series, 273:4 (19pp), 2024 July https://doi.org/10.3847/1538-4365/ad452e

Microlensing Optical Depth and Event Rate toward the Large Magellanic Cloud Based on 20 yr of OGLE Observations

Przemek Mróz[1], Andrzej Udalski[1], Michał K. Szymański[1], Mateusz Kapusta[1], Igor Soszyński[1], Łukasz Wyrzykowski[1], Paweł Pietrukowicz[1], Szymon Kozłowski[1], Radosław Poleski[1], Jan Skowron[1], Dorota Skowron[1], Krzysztof Ulaczyk[1,2], Mariusz Gromadzki[1], Krzysztof Rybicki[1,3], Patryk Iwanek[1], Marcin Wrona[1], and Milena Ratajczak[1]

[1] Astronomical Observatory, University of Warsaw, Al. Ujazdowskie 4, 00-478 Warszawa, Poland; pmroz@astrouw.edu.pl
[2] Department of Physics, University of Warwick, Coventry CV4 7AL, UK
[3] Department of Particle Physics and Astrophysics, Weizmann Institute of Science, Rehovot 76100, Israel
Received 2024 March 3; revised 2024 April 22; accepted 2024 April 22; published 2024 June 24

Abstract

Measurements of the microlensing optical depth and event rate toward the Large Magellanic Cloud (LMC) can be used to probe the distribution and mass function of compact objects in the direction toward that galaxy—in the Milky Way disk, the Milky Way dark matter halo, and the LMC itself. The previous measurements, based on small statistical samples of events, found that the optical depth is an order of magnitude smaller than that expected from the entire dark matter halo in the form of compact objects. However, these previous studies were not sensitive to long-duration events with Einstein timescales longer than 2.5–3 yr, which are expected from massive (10–100 $M_\odot$) and intermediate-mass (10^2–10^5 $M_\odot$) black holes. Such events would have been missed by the previous studies and would not have been taken into account in calculations of the optical depth. Here, we present the analysis of nearly 20 yr long photometric monitoring of 78.7 million stars in the LMC by the Optical Gravitational Lensing Experiment (OGLE) from 2001 through 2020. We describe the observing setup, the construction of the 20 yr OGLE data set, the methods used for searching for microlensing events in the light-curve data, and the calculation of the event detection efficiency. In total, we find 16 microlensing events (13 using an automated pipeline and three with manual searches), all of which have timescales shorter than 1 yr. We use a sample of 13 events to measure the microlensing optical depth toward the LMC $\tau = (0.121 \pm 0.037) \times 10^{-7}$ and the event rate $\Gamma = (0.74 \pm 0.25) \times 10^{-7}\,\mathrm{yr}^{-1}\,\mathrm{star}^{-1}$. These numbers are consistent with lensing by stars in the Milky Way disk and the LMC itself, and they demonstrate that massive and intermediate-mass black holes cannot comprise a significant fraction of the dark matter.

Microlensing en M31

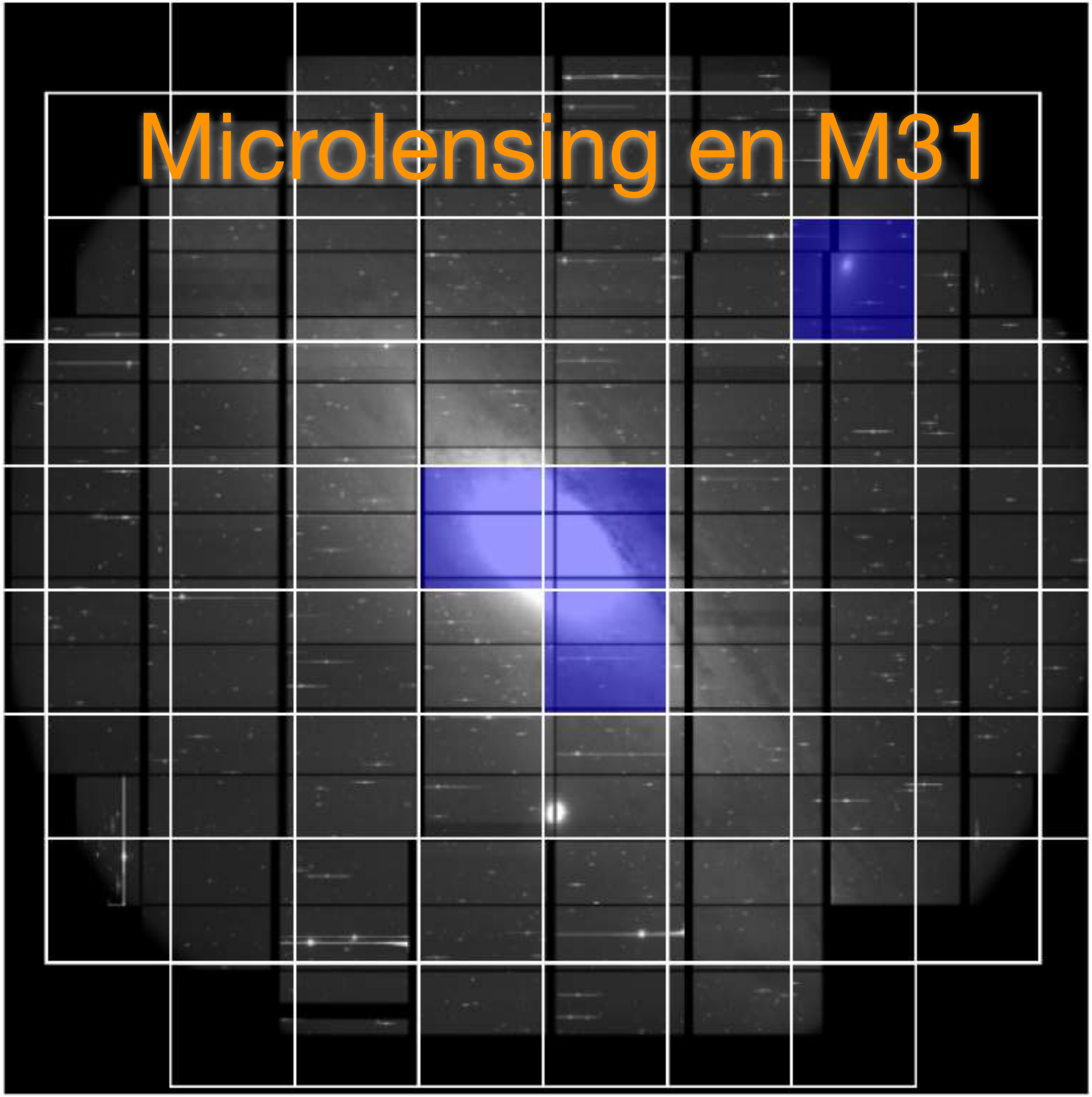

Resultados en M31

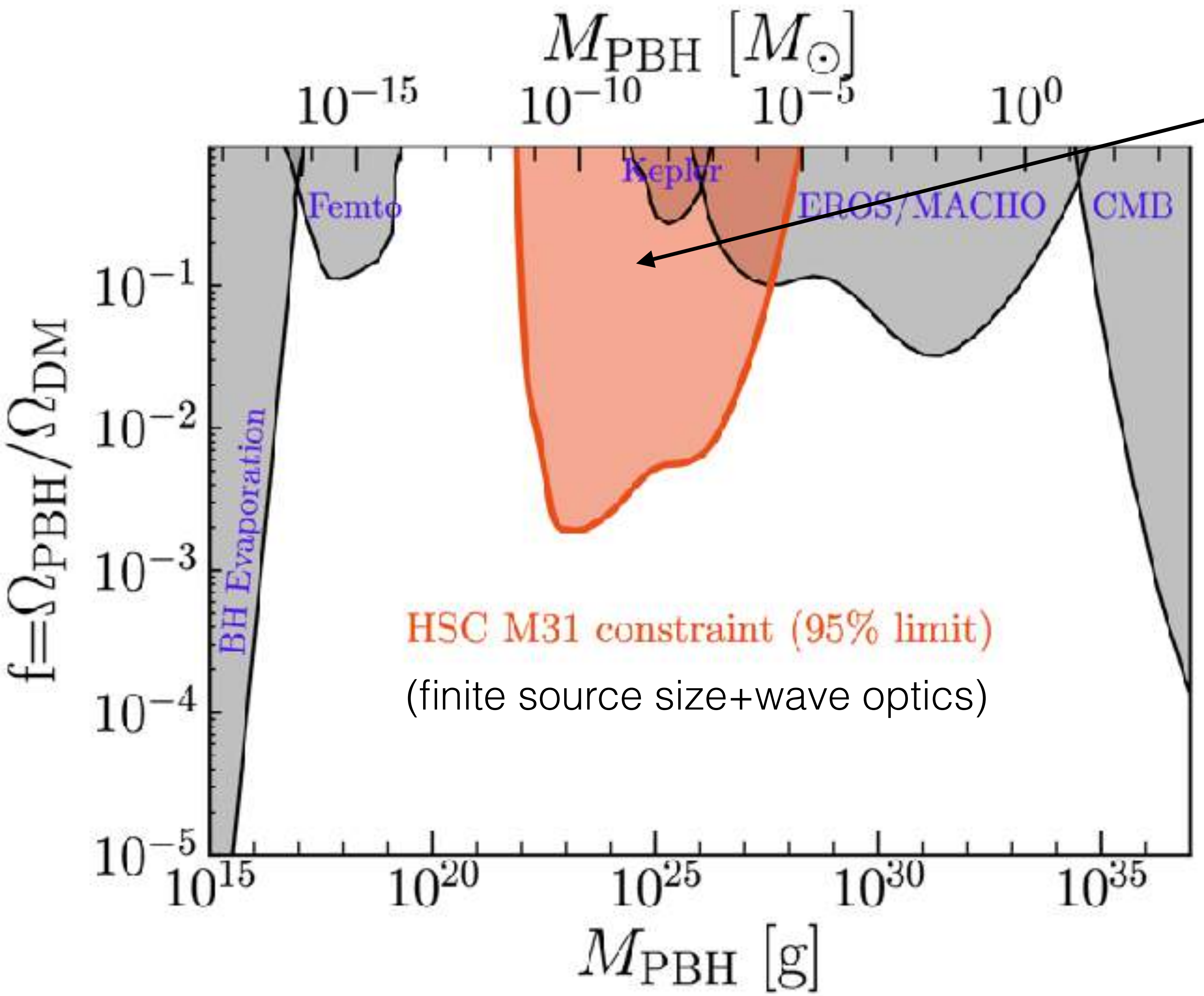

- HyperSuprimeCam
- Telescópio Subaru de 8m
- Gran campo de visión (M31 entera)
- Microlensing de los pixeles (no puntos)
- Linea de base: 8h
- cadencia minutos

arXiv:1701.02151

Límites de materia oscura en objetos compactos

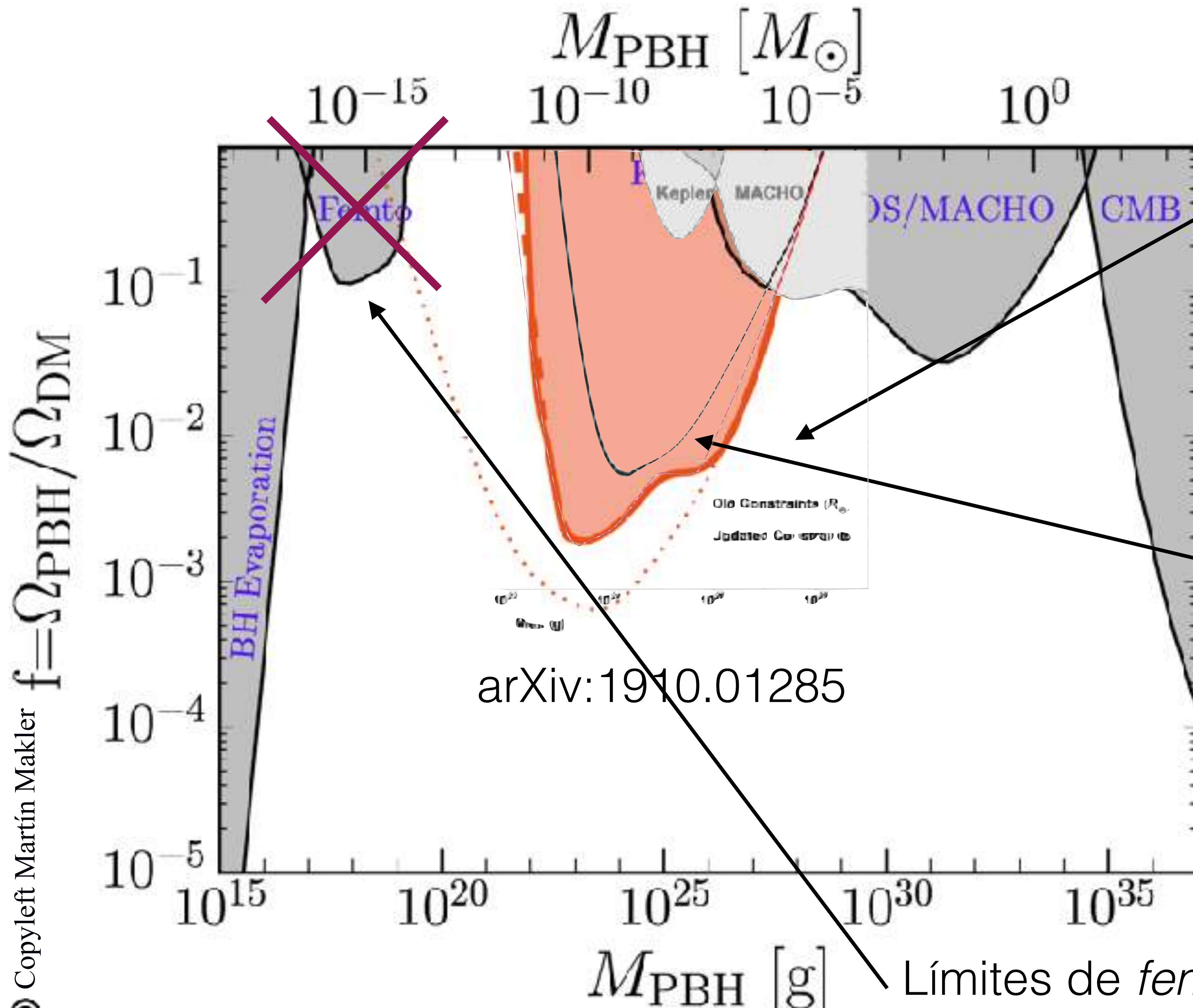

arXiv:1910.01285

Considerando el efecto de fuente finita y óptica ondulatória, el límite es menos restrictivo

Considerando una distribución realista de la dimensión de las estrellas, el límite se vuelve aún menos restritivo

Límites de *femtolensing* no sobreviven al efecto de fuente finita

arXiv:1701.02151v3

Ventanas para PBH

Estudiar con micro y femtolensing

ondas gravitacionales

Macrolensing: busca + modelos! ← escala de cúmulos de galaxias

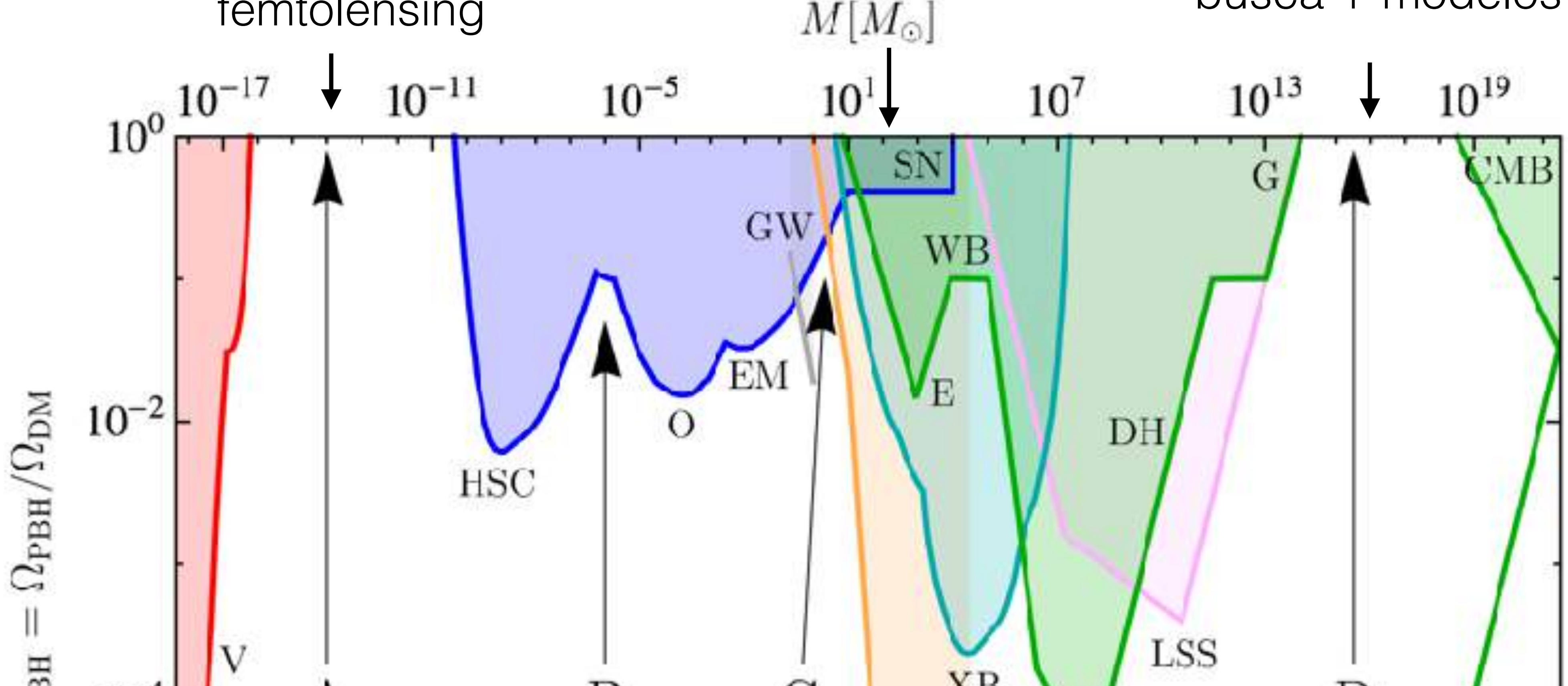

https://www.ligo.org/detections/GW190521.php

"On 2 September 2020, the LIGO Scientific Collaboration and the Virgo Collaboration announced the discovery of GW190521, the most massive gravitational wave binary observed to date. The two inspiralling black holes had masses of about 85 and 66 solar masses, and resulted in the formation of a black hole remnant of 142 solar masses. This remnant provides the first clear detection of an "intermediate-mass" black hole."

¡Generación de arcos gravitacionales y anillos de Einstein!

¿Seriam detectados?

¿Límites actuales?

¿Se pueden predecir y obtener límites?

Otros modelos de lentes

Límites por microlensing en matéria oscura extendida

Gravitational microlensing by dark matter in extended structures

Djuna Croon, David McKeen, and Nirmal Raj
Phys. Rev. D **101**, 083013 – Published 8 April 2020

- Matéria escura en la forma de objetos condensados
  - agujeros negros primordiales
  - estrellas de bosones
  - micro-halos de materia oscura
  - mini-grumos de axiones

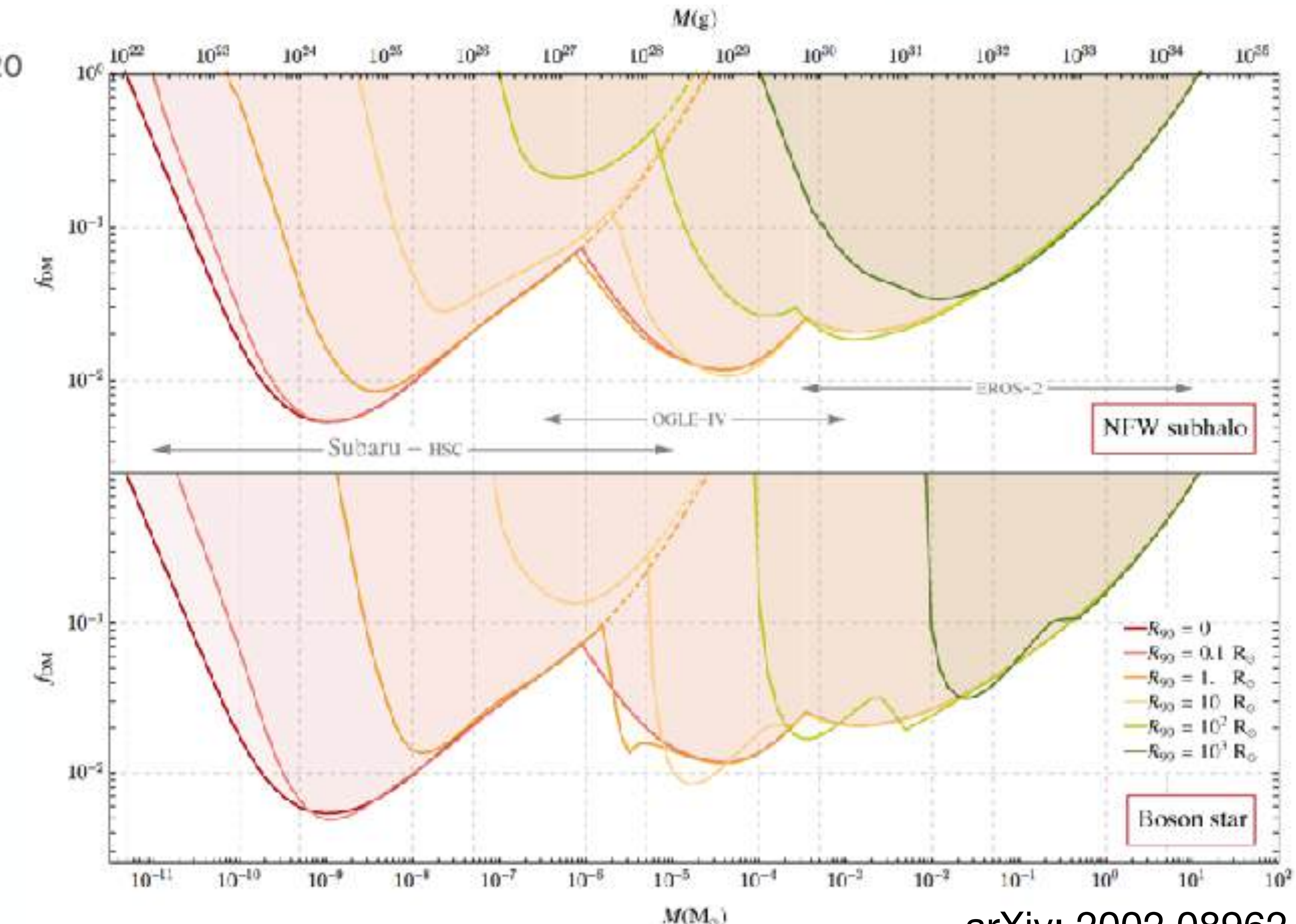

arXiv: 2002.08962

Ver también: *Repository for extended dark matter object constraints*,

Djuna Croon, Sergio Sevillano Muñoz, arXiv:2407.02573

Otras poblaciones de lentes

Gaudi, 2012, Ann. Rev. Astron. Astrophys. 50, 411

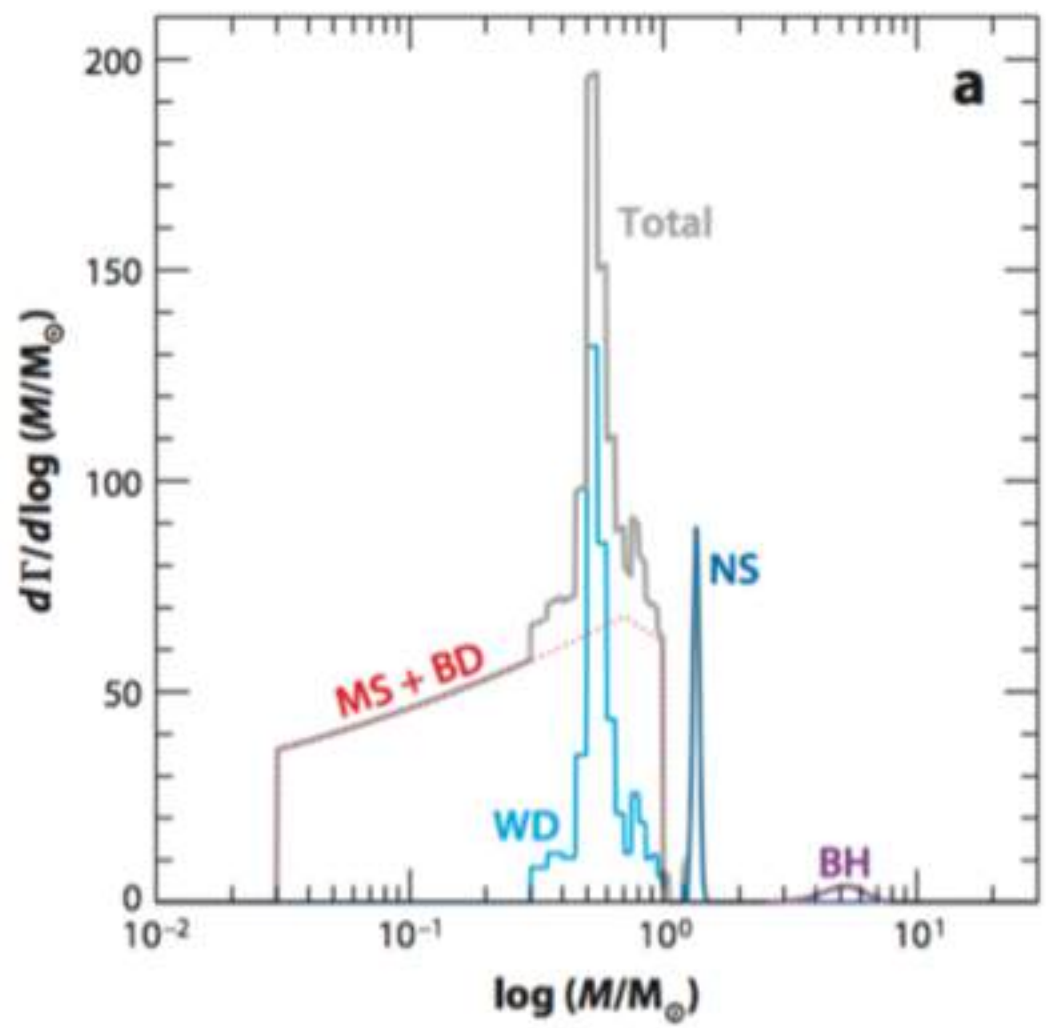

Theoretical estimate of the rate of microlensing events towards the galactic bulge

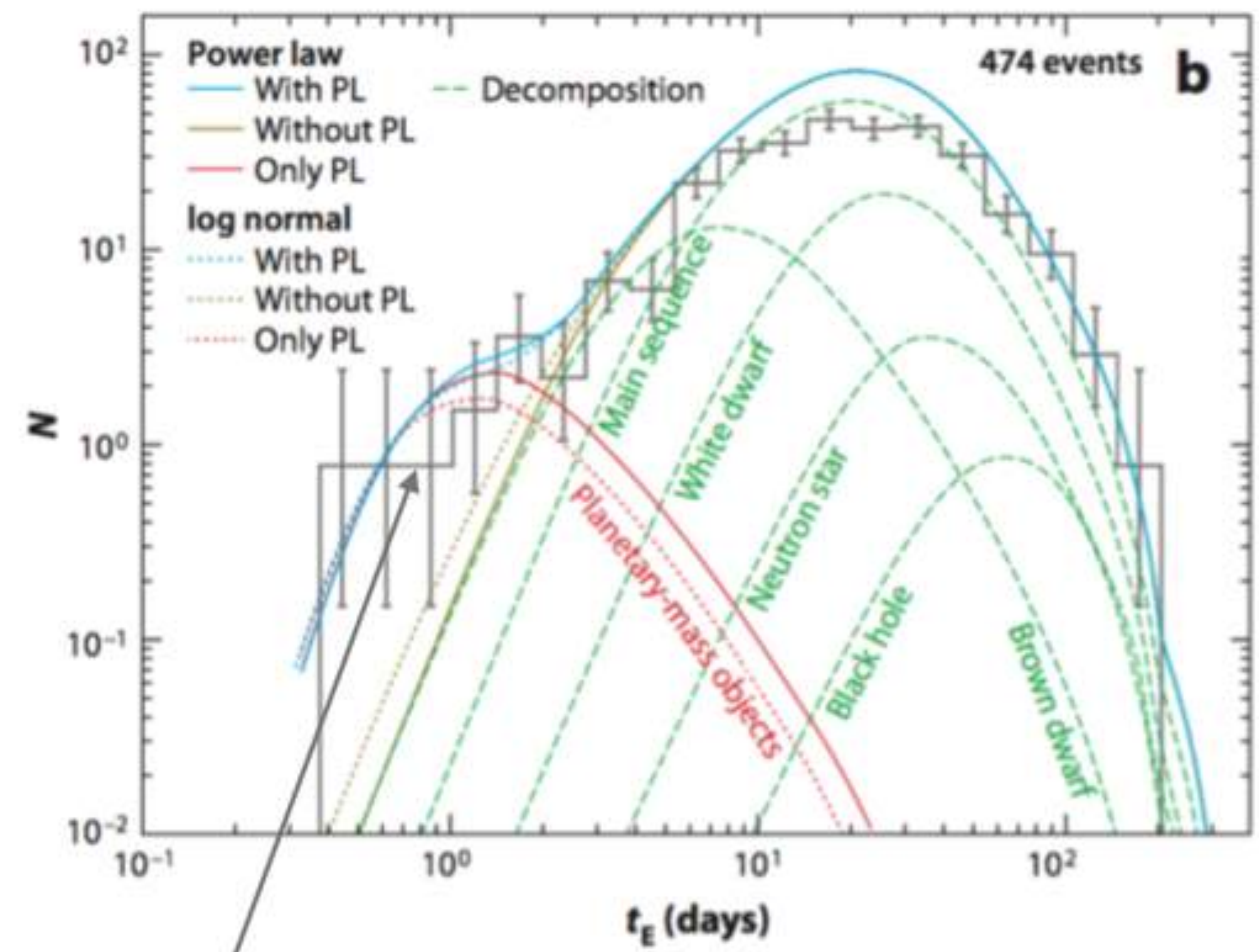

Distribution of microlensing event timescales observed by the MOA collaboration (2006-2007)

Exceso de eventos por planetas?

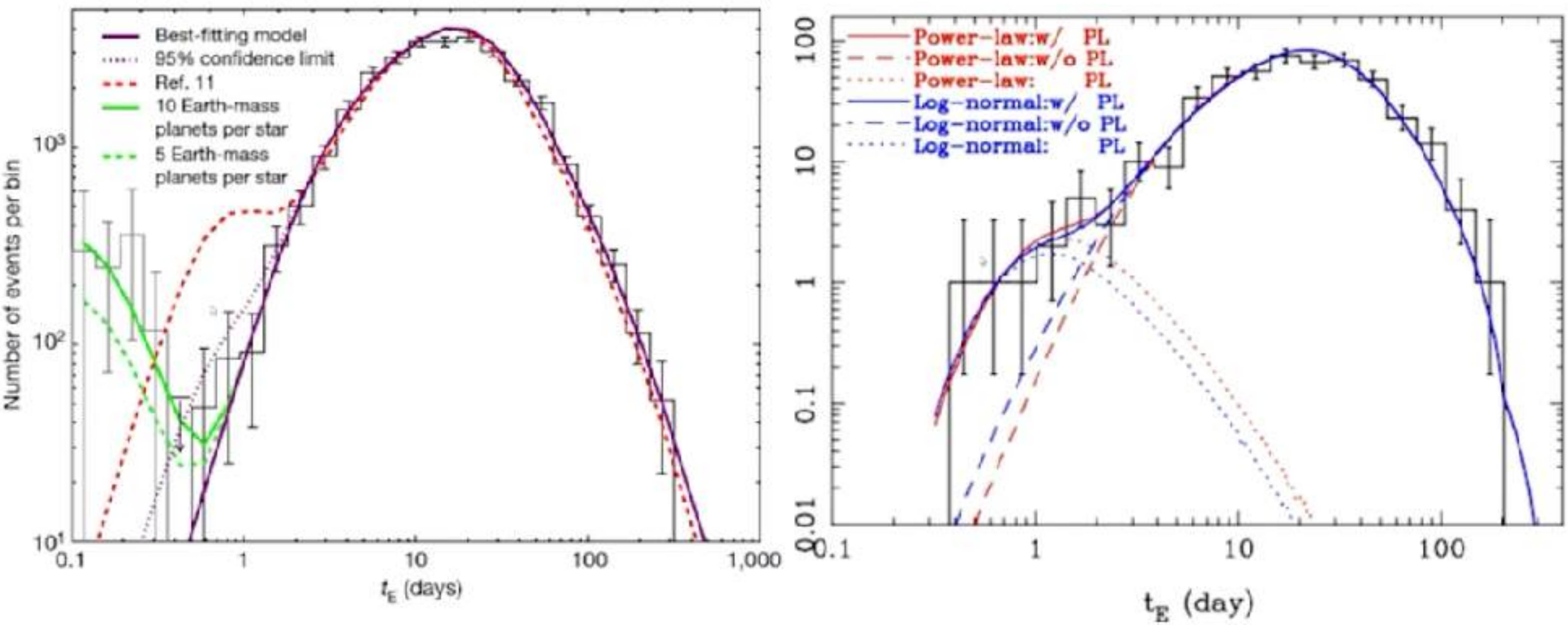

Mróz et al. (2017)

No hay exceso? Hay exceso para masas menores?

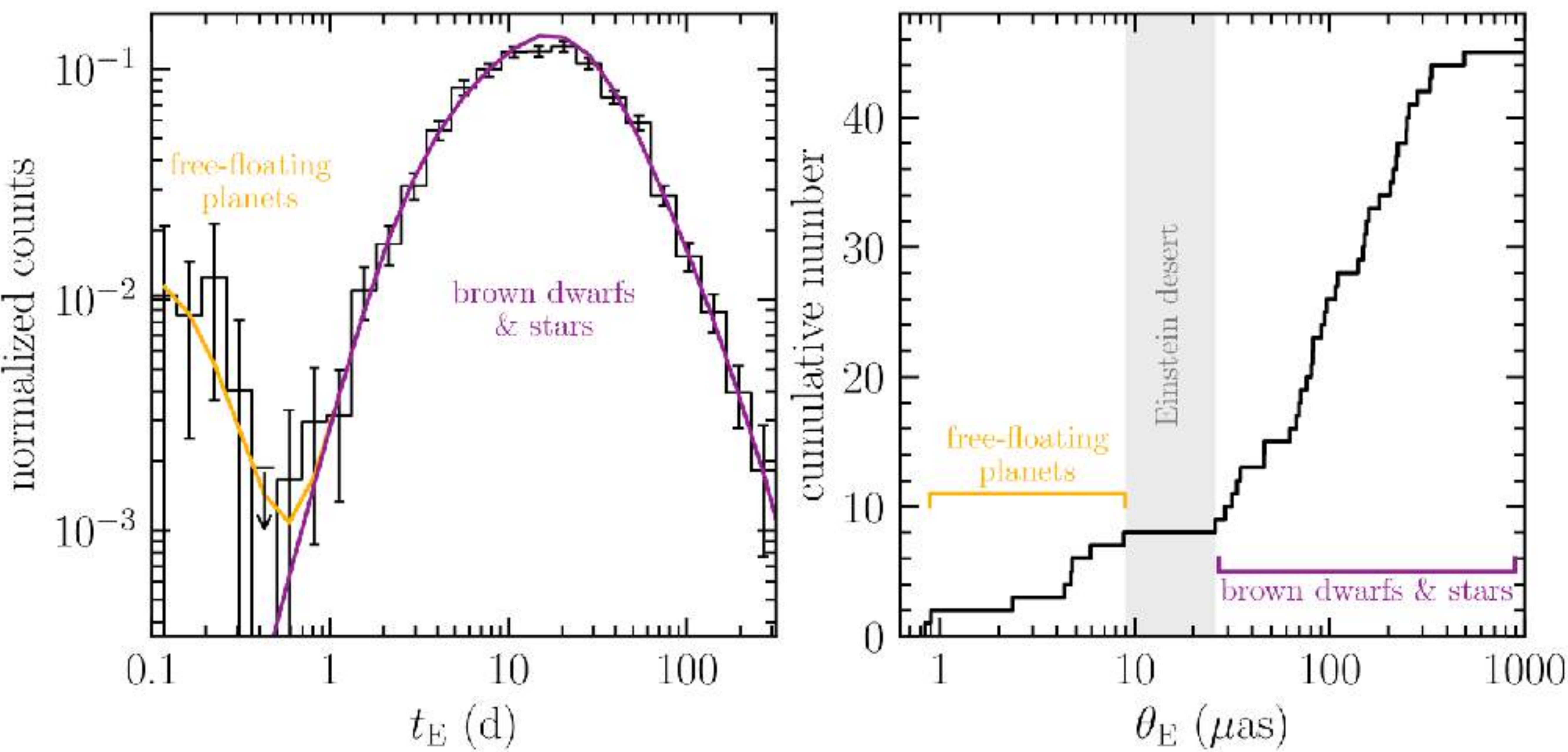

free-floating
planets
brown dwarfs
& stars
normalized counts
t_E (d)
Einstein desert
free-floating
planets
brown dwarfs & stars
cumulative number
θ_E (μas)

Para pensar

- Para pensar: ¿es realista el cálculo de la estadística de lentes usando un umbral fijo de magnificación? ¿Qué hipótesis conlleva?
- ¿Eso podría llevar a descartar eventos o poner un sesgo de selección?
- ¿Cómo tomar en cuenta la eficiencia de detección, modificando la sección eficaz o agregando una función de selección?
- ¿Qué cambiaria en el cálculo de la tasa de eventos si consideramos el efecto de fuente finita?

Qué se puede estudiar con *microlensing*?

- Descubierta de planetas extra-solares: > 300 planetas (> 60 en 2022!)
- Propiedades y distribución de objetos compactos: agujeros negros, estrellas de neutrones, enanas blancas y marrones, estrellas comunes, etc.
- Existencia y propiedades de objetos condensados candidatos a **materia oscura** (agujeros negros primordiales, estrellas de bosones, etc.)
- Límites en la contribución de esos objetos a la materia oscura en el Universo
- En resumen, pueden sondear **cualquier cosa en nuestra galaxia (o en otras galáxias) que sea lo suficientemente condensada y posea masa mayor a la de asteroides**!

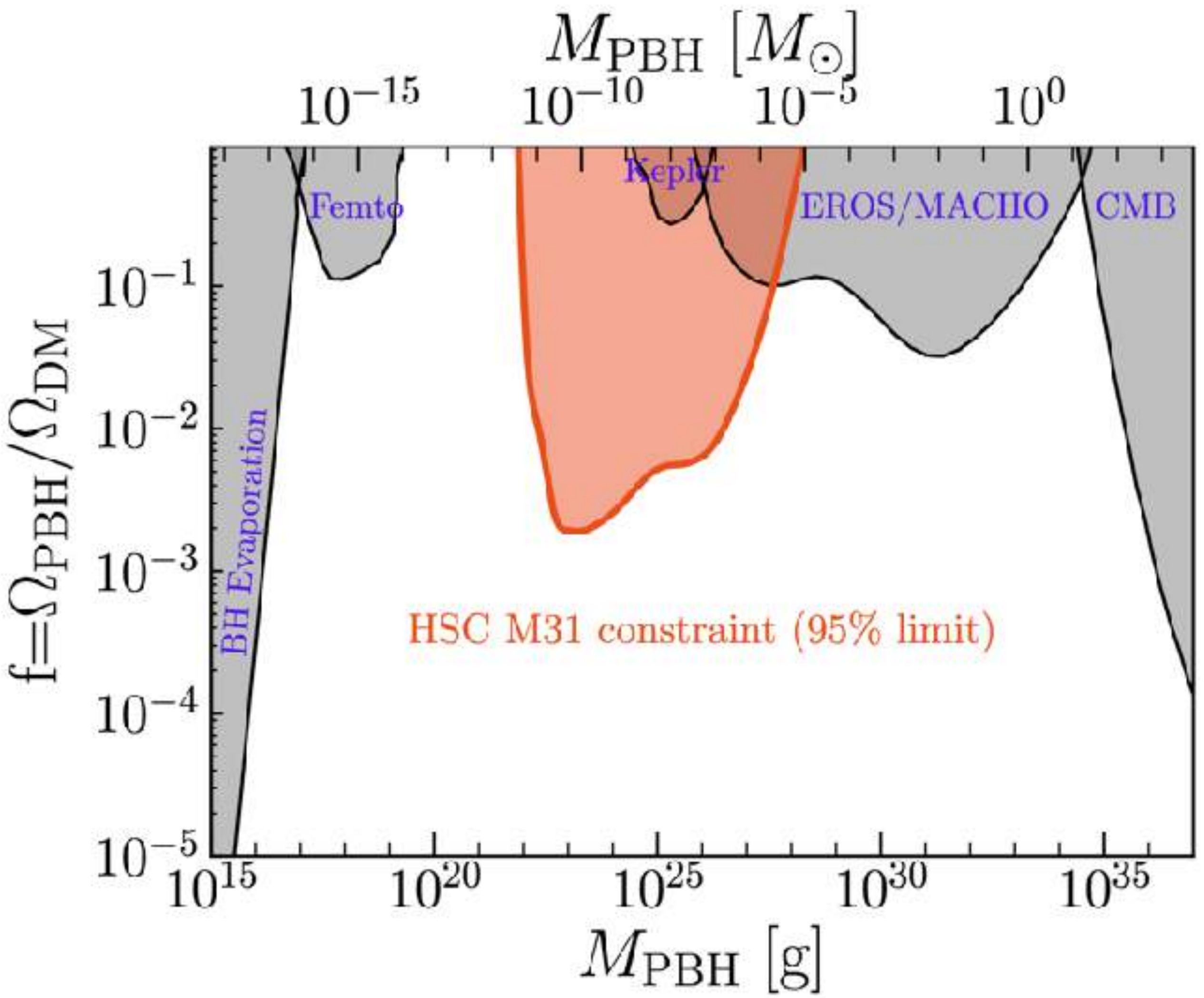

arXiv:1701.02151v3

Para pensar

- ¿Qué más se podría medir con microlensing?
- ¿Qué otras aplicaciones podría tener?
- ¿Qué tipo de instrumentación nueva podría llevar a nuevas descubiertas o nuevas medidas en el campo?

Plan de la Parte II

lentes por galáxias y cúmulos de galáxias

- Ecuación de la lente en un universo en expansión
- Jacobiana de la transformación: cáusticas y curvas críticas
- Modelos de lentes extendidas
- Retraso temporal y aplicaciones
- Efecto débil de lentes (fundamentos de *weak lensing*, regímenes y métodos)

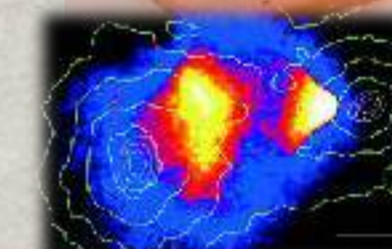

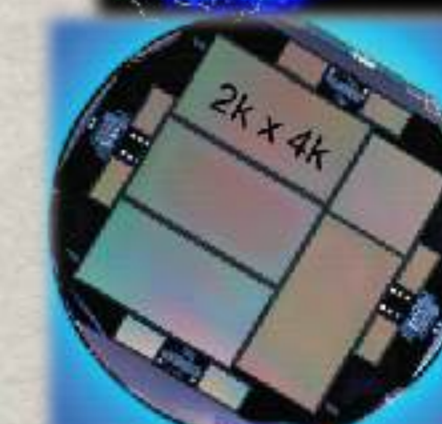

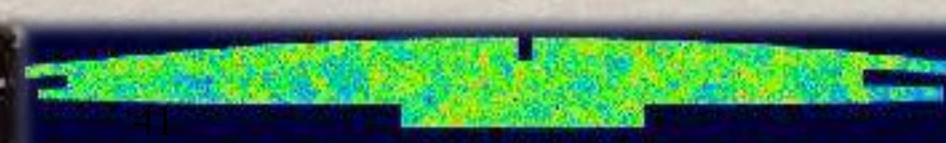

Límite newtoniano y teoria de perturbación relativista

- Límite newtoniano: $\dfrac{\phi}{c^2} \ll 1$ e $\left(\dfrac{v}{c}\right)^2 \ll 1$

- Teoria de perturbación cosmológica: métrica de Robertson-Walker perturbada

$$
\begin{aligned}
ds^2 &= \left[g^{(0)}_{\mu\nu} + g^{(1)}_{\mu\nu}\right] dx^\mu dx^\nu \\
&= a^2(\tau)\left[-d\tau^2 + \gamma_{ij}(\vec{x})dx^i dx^j + h_{\mu\nu}(\vec{x},\tau)dx^\mu dx^\nu\right] \quad ,
\end{aligned}
$$

- Desacople entre los modos en el regimen lineal
- Perturbaciones escalares:

$$\boxed{ds^2 = a^2(\tau)\left[-(1+2\Psi)d\tau^2 + (1-2\phi)\gamma_{ij}\, dx^i dx^j\right]}$$

(para um fluido perfecto $\Phi = \Psi$)

Comentario/recordatorio

- Observaciones se realizan en el llamado cono de luz
- Relación entre distancia y tiempo
- Relación entre distancia y corrimiento al rojo z
- Utilizados de forma intercambiable
- z es directamente observable,
- t y r dependen del modelo

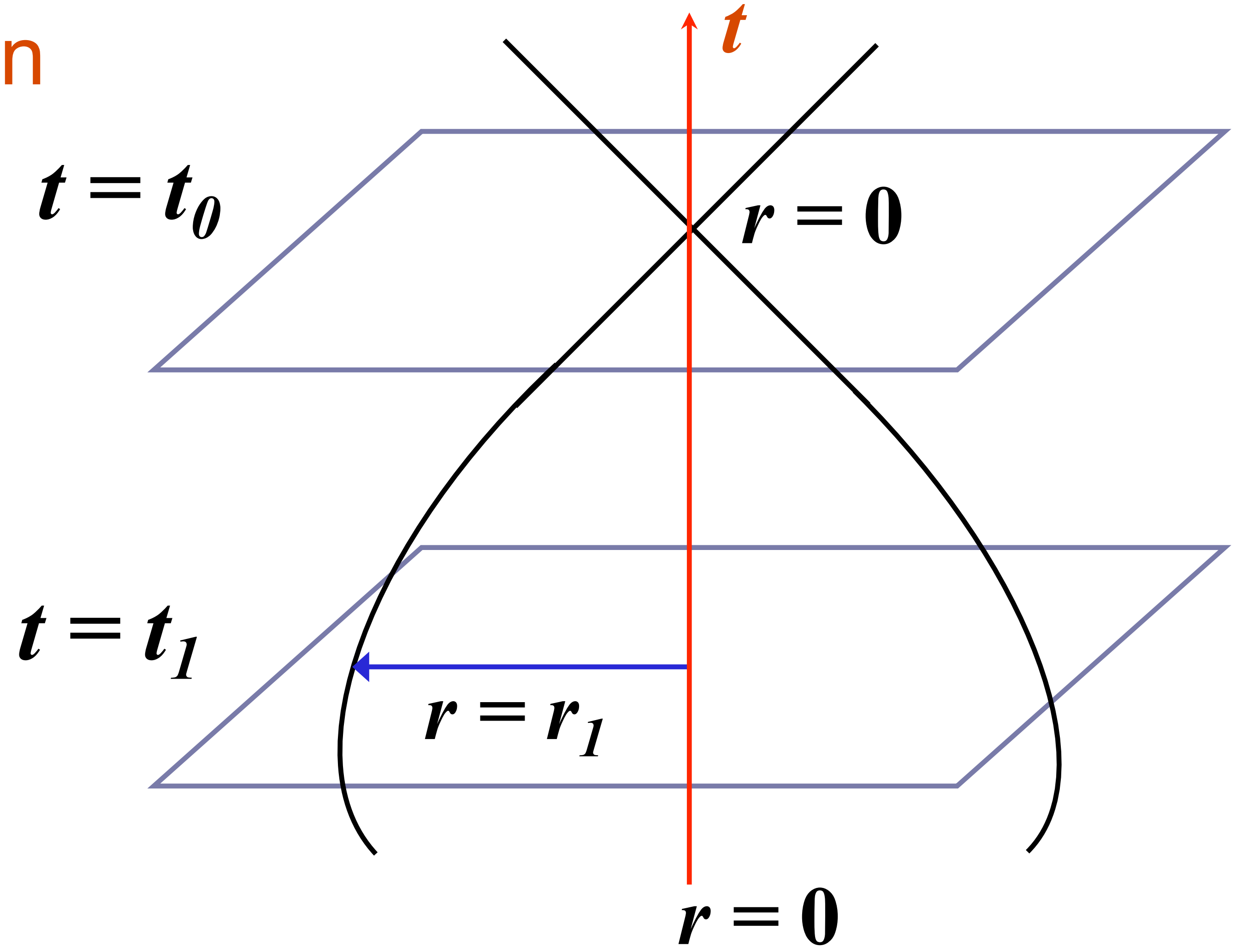

$$z = \frac{\lambda_r - \lambda_e}{\lambda_e}$$

$$d_i = f(z; \text{cosmologia})$$

Distancia de diámetro angular entre dos puntos

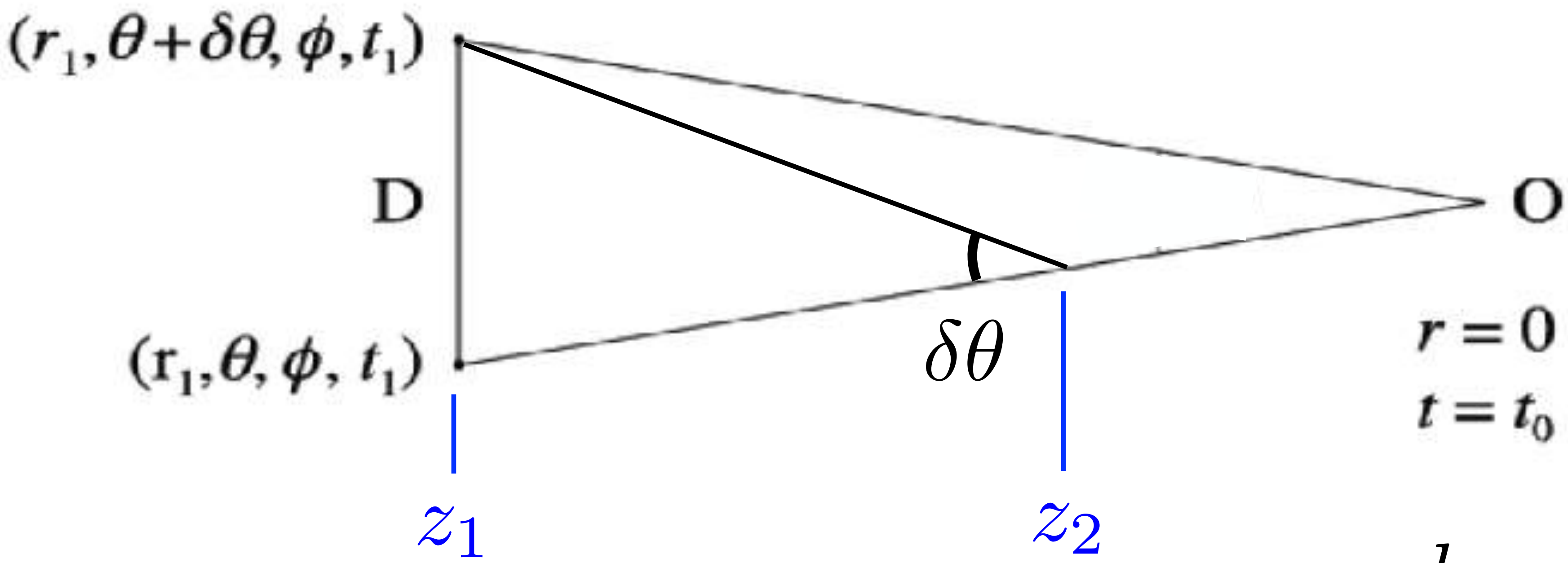

$$d_A \equiv \frac{D}{\delta\theta}$$

$(\text{para}\, \delta\theta \ll 1)$

$$d_A = a(t_2) r_{12} = a(z_2) r_{12}$$

$$\boxed{d_A = (1+z_2)^{-1} \operatorname{sen}_K \left(H_0 \sqrt{|1-\Omega_0|} \int_{z_1}^{z_2} \frac{dz'}{H(z')} \right) \Big/ H_0 \sqrt{|1-\Omega_0|}}$$

Caso plano: $D_A(z_1, z_2) = \dfrac{1}{1+z_2} \displaystyle\int_{z_1}^{z_2} \frac{dz}{H(z)}$

Distância de diámetro angular entre dos puntos

Caso plano:

$$D_A\left(z_1, z_2\right) = \frac{1}{1+z_2}\int_{z_1}^{z_2}\frac{dz}{H(z)}$$

En el modelo wCDM $\qquad p = w\rho$

$$H^2(a) = H_0^2\left[\Omega_r a^{-4} + \Omega_M a^{-3} + \Omega_k a^{-2} + \Omega_{DE} a^{-3(1+w)}\right]$$

de forma que

$$D_A\left(z_1, z_2\right) = \frac{\left(1+z_2\right)^{-1}}{H_0}\int_{z_1}^{z_2}\frac{dz'}{\sqrt{\Omega_M(1+z')^3 + \left(1-\Omega_M\right)\left(1+z'\right)^{3(1+w)}}}$$

$D_{LS} = D_A(z_L, z_S)$, etc.

Desviación de la luz por la gravedad

Geodésica nula,
Principio de Fermat

$$ds^2 = \left(1 + \frac{2\phi}{c^2}\right) c^2 dt^2 - \left(1 - \frac{2\phi}{c^2}\right) d\sigma^2$$

Parte espacial
de la métrica
de FLRW

$$\frac{d\sigma}{dt} := c' = \sqrt{\frac{1 + 2\phi/c^2}{1 - 2\phi/c^2}} \simeq c\left(1 + \frac{2\phi}{c^2}\right)$$

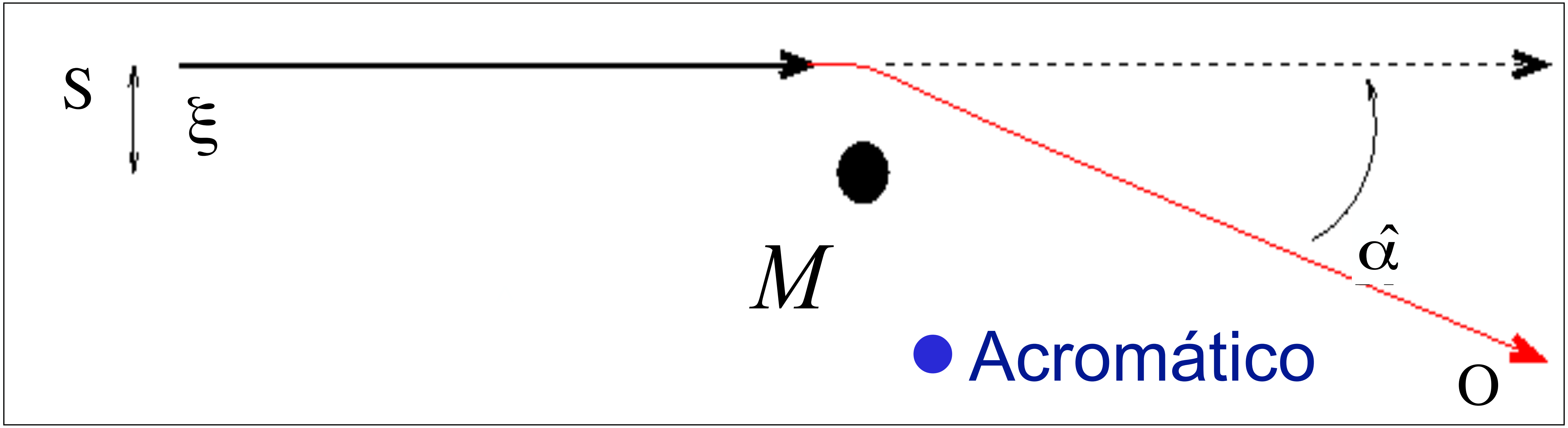

- Acromático

Desvío causado por una lente puntual:

$$\hat{\alpha} = \frac{4GM}{c^2}\frac{1}{\xi}$$

(factor 2 en comparación con "Newton")

Geometría del efecto de lentes por plano único
(aproximación de lente fina)

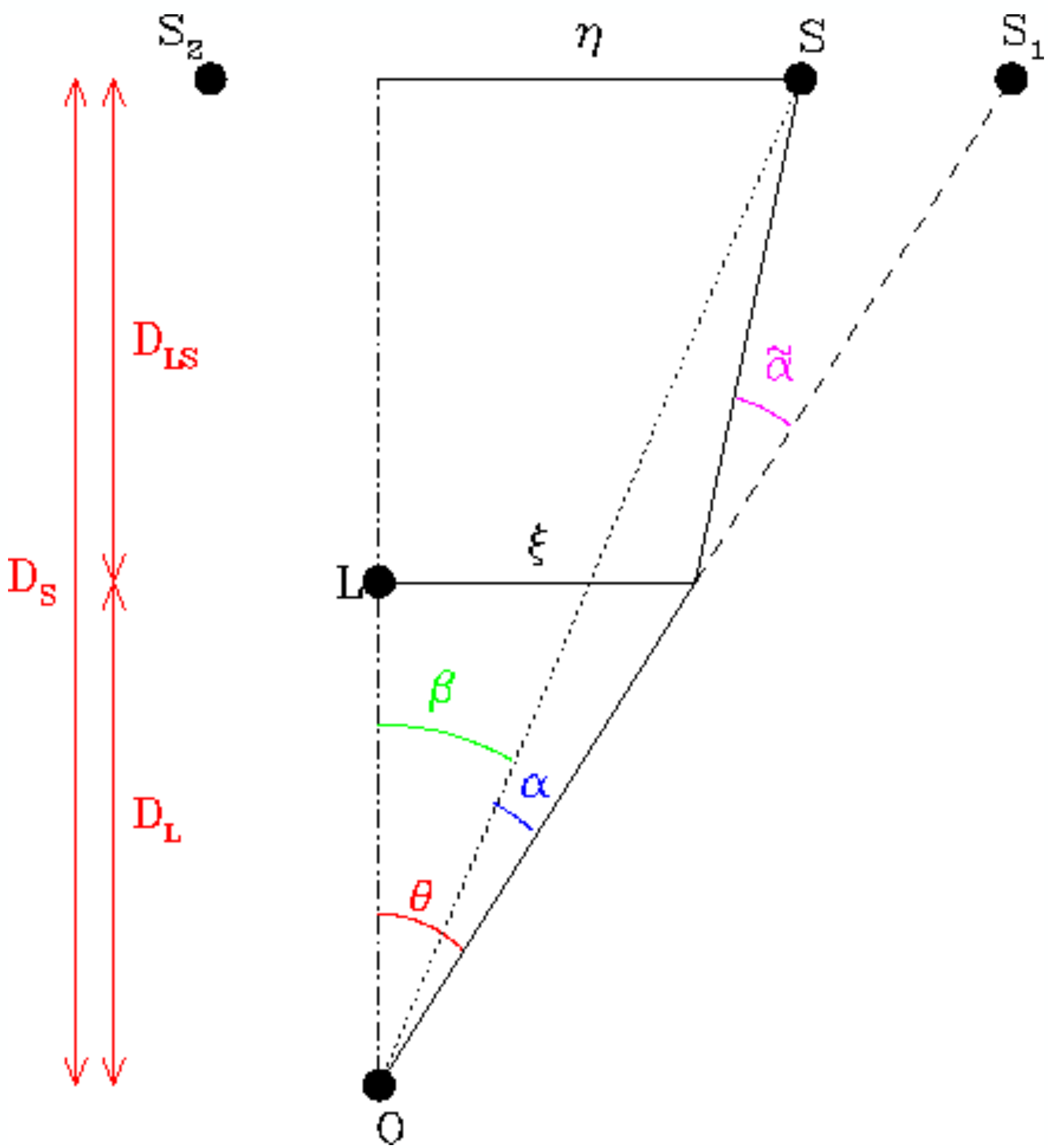

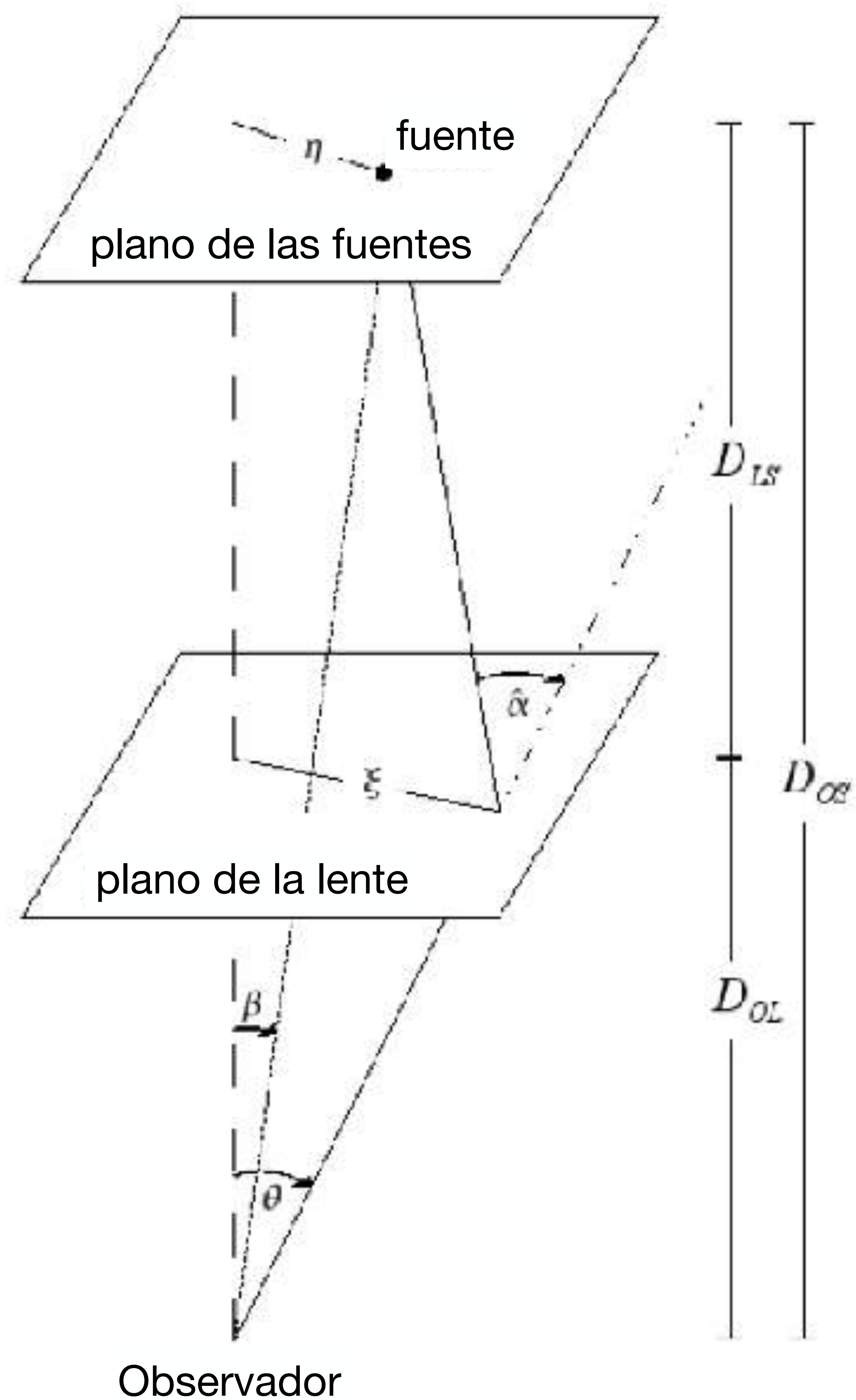

La ecuación de la lente

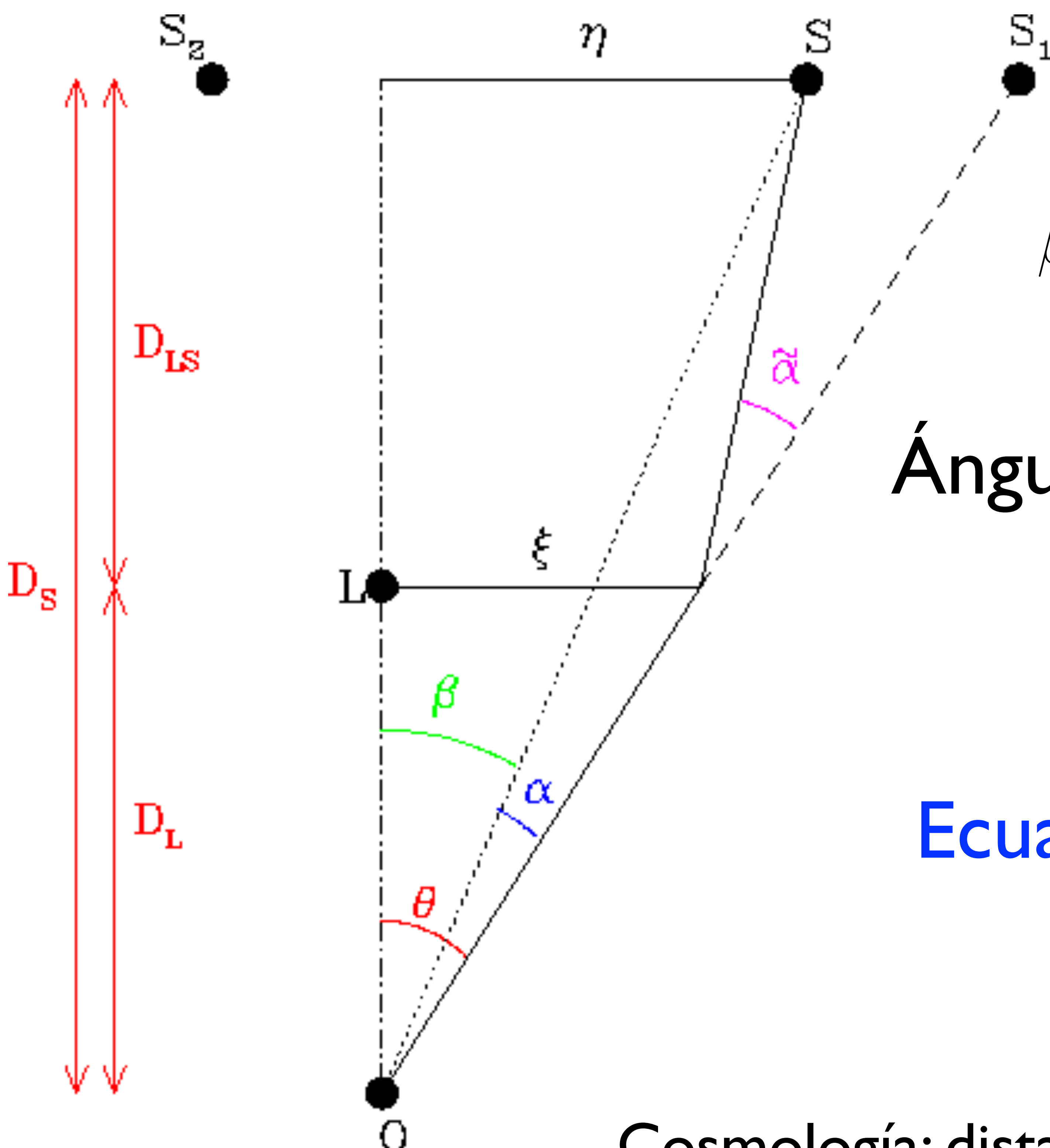

¡(*Strong*) *lensing* es resolver la ecuación de la lente!

$$\vec{\beta} D_{OS} = \vec{\theta} D_{OS} - \hat{\vec{\alpha}} D_{LS} \left(\vec{\theta}\right)$$

Ángulo de deflexión reducido

$$\vec{\alpha} = \hat{\vec{\alpha}} \frac{D_{LS}}{D_{OS}}$$

Ecuación de la lente

$$\vec{\beta} = \vec{\theta} - \vec{\alpha}\left(\vec{\theta}\right)$$

Cosmología: distancias de diámetro angular!

Deducciones formales

- Lentes gravitacionales en relatividad general: Schneirder, Ehlers, Falco: capítulos 3 (*Optics in curved spacetime*) y 4 (contexto cosmológico)

- Ángulo de reflexión en las 3 geometrías de fondo: Petters, Lavine, Wambsganss


Lentes Extensas

Extended Lenses

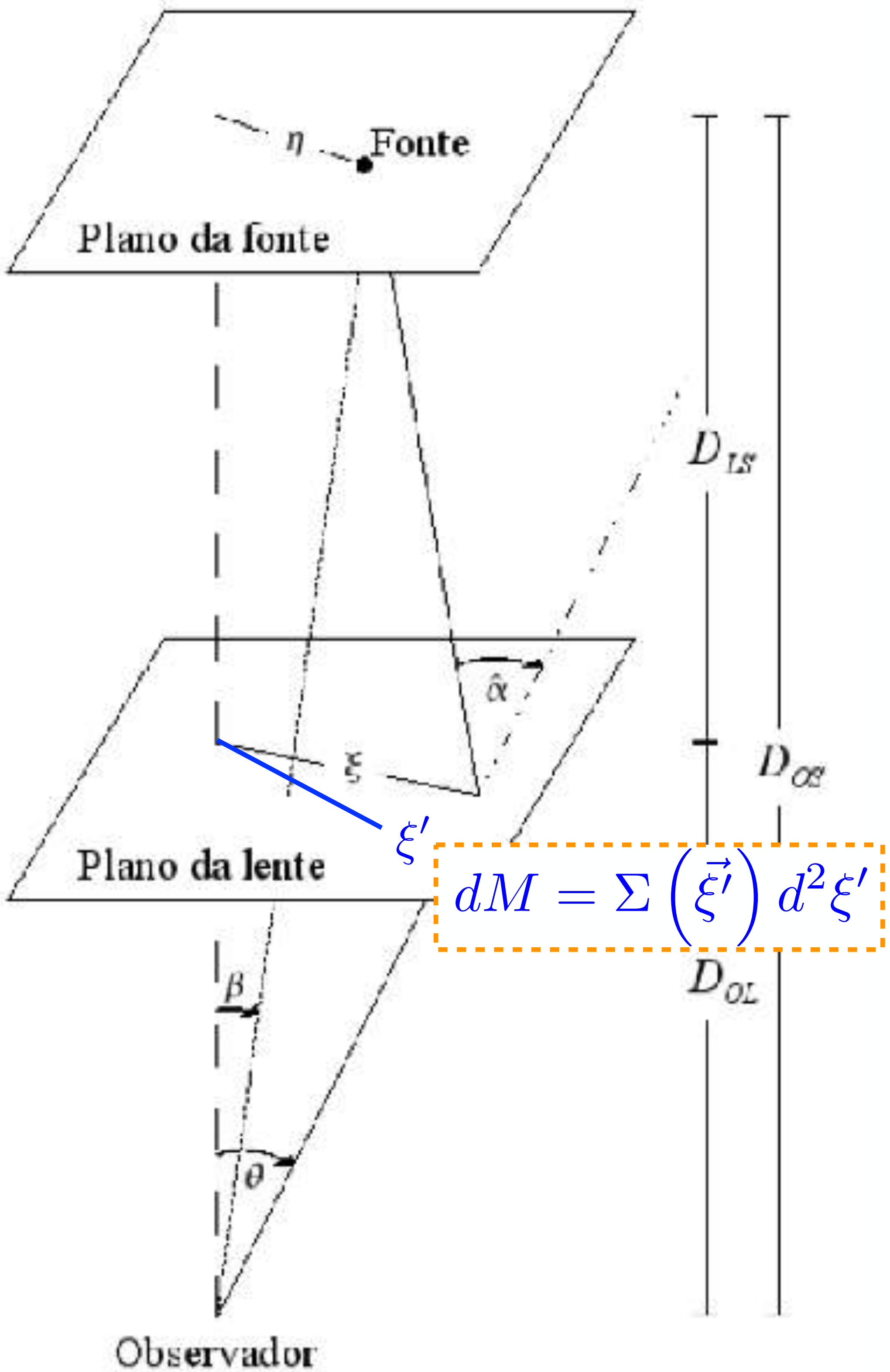

Point mass $\hat{\vec{\alpha}} = \frac{4GM}{c^2\xi}$

Surface mass density

$$\Sigma\left(\vec{\xi}\right) = \int_0^\infty dz\rho\left(\vec{\xi}, z\right)$$

Contribution of the area element

$$d\hat{\vec{\alpha}} = \frac{4G}{c^2}\Sigma\left(\vec{\xi'}\right) d^2\xi' \frac{\vec{\xi} - \vec{\xi'}}{|\vec{\xi} - \vec{\xi'}|^2}$$

Deflection angle

$$\hat{\vec{\alpha}} = \frac{4G}{c^2}\int d^2\xi'\Sigma\left(\vec{\xi'}\right) \frac{\vec{\xi} - \vec{\xi'}}{|\vec{\xi} - \vec{\xi'}|^2}$$

Extended Lenses

Projected potential $\psi\left(\vec{\xi}\right) = \int dz \varphi(\vec{\xi}, z)$

Poisson equation $\nabla^2_\xi \psi\left(\vec{\xi}\right) = 4\pi G \Sigma\left(\vec{\xi}\right)$

Using the 2D Green function

$$\psi\left(\vec{\xi}\right) = 2G \int d^2\xi' \Sigma\left(\vec{\xi'}\right) \ln|\xi - \xi'|$$

Comparing with the deflection angle

$$\hat{\vec{\alpha}} = \frac{4G}{c^2} \int d^2\xi' \Sigma\left(\vec{\xi'}\right) \frac{\vec{\xi} - \vec{\xi'}}{|\vec{\xi} - \vec{\xi'}|^2}$$

We obtain $\hat{\vec{\alpha}} = \frac{2}{c^2} \vec{\nabla}_\xi \psi\left(\vec{\xi}\right)$

Extended Lenses

Projected potential $\psi\left(\vec{\xi}\right) = \int dz \varphi(\vec{\xi}, z)$

Deflection angle $\vec{\hat{\alpha}} = \frac{2}{c^2}\vec{\nabla}_\xi \psi\left(\vec{\xi}\right)$

Reduced deflection angle

$$\vec{\alpha} = \vec{\hat{\alpha}}\frac{D_{LS}}{D_{OS}} = \frac{2}{c^2}\frac{D_{LS}}{D_{OS}D_{OL}}\vec{\nabla}_\theta \psi\left(\vec{\theta}\right)$$

Lensing potential $\Psi(\vec{x}) \equiv \frac{2}{c^2}\frac{D_{LS}}{D_{OS}D_{OL}}\psi$

Lens equation $\vec{\beta} = \vec{\theta} - \vec{\alpha}\left(\vec{\theta}\right) = \boxed{\vec{\theta} - \vec{\nabla}_\theta \Psi\left(\vec{\theta}\right)}$

Lentes extensas

Ángulo de deflexión

$$\hat{\vec{\alpha}} = \frac{4G}{c^2} \int d^2\xi' \Sigma\left(\vec{\xi'}\right) \frac{\vec{\xi} - \vec{\xi'}}{|\vec{\xi} - \vec{\xi'}|^2}$$

Ecuación de Poisson $\nabla^2_{\xi}\psi\left(\vec{\xi}\right) = 4\pi G \Sigma\left(\vec{\xi}\right)$

Ecuación de la lente

$$\vec{\beta} = \vec{\theta} - \vec{\alpha}\left(\vec{\theta}\right) = \boxed{\vec{\theta} - \vec{\nabla}_{\theta}\Psi\left(\vec{\theta}\right)}$$

Potencial de Lente(amiento) $\Psi \equiv \frac{2}{c^2}\frac{D_{\rm LS}}{D_{\rm OS}D_{\rm OL}}\psi$

convirtiendo variables $d\xi_i = D_{OL} d\theta_i$

$$\nabla^2_{\theta}\Psi = \frac{2}{c^2}\frac{D_{\rm LS}}{D_{\rm OS}D_{\rm OL}} D^2_{\rm OL} 4\pi G\, \Sigma$$

Convergencia

Ecuación de Poisson

$$\nabla_\theta^2 \Psi = \frac{2}{c^2} \frac{D_{\rm LS}}{D_{\rm OS} D_{\rm OL}} D_{\rm OL}^2 4\pi G \, \Sigma\left(\vec{\theta}\right) = 2 \frac{\Sigma\left(\vec{\theta}\right)}{\Sigma_{\rm crit}}$$

Densidad superficial crítica

$$\boxed{\Sigma_{\rm crit} = \frac{c^2}{4\pi G} \frac{D_{\rm OS}}{D_{\rm OL} D_{\rm LS}}}$$

Convergencia

$$\kappa\left(\vec{\theta}\right) = \frac{\Sigma\left(\vec{\theta}\right)}{\Sigma_{\rm crit}}$$

Ecuación de Poisson $\boxed{\nabla_\theta^2 \Psi = 2\kappa\left(\vec{\theta}\right)}$

Jacobiana de la transformación

$$\vec{\beta} = \vec{\theta} - \vec{\nabla}_\theta \Psi \left(\vec{\theta} \right)$$

$$J_{ij} = \left(\frac{\partial \vec{\beta}}{\partial \vec{\theta}} \right)_{ij} = \delta_{ij} - \frac{\partial^2 \Psi}{\partial \theta_i \partial \theta_j},$$ definiendo $\Psi_{ij} = \dfrac{\partial^2 \Psi}{\partial \theta_i \partial \theta_j}$

tenemos $\mathbf{J} = \begin{pmatrix} 1 - \Psi_{11} & -\Psi_{12} \\ -\Psi_{21} & 1 - \Psi_{22} \end{pmatrix}$

como $\nabla_\theta^2 \Psi = \Psi_{11} + \Psi_{22} = 2\kappa$

$$\mathbf{J} = (1-\kappa)\mathbf{I} - \begin{pmatrix} \frac{1}{2}\left(\Psi_{11} - \Psi_{22}\right) & \Psi_{12} \\ \Psi_{21} & -\frac{1}{2}\left(\Psi_{11} - \Psi_{22}\right) \end{pmatrix}$$

Jacobiana de la transformación

$$\mathbf{J} = (1-\kappa)\mathbf{I} - \begin{pmatrix} \frac{1}{2}\left(\Psi_{11} - \Psi_{22}\right) & \Psi_{12} \\ \Psi_{21} & -\frac{1}{2}\left(\Psi_{11} - \Psi_{22}\right) \end{pmatrix}$$

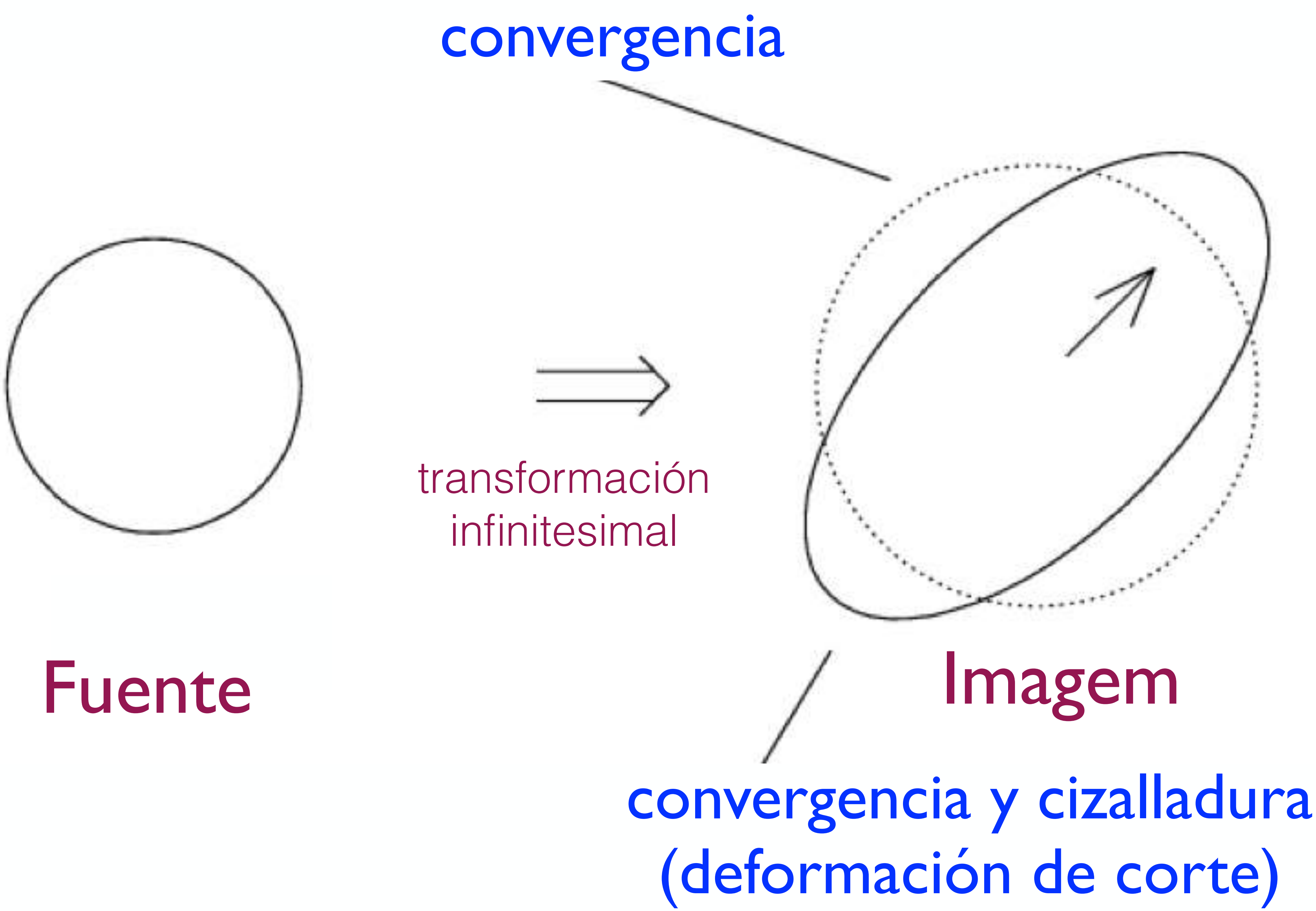

Cizalladura

$$\mathbf{J} = (1-\kappa)\mathbf{I} - \begin{pmatrix} \frac{1}{2}\left(\Psi_{11} - \Psi_{22}\right) & \Psi_{12} \\ \Psi_{21} & -\frac{1}{2}\left(\Psi_{11} - \Psi_{22}\right) \end{pmatrix}$$

Cizalladura:

$$\gamma_1(\vec{\theta}) = \frac{1}{2}(\Psi_{11} - \Psi_{22})$$

$$\gamma_2(\vec{\theta}) = \Psi_{12} = \Psi_{21}$$

$$\gamma = \sqrt{\gamma_1^2 + \gamma_2^2}$$

Em términos de la cizalladura y la convergencia tenemos

$$\mathbf{J} = (1-\kappa)\mathbf{I} + \begin{pmatrix} -\gamma_1 & -\gamma_2 \\ -\gamma_2 & \gamma_1 \end{pmatrix}$$

Autovalores de $\mathbf{J}^{-1}$

$$\mu_1 = \frac{1}{1-\kappa-\gamma}, \quad \mu_2 = \frac{1}{1-\kappa+\gamma}$$

Mapeo de Lentes

- mapeo imagem → fuente

$$\frac{\partial \beta_i}{\partial \theta_j} = \delta_{ij} - \frac{\partial^2 \Psi\left(\vec{\theta}\right)}{\partial \theta_i \partial \theta_j}$$

- plano único

$$\Psi = \frac{2}{c^2} \frac{D_{LS}}{D_{OS} D_{OL}} \int \phi\left(\xi, z\right) dz$$

potencial gravitacional

distâncias cosmológicas

$$D_{LS} = D_A\left(z_L, z_S\right) \ldots$$

- autovalores:

$$\mu_1 = \frac{1}{1-\kappa+\gamma}, \mu_2 = \frac{1}{1-\kappa-\gamma}$$

- magnificación local y razón axial:

$$\mu = \mu_1 \, \mu_2$$

$$r = \left| \frac{\mu_1}{\mu_2} \right|$$

Mapeo Lineal

Fuente circular

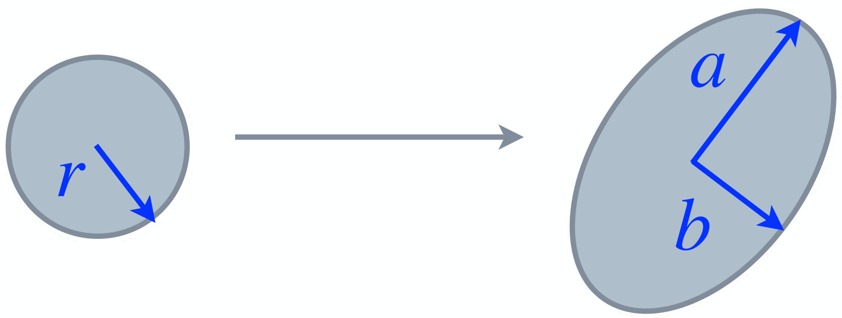

$$a = \left(\frac{1}{1-\kappa-\gamma}\right) r$$

$$b = \left(\frac{1}{1-\kappa+\gamma}\right) r$$

- Magnificación

$$\mu = \frac{A_{\text{imagem}}}{A_{\text{fonte}}} = \left[(1-\kappa)^2 - \gamma^2\right]^{-1}$$

- Elipticidad

$$\boxed{\epsilon := \frac{a-b}{a+b} = \frac{\gamma}{1-\kappa} =: g}$$

Mapeo de Lentes

- mapeo imagem → fuente

$$\frac{\partial \beta_i}{\partial \theta_j} = \delta_{ij} - \frac{\partial^2 \Psi(\vec{\theta})}{\partial \theta_i \partial \theta_j}$$

- plano único

$$\Psi = \frac{2}{c^2} \frac{D_{LS}}{D_{OS} D_{OL}} \int \phi(\xi, z) dz$$

potencial gravitatorio

distancias cosmológicas

$$D_{LS} = D_A(z_L, z_S)\ldots$$

- autovalores:

$$\mu_1 = \frac{1}{1-\kappa+\gamma}, \mu_2 = \frac{1}{1-\kappa-\gamma}$$

- magnificación local y razón axial:

$$\mu = \mu_1 \, \mu_2 \qquad r = \left| \frac{\mu_1}{\mu_2} \right|$$

- densidad superficial crítica

$$\Sigma_{\rm crit} = \frac{c^2}{4\pi G} \frac{D_{OS}}{D_{OL} D_{LS}}$$

- convergencia

$$\kappa = \frac{\Sigma}{\Sigma_{\rm crit}}$$

Mapeo de Lentes

- mapeo imagem → fuente

$$\frac{\partial \beta_i}{\partial \theta_j} = \delta_{ij} - \frac{\partial^2 \Psi(\vec{\theta})}{\partial \theta_i \partial \theta_j}$$

- autovalores:

$$\mu_1 = \frac{1}{1-\kappa+\gamma}, \mu_2 = \frac{1}{1-\kappa-\gamma}$$

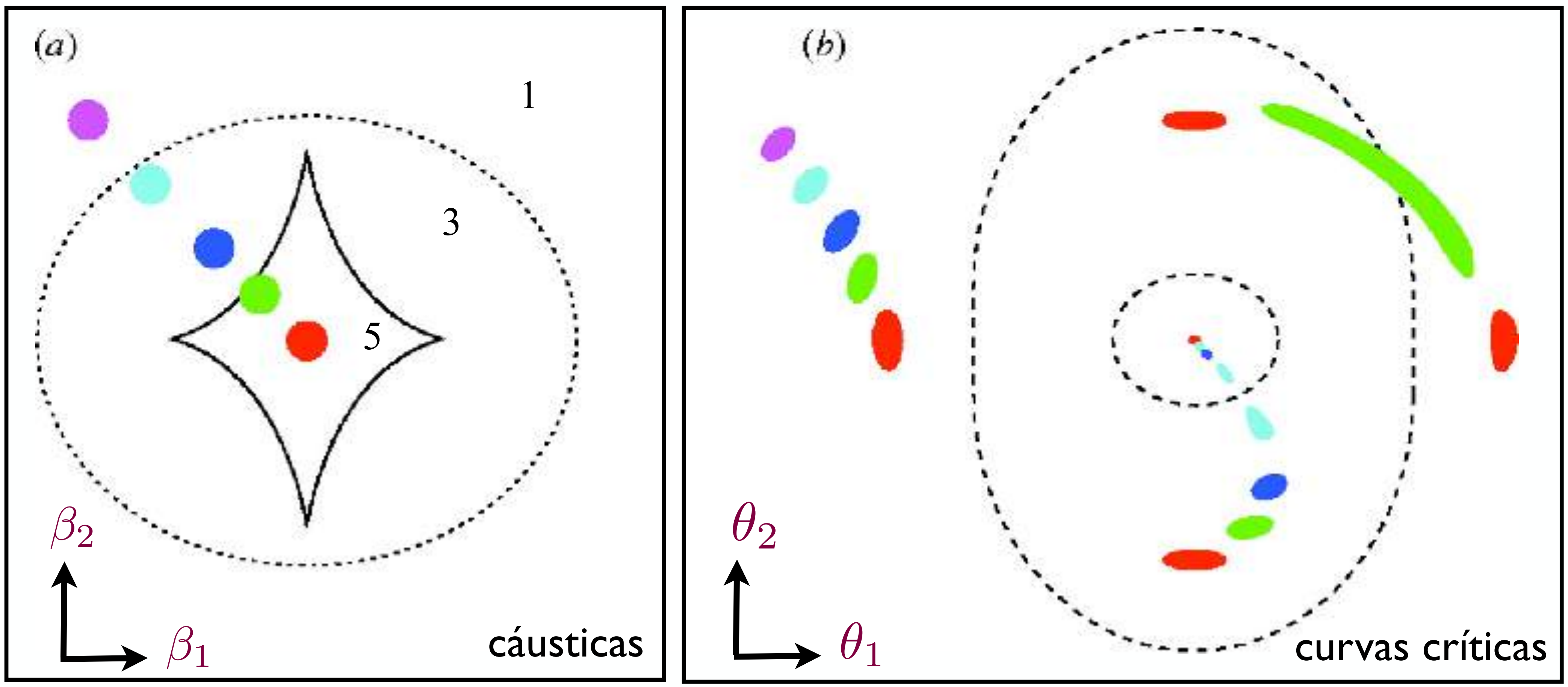

Plano de las fuentes

Lente/imágenes

Los números en el plano de las fuentes indicam la multiplicidad de las imágenes

Esfera isoterma singular

Esfera isoterma singular

- Modelo más simple de lente extendida
- Caso típico para soluciones más generales
- Mas allá de su valor didáctico, es un modelo realista para la distribución de massa en la escala de galáxias (*bulge-halo conspiracy*)
- Muy usado en el caso de galáxias de tipo temprano (elípticas)
- Quizás aplicabilidad más amplia (e.g. arXiv: 2406.0965)

Esfera Isotérmica Singular

$$\rho(r) = \frac{\sigma_v^2}{2\pi G r^2}$$

Densidad proyectada (superficial)

$$\Sigma(\xi) = \frac{\sigma_v^2}{2\pi G} 2 \int_0^\infty \frac{dz}{\xi^2 + z^2} = \frac{\sigma_v^2}{2G\xi}$$

Masa contenida en radio ξ

$$M(\xi) = \int_0^\xi \Sigma(\xi')\, 2\pi\xi'\, \mathrm{d}\xi' = \sigma_v^2 \frac{\pi}{G} \xi$$

Ángulo de deflexión

$$\Rightarrow \quad \hat{\vec{\alpha}} = \frac{4GM(\xi)}{c^2\xi}\hat{\xi} = 4\pi \left(\frac{\sigma_v}{c}\right)^2 \hat{\xi}$$

constante!

Lens Equation

Reduced deflexion angle

$$\vec{\alpha} = \hat{\vec{\alpha}} \frac{D_{LS}}{D_{OS}} \qquad\qquad \hat{\vec{\alpha}} = 4\pi \left(\frac{\sigma_v}{c} \right)^2 \hat{\xi}$$

$$\vec{\alpha} = \hat{\vec{\alpha}} \frac{D_{LS}}{D_{OS}} = \boxed{4\pi \left(\frac{\sigma_v}{c} \right)^2 \frac{D_{LS}}{D_{OS}}} \hat{\xi} = \theta_E \, \hat{\xi}$$

$$\vec{\beta} = \vec{\theta} - \theta_E \, \hat{\theta} = \left(1 - \frac{\theta_E}{\theta} \right) \vec{\theta}$$

$$\Rightarrow \quad \beta = \left| 1 - \frac{\theta_E}{\theta} \right| \theta$$

Solutions: 1) if $\quad 1 - \frac{\theta_E}{\theta} > 0$

then $\quad \beta = \left(1 - \frac{\theta_E}{\theta} \right) \theta = \theta - \theta_E \Rightarrow \boxed{\theta = \beta + \theta_E}$

Lens Equation

$$\beta = \left|1 - \frac{\theta_E}{\theta}\right| \theta$$

Solutions: I) if $\quad 1 - \frac{\theta_E}{\theta} > 0$

then $\quad \beta = \left(1 - \frac{\theta_E}{\theta}\right)\theta \; = \theta - \theta_E \Rightarrow \boxed{\theta = \beta + \theta_E}$

II) if $\quad 1 - \frac{\theta_E}{\theta} < 0$

then $\quad \beta = -\left(1 - \frac{\theta_E}{\theta}\right)\theta = \theta_E - \theta \Rightarrow \boxed{\theta = \theta_E - \beta}$

Fuente circular

Círculo en el plano de las fuentes: $\left|\vec{\beta} - \vec{\beta}_0\right| = R$

$$\beta = \beta_0 \cos\phi \pm \sqrt{R^2 - \beta_0^2 \mathrm{sen}^2\phi}$$

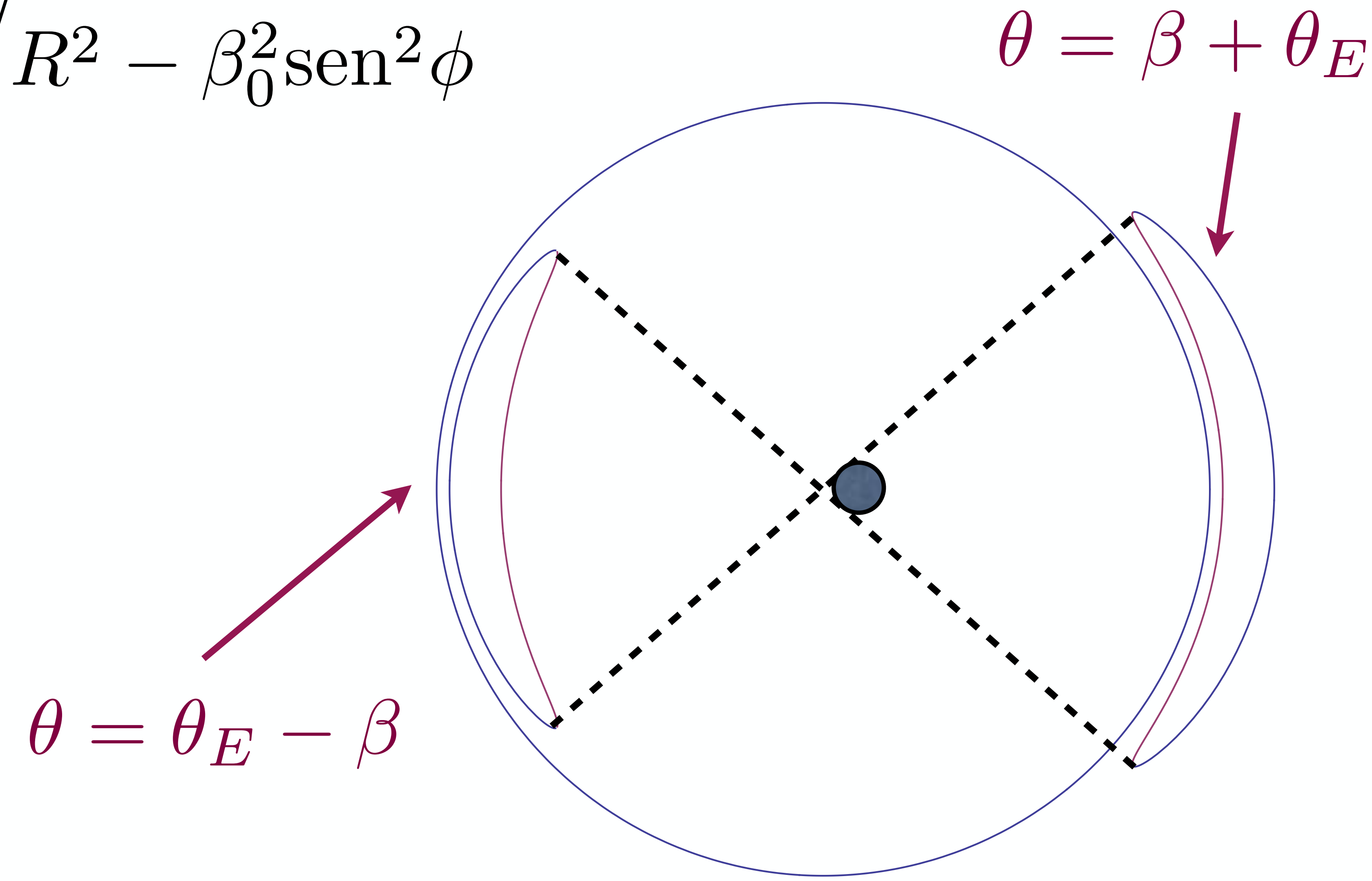

Caso general $\beta = \beta_0 \cos(\phi - \phi_0) \pm \sqrt{R^2 - \beta_0^2 \mathrm{sen}^2(\phi - \phi_0)}$

"Anillos de Chwolson-Einstein"

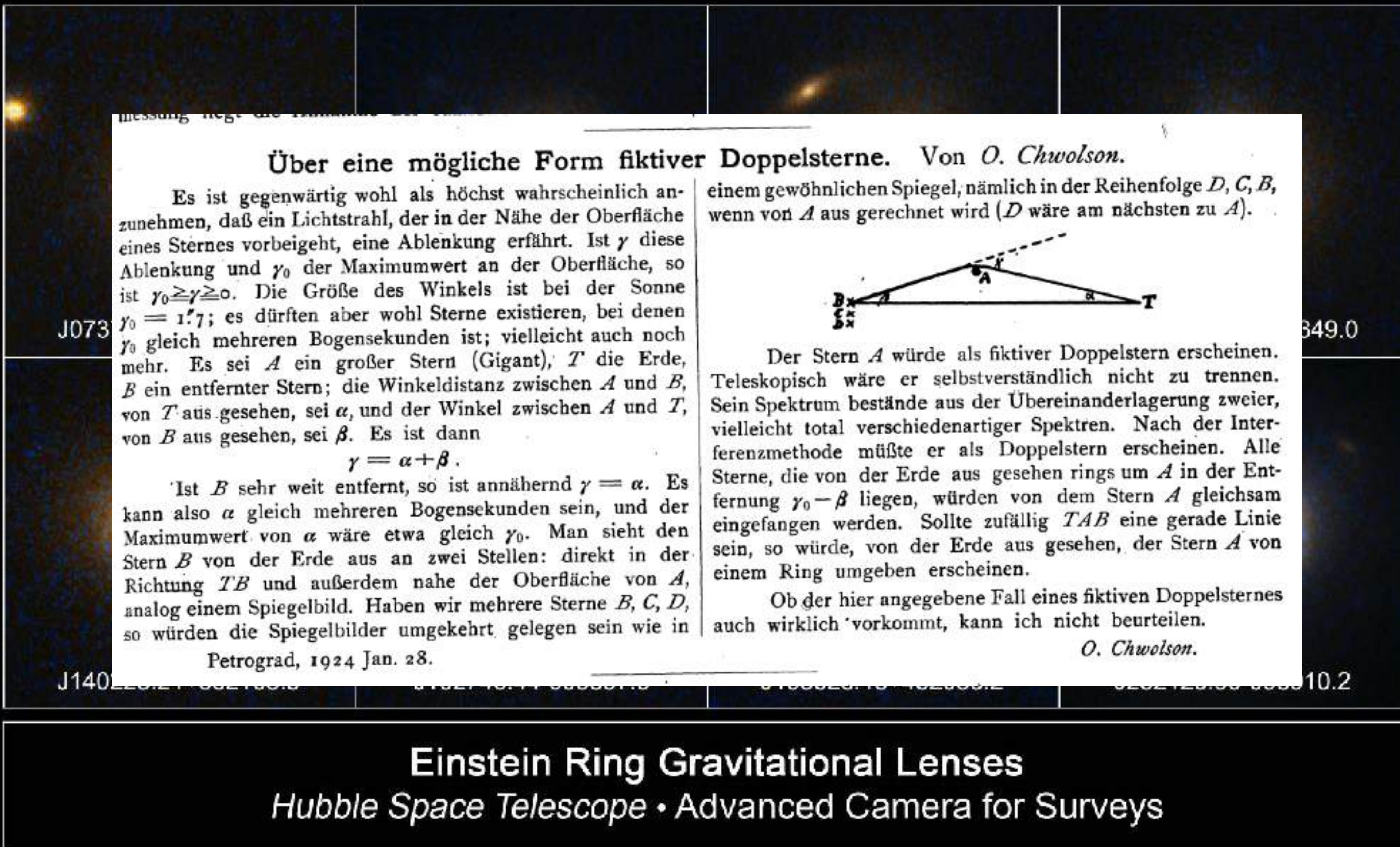

Über eine mögliche Form fiktiver Doppelsterne. Von *O. Chwolson.*

Es ist gegenwärtig wohl als höchst wahrscheinlich anzunehmen, daß ein Lichtstrahl, der in der Nähe der Oberfläche eines Sternes vorbeigeht, eine Ablenkung erfährt. Ist γ diese Ablenkung und γ_0 der Maximumwert an der Oberfläche, so ist $\gamma_0 \geqq \gamma \geqq 0$. Die Größe des Winkels ist bei der Sonne $\gamma_0 = 1\overset{''}{.}7$; es dürften aber wohl Sterne existieren, bei denen γ_0 gleich mehreren Bogensekunden ist; vielleicht auch noch mehr. Es sei A ein großer Stern (Gigant), T die Erde, B ein entfernter Stern; die Winkeldistanz zwischen A und B, von T aus gesehen, sei α, und der Winkel zwischen A und T, von B aus gesehen, sei β. Es ist dann

$$\gamma = \alpha + \beta .$$

Ist B sehr weit entfernt, so ist annähernd $\gamma = \alpha$. Es kann also α gleich mehreren Bogensekunden sein, und der Maximumwert von α wäre etwa gleich γ_0. Man sieht den Stern B von der Erde aus an zwei Stellen: direkt in der Richtung TB und außerdem nahe der Oberfläche von A, analog einem Spiegelbild. Haben wir mehrere Sterne B, C, D, so würden die Spiegelbilder umgekehrt gelegen sein wie in einem gewöhnlichen Spiegel, nämlich in der Reihenfolge D, C, B, wenn von A aus gerechnet wird (D wäre am nächsten zu A).

Der Stern A würde als fiktiver Doppelstern erscheinen. Teleskopisch wäre er selbstverständlich nicht zu trennen. Sein Spektrum bestände aus der Übereinanderlagerung zweier, vielleicht total verschiedenartiger Spektren. Nach der Interferenzmethode müßte er als Doppelstern erscheinen. Alle Sterne, die von der Erde aus gesehen rings um A in der Entfernung $\gamma_0 - \beta$ liegen, würden von dem Stern A gleichsam eingefangen werden. Sollte zufällig TAB eine gerade Linie sein, so würde, von der Erde aus gesehen, der Stern A von einem Ring umgeben erscheinen.

Ob der hier angegebene Fall eines fiktiven Doppelsternes auch wirklich vorkommt, kann ich nicht beurteilen.

Petrograd, 1924 Jan. 28.

O. Chwolson.

NASA, ESA, A. Bolton (Harvard-Smithsonian CfA), and the SLACS Team

STScI-PRC05-32

“Anillos de Chwolson-Einstein”

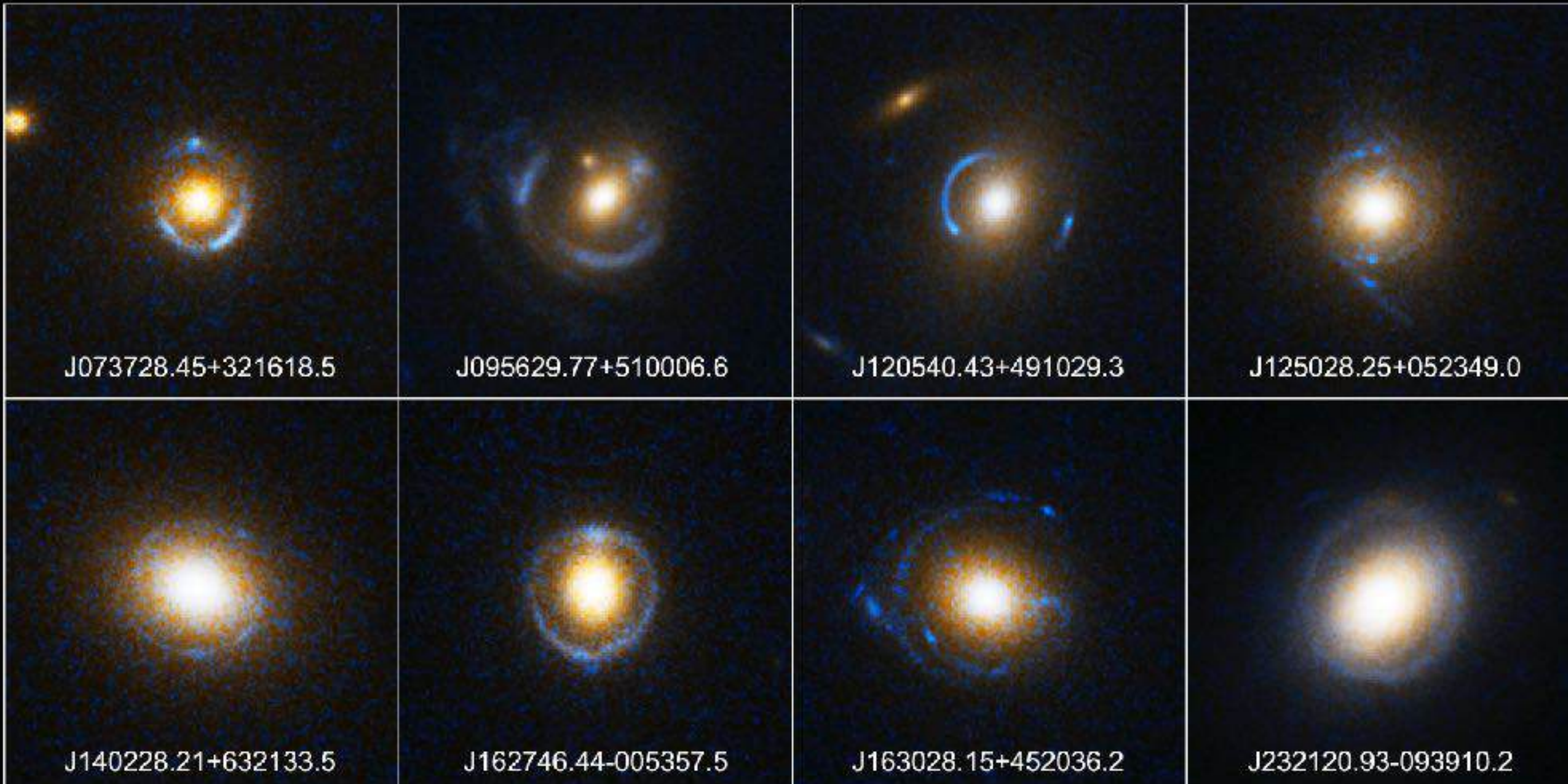

Einstein Ring Gravitational Lenses

Hubble Space Telescope • Advanced Camera for Surveys

NASA, ESA, A. Bolton (Harvard-Smithsonian CfA), and the SLACS Team STScI-PRC05-32

A Relativistic Eclipse

What Might be Seen from a Planet Conveniently Placed Near the Companion of Sirius . . . Perfect Tests of General Relativity that are Unavailable

By HENRY NORRIS RUSSELL, Ph. D.
Chairman of the Department of Astronomy and Director of the Observatory at Princeton University; Research Associate of the Mount Wilson Observatory of the Carnegie Institution of Washington; President of the American Astronomical Society

It is a familiar aphorism that the theory of relativity, despite its enormous importance, both in physics and philosophy, may be forgotten in ordinary practical life. There is a good reason. In almost every known case its results agree so closely with those of the older "classical" theories that very accurate observations are required to distinguish between them. Thus, for example, the famous Michelson-Morley experiment requires long series of the

No one predicted gravitational arcs?

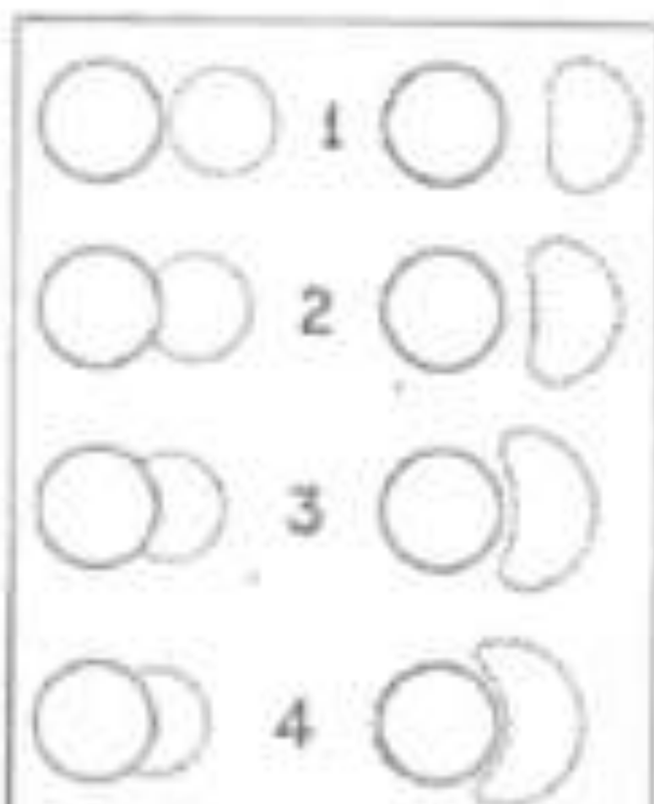

My hearty thanks are due to Professor Einstein, who permitted me to see the manuscript of his note before its publication.—*Princeton University Observatory, December 2, 1936.*


Lentes com
Simetria Axial

Teorema de Gauss

Equación de Poisson $\nabla^2_{\xi}\psi\left(\vec{\xi}\right) = 4\pi G\Sigma\left(\vec{\xi}\right)$

Ángulo de deflexión $\hat{\vec{\alpha}} = \frac{2}{c^2}\vec{\nabla}_{\xi}\psi\left(\vec{\xi}\right)$

Así: $\vec{\nabla}\cdot\hat{\vec{\alpha}} = \frac{8\pi G}{c^2}\Sigma\left(\vec{\xi}\right)$

Teorema de Gauss 2D

$$\int_{S_\xi}\vec{\nabla}\cdot\hat{\vec{\alpha}}\,dS = \oint_{C_\xi}\left(\hat{\vec{\alpha}}\cdot\hat{n}\right)dl$$

Como en la lente puntual!
Radio de Einstein, etc.

$$\Downarrow$$

$$\frac{8\pi G}{c^2}\underbrace{\int_{S_\xi}\Sigma\left(\xi\right)dS}_{M(\xi)} = \int_0^{2\pi}\hat{\alpha}\,\xi\,d\phi \quad\Rightarrow\quad \hat{\vec{\alpha}} = \frac{4GM(\xi)}{c^2\xi}\hat{\xi}$$

Lens equation with axial symmetry

Deflection angle $$\hat{\vec{\alpha}} = \frac{4GM(\xi)}{c^2 \xi} \hat{\xi}$$

Lens equation $$\vec{\beta} = \vec{\theta} - \hat{\vec{\alpha}} \frac{D_{LS}}{D_{OS}} = \vec{\theta} - \frac{4GM(\theta)}{c^2 \theta^2 D_{OL}} \vec{\theta} \frac{D_{LS}}{D_{OS}}$$

$$\vec{\beta} = \left(1 - \frac{4GM(\theta) D_{LS}}{c^2 D_{OL} D_{OS}} \frac{1}{\theta^2}\right) \vec{\theta}$$

Einstein angle $\left(\vec{\beta} = 0\right)$

$$\theta_E = \sqrt{\frac{D_{LS}}{D_{OS} D_{OL}} \frac{4GM\left(\theta_E\right)}{c^2}}$$

Mass estimate at $\theta < \theta_E$

Ecuación de la Lente

Ecuación de la Lente $\vec{\beta} = \left(1 - \frac{4GM(\theta)D_{LS}}{c^2 D_{OL} D_{OS}} \frac{1}{\theta^2}\right)\vec{\theta}$

Densidad superficial crítica $\Sigma_{\rm crit} = \frac{c^2}{4\pi G} \frac{D_{\rm OS}}{D_{\rm OL} D_{\rm LS}}$

Ecuación de la Lente $\vec{\beta} = \left(1 - \frac{M(\theta)}{\pi \Sigma_{\rm crit} \left(D_{OL}\theta\right)^2}\right)\vec{\theta}$

$$\frac{\text{Massa contida em}\,\theta}{\text{Massa se}\,\Sigma = \Sigma_{\rm crit}}$$

Anillo de Einstein e imágenes múltiplas si

$\Sigma(\theta = 0) > \Sigma_{\rm crit}$ (si densidad monótonamente decreciente)

Magnificación

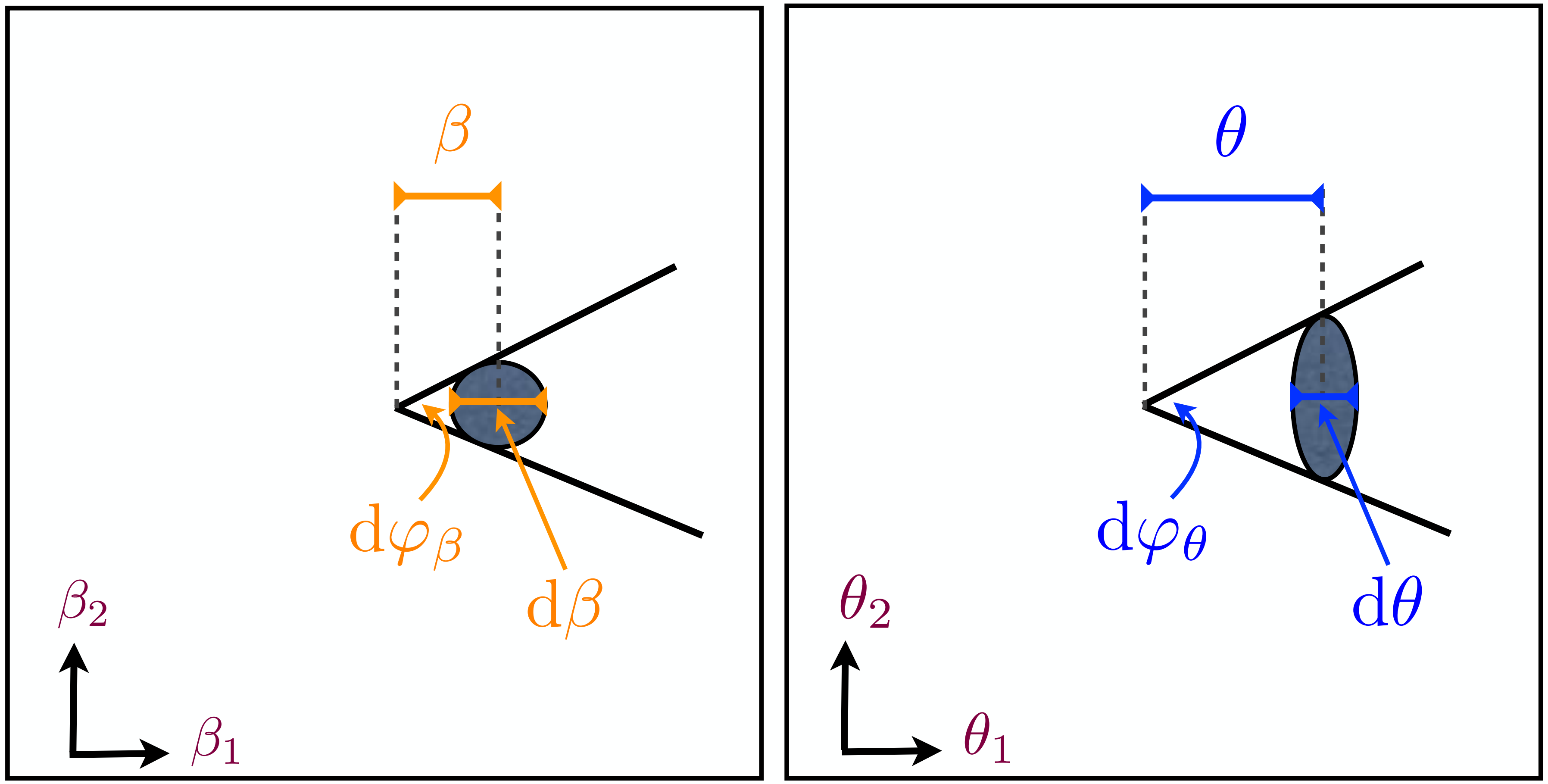

Plano de las fuentes | Lente/imágenes

Longitud radial	$\mathrm{d}\beta$	$\mathrm{d}\theta$	Magnificación radial	$\dfrac{\mathrm{d}\theta}{\mathrm{d}\beta}$
Longitud tangencial	$\beta\,\mathrm{d}\varphi_\beta$	$\theta\,\mathrm{d}\varphi_\theta$	Magnificación tangencial	$\underbrace{\dfrac{\mathrm{d}\varphi_\theta}{\mathrm{d}\varphi_\beta}}_{=1}\dfrac{\theta}{\beta}$

Magnificación

Ecuación de la Lente $\vec{\beta} = \left(1 - \frac{4GM(\theta)D_{LS}}{c^2 D_{OL} D_{OS}} \frac{1}{\theta^2}\right) \vec{\theta}$

$$\beta = \theta - \frac{M(\theta)}{\pi \Sigma_{\rm crit} D_{OL}^2 \theta}$$

Magnificación tangencial

$$\frac{\theta}{\beta} = \left(\frac{\beta}{\theta}\right)^{-1} = \left(1 - \frac{M(\theta)}{\pi \Sigma_{\rm crit} D_{OL}^2 \theta^2}\right)^{-1}$$

Magnificación radial

$$\frac{\mathrm{d}\theta}{\mathrm{d}\beta} = \left(\frac{\mathrm{d}\beta}{\mathrm{d}\theta}\right)^{-1} = \left[1 - \frac{1}{\pi \Sigma_{\rm crit} D_{OL}^2} \frac{\mathrm{d}}{\mathrm{d}\theta} \left(\frac{M(\theta)}{\theta}\right)\right]^{-1}$$

Ejercicio: $\gamma_{1,2}$ e κ, variables adimensionales

Esfera isoterma singular

$$M = \sigma_v^2 \frac{\pi}{G} \xi = \sigma_v^2 \frac{\pi}{G} D_{OL} \theta$$

Magnificación tangencial

$$\frac{\theta}{\beta} = \left(1 - \frac{M(\theta)}{\pi \Sigma_{\rm crit} D_{OL}^2 \theta^2}\right)^{-1} = \left(1 - \boxed{\overbrace{4\pi \left(\frac{\sigma_v}{c}\right)^2 \frac{D_{LS}}{D_{OS}}}^{\theta_E}} \frac{1}{\theta}\right)^{-1}$$

Magnificación radial

$$\frac{\mathrm{d}\theta}{\mathrm{d}\beta} = \left[1 - \frac{1}{\pi \Sigma_{\rm crit} D_{OL}^2} \frac{\mathrm{d}}{\mathrm{d}\theta} \left(\frac{M(\theta)}{\theta}\right)\right]^{-1} = 1$$

No hay cáustica/
curva crítica
radial

Modelos de Lentes

Dos caminos

Ecuación de la lente $\vec{\beta} = \vec{\theta} - \vec{\alpha}\left(\vec{\theta}\right) = \vec{\theta} - \vec{\nabla}_\theta \Psi\left(\vec{\theta}\right)$

Obtener $\vec{\alpha}\left(\vec{\theta}\right)$ o $\Psi\left(\vec{\theta}\right)$

Solución de la ecuación de la lente y jacobiana

$$\hat{\vec{\alpha}} = \frac{4G}{c^2}\int d^2\xi' \Sigma\left(\vec{\xi'}\right)\frac{\vec{\xi}-\vec{\xi'}}{|\vec{\xi}-\vec{\xi'}|^2}.$$

$$\psi\left(\vec{\xi}\right) = 2G\int d^2\xi' \Sigma\left(\vec{\xi'}\right)\ln|\xi - \xi'|$$

Camino I: Elegir $\Sigma\left(\vec{\xi}\right)$ o $\rho\left(\vec{r}\right)$

Camino II: Modelo para $\Psi\left(\vec{\theta}\right)$

Modelos de potencial

Esfera isotermica singular $\Psi = \theta_E \left| \vec{\theta} \right|$

Esfera isotermica con core $\Psi = \theta_0 \sqrt{\theta^2 + \theta_c^2}$

Convergencia $\kappa = \theta_0 \frac{\theta^2 + 2\theta_c^2}{2\left(\theta^2 + \theta_c^2\right)^{3/2}}$

Perfil de densidad

Esfera isotermica suavizada
$$\rho(r) = \frac{\sigma^2}{2\pi G(r^2 + r_c^2)}$$

Densidad proyectada
$$\Sigma(\theta) = \frac{\sigma^2}{2GD_{OL}} \frac{1}{\sqrt{\theta^2 + \theta_c^2}}$$

Potencial de lente

$$\Psi(\vec{\theta}) = \theta_0 \left[\sqrt{\theta^2 + \theta_c^2} - \theta_c \ln \left(\sqrt{\theta^2 + \theta_c^2} + \theta_c \right) \right]$$

Modelo axial no singular

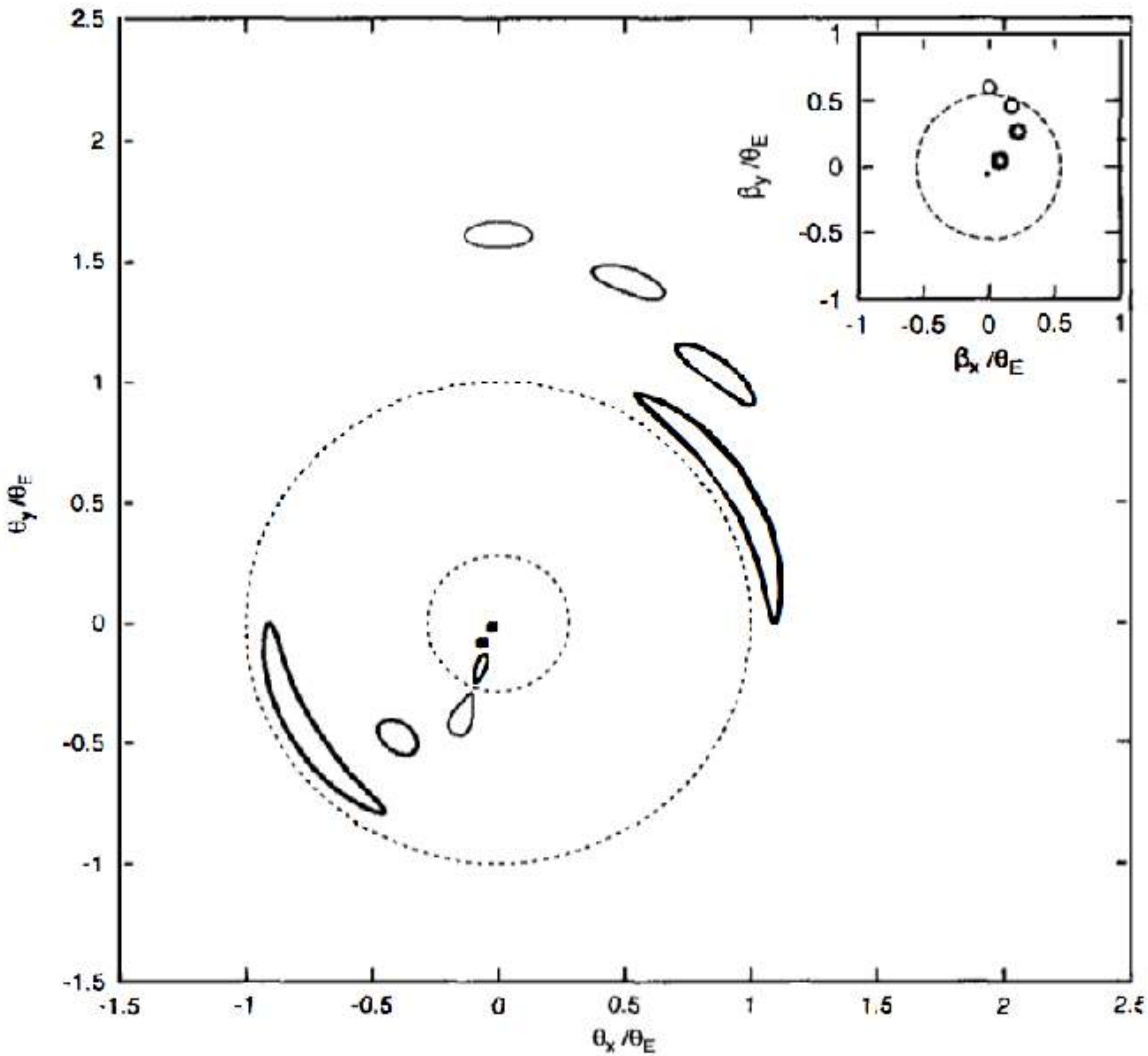

Modelo Navarro-Frenk-White

Simulaciones computacionales de *N-cuerpos* en un contexto cosmológico

Densidad media radial: $$\rho(r) = \frac{\rho_s}{(r/r_s)(1 + r/r_s)^2}$$

Universalidad de los perfiles de materia oscura!

El perfil de Navarro-Frenk-White

https://wwwmpa.mpa-garching.mpg.de/~swhite/pictures/NFW_profile1.jpg


LOS SIMULADORES

Perfiles (radiales) de densidad

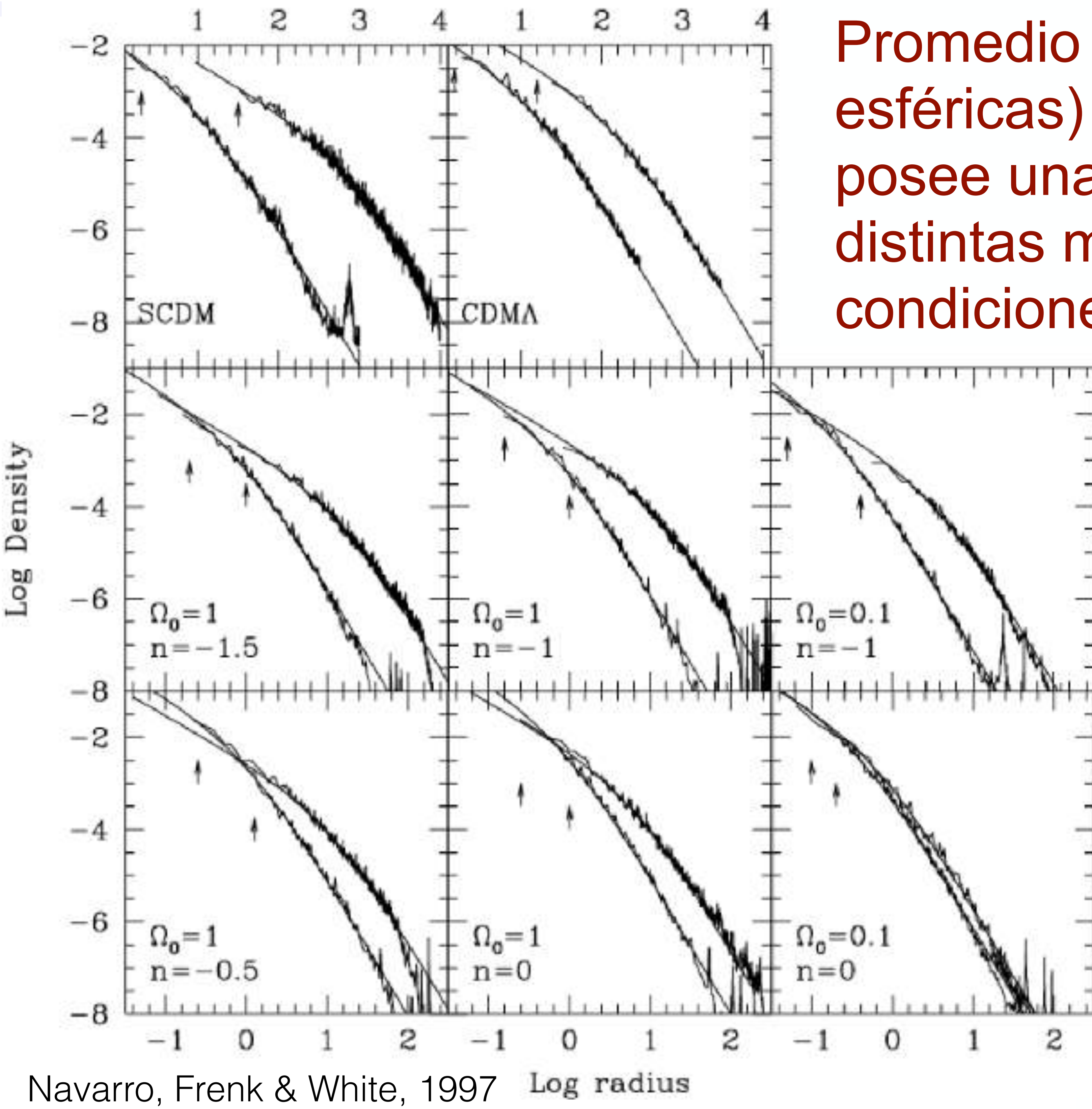

Navarro, Frenk & White, 1997

Promedio angular (cáscaras esféricas) de la densidad en halos posee una forma universal para distintas masas, cosmologias y condiciones iniciales

$$\rho(r) = \frac{\rho_0}{(r/r_s)\,(1 + r/r_s)^2}$$

Se puede expresar en términos de la masa M_Δ y de la concentración

$$c = r_\Delta / r_s$$

Valores de los parámetros dependem de la massa y de la história de formación de los halos

Modelo Navarro-Frenk-White

Densidad promedio radial: $$\rho(r) = \frac{\rho_s}{(r/r_s)(1+r/r_s)^2}$$

Convergencia:

$$\kappa(x) = 2\kappa_s \frac{1-F(x)}{x^2-1}, \qquad x = \frac{\xi}{r_s} \quad \text{e} \quad k_s = \frac{\rho_s r_s}{\Sigma_{cr}}$$

$$F(x) = \begin{cases} \frac{\mathrm{ArcTan}\left(\sqrt{x^2-1}\right)}{\sqrt{x^2-1}} & , \quad x > 1 \\ 1 & , \quad x = 1 \\ \frac{\mathrm{ArcTanh}\left(\sqrt{1-x^2}\right)}{\sqrt{1-x^2}} & , \quad x < 1 \end{cases} ,$$

Potencial de lente:

$$\Psi(x) = 2\kappa_s r_s^2 \left[\ln^2 \frac{x}{2} - \mathrm{ArcTanh}^2 \sqrt{1-x^2}\right]$$

Potencial mais suave que el de la Esfera Isotermica:
curvas críticas menores, mayor amplificación, menor separación angular

Other lens models

Implemented in *gravlens* and several public codes (+ Sérsic, Einasto, etc.)

Model	N_r	Density $\rho(r)$	Surface Density $\kappa(r)$
Point mass	0	$\delta(\mathbf{x})$	$\delta(\mathbf{x})$
Power law or α-models	2	$\left(s^2+r^2\right)^{(\alpha-3)/2}$	$\left(s^2+r^2\right)^{(\alpha-2)/2}$
Isothermal ($\alpha=1$)	1	$\left(s^2+r^2\right)^{-1}$	$\left(s^2+r^2\right)^{-1/2}$
$\alpha=-1$	1	$\left(s^2+r^2\right)^{-2}$	$\left(s^2+r^2\right)^{-3/2}$
Pseudo-Jaffe	2	$\left(s^2+r^2\right)^{-1}\left(a^2+r^2\right)^{-1}$	$\left(s^2+r^2\right)^{-1/2}-\left(a^2+r^2\right)^{-1/2}$
King (approximate)	1	$\cdots$	$2.12\left(0.75r_s^2+r^2\right)^{-1/2}$ $-1.75\left(2.99r_s^2+r^2\right)^{-1/2}$
de Vaucouleurs	1	$\cdots$	$\exp\left[-7.67(r/R_e)^{1/4}\right]$
Hernquist	1	$r^{-1}\left(r_s+r\right)^{-3}$	see eq. (47)
NFW	1	$r^{-1}\left(r_s+r\right)^{-2}$	see eq. (53)
Cuspy NFW	2	$r^{-\gamma}\left(r_s+r\right)^{\gamma-3}$	see eq. (57)
Cusp	3	$r^{-\gamma}\left(r_s^2+r^2\right)^{(\gamma-n)/2}$	see eq. (64)
Nuker	4	$\cdots$	see eq. (71)
Exponential disk	1	$\cdots$	$\exp[-r/R_d]$
Kuzmin disk	1	$\cdots$	$\left(r_s^2+r^2\right)^{-3/2}$

Modelos Elípticos y Pseudo-Elípticos

Modelos elípticos

Sustituir $\theta \to \sqrt{q_1\theta_1^2 + q_2\theta_2^2}$

- en el potencial (modelos pseudo-elípticos)
- en la densidad proyectada (modelos elípticos)

Ejemplo: Esfera isotérmica com *core* pseudo-elíptico

$$\Psi(\theta_1, \theta_2) = \frac{\Psi_0}{\theta_c}\sqrt{(1-\epsilon)\theta_1^2 + (1+\epsilon)\theta_2^2 + \theta_c^2}$$

Elipticidad en la densidad proyectada

Ejemplo: Esfera isoterma elíptica con *core*

$$\Sigma(\theta_1, \theta_2) = \frac{\Sigma_0 \theta_c}{\sqrt{(1-\epsilon)\theta_1^2 + (1+\epsilon)\theta_2^2 + \theta_c^2}}$$

Solución para modelos elípticos

$$
\begin{aligned}
\phi(x,y) &= \frac{q}{2}\, I(x,y) \\
\phi_{,x}(x,y) &= q\, x\, J_0(x,y) \\
\phi_{,y}(x,y) &= q\, y\, J_1(x,y) \\
\phi_{,xx}(x,y) &= 2\, q\, x^2\, K_0(x,y) + q\, J_0(x,y) \\
\phi_{,yy}(x,y) &= 2\, q\, y^2\, K_2(x,y) + q\, J_1(x,y) \\
\phi_{,xy}(x,y) &= 2\, q\, x\, y\, K_1(x,y)
\end{aligned}
$$

$$
\begin{aligned}
I(x,y) &= \int_0^1 \frac{\xi}{u} \frac{\phi_{,r}\left(\xi(u)\right)}{\left[1-(1-q^2)u\right]^{1/2}}\, du \\
J_n(x,y) &= \int_0^1 \frac{\kappa\left(\xi(u)^2\right)}{\left[1-(1-q^2)u\right]^{n+1/2}}\, du \\
K_n(x,y) &= \int_0^1 \frac{u\, \kappa'\left(\xi(u)^2\right)}{\left[1-(1-q^2)u\right]^{n+1/2}}\, du \\
\xi(u)^2 &= u\left(x^2 + \frac{y^2}{1-(1-q^2)u}\right)
\end{aligned}
$$

Campos externos

Expansión hasta segundo ordem del potencial

$$\Psi(\theta_1, \theta_2) = \frac{\kappa}{2}\left(\theta_1^2 + \theta_2^2\right) + \frac{\gamma_1}{2}\left(\theta_1^2 - \theta_2^2\right) + \gamma_2 \theta_1 \theta_2$$

Model for the source

Surface brightness distribution of the source

Example: Sérsic profile

$$\boxed{I(R) = I_0 \exp\left\{-b_n \left(\frac{R}{R_e}\right)^{1/n}\right\}}$$

Elliptical brightness distribution

source centered at (S_1, S_2)

$$\begin{aligned} R^2 = &(1-\varepsilon_S)[(\beta_1 - S_1)\cos\phi_e + (\beta_2 - S_2)\sin\phi_e]^2 \\ &+(1+\varepsilon_S)[(\beta_2 - S_2)\cos\phi_e - (\beta_1 - S_1)\sin\phi_e]^2 \end{aligned}$$

Simulating Strong Lensing Images

Map the brightness distribution of the source to the lens plane

$$I(R) = I\left(\vec{\beta}\right) = I\left(\vec{\beta}\left(\vec{\theta}\right)\right)$$

Use the lens equation (no need to solve it!)

Add PSF and noise

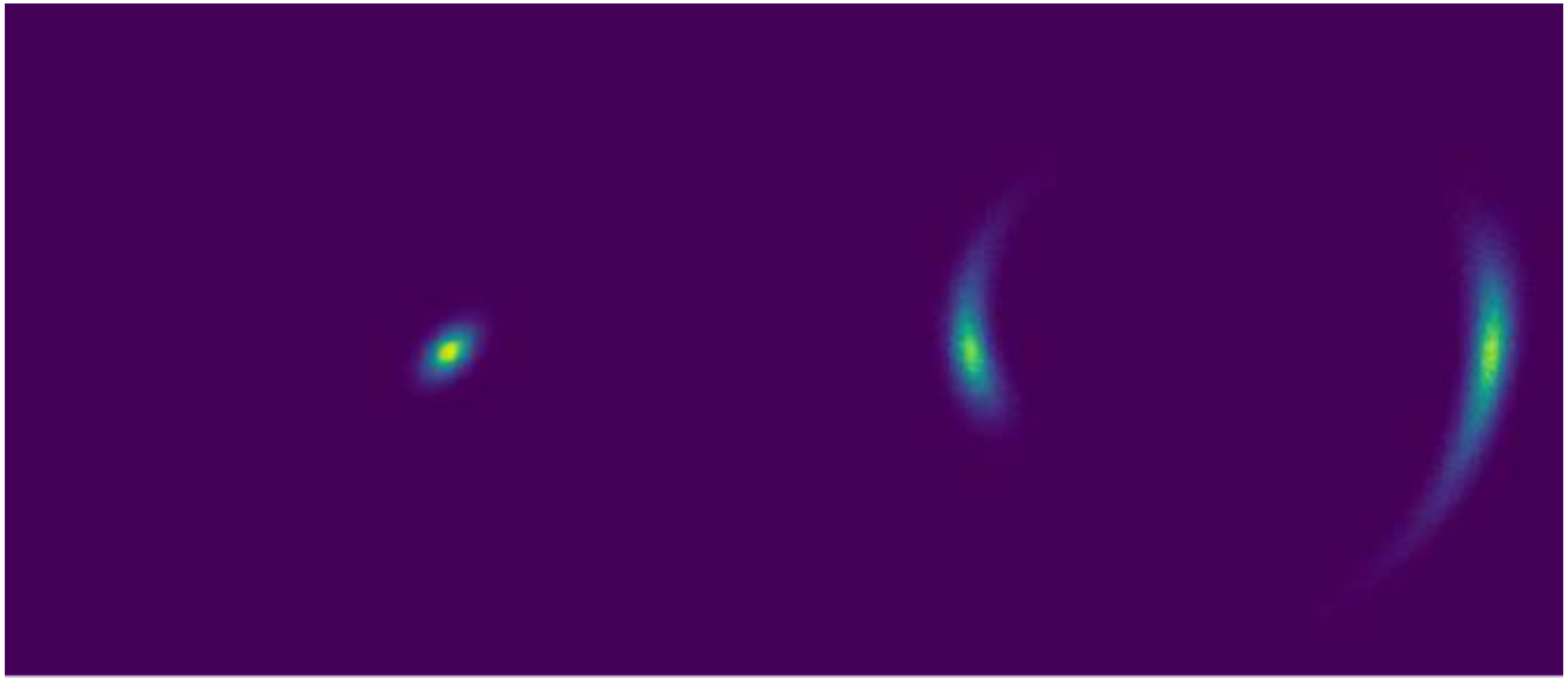

AddArcs v2.0

Actividad Práctica

Reconstrucción de la distribución de materia en la lente

Inverse Modeling

Use systems of multiple images to determine the lensing potential

$$\chi^2_{\mathrm{lente}} := \sum_i \left(\frac{\vec{\theta}_i^{\mathrm{obs}} - \vec{\theta}^{\mathrm{mod}}\left(\vec{\beta}, \vec{\Pi}\right)}{\sigma_i^{\mathrm{obs}}} \right)^2$$

Position of the multiple images

Uncertainty on the image positions

Available codes: *lenstool*, *gravlens*, *glafic*, etc. + “home-made”

- Parameters that minimize this function (or maximize the likelihood) are the best fitting lens model
- Combination with independent mass constraints (e.g., x-ray, Sunyaev Zel’dovich, velocity dispersions) yields limits on cosmology or gravity

Inverse Modeling: Mapping the Mass

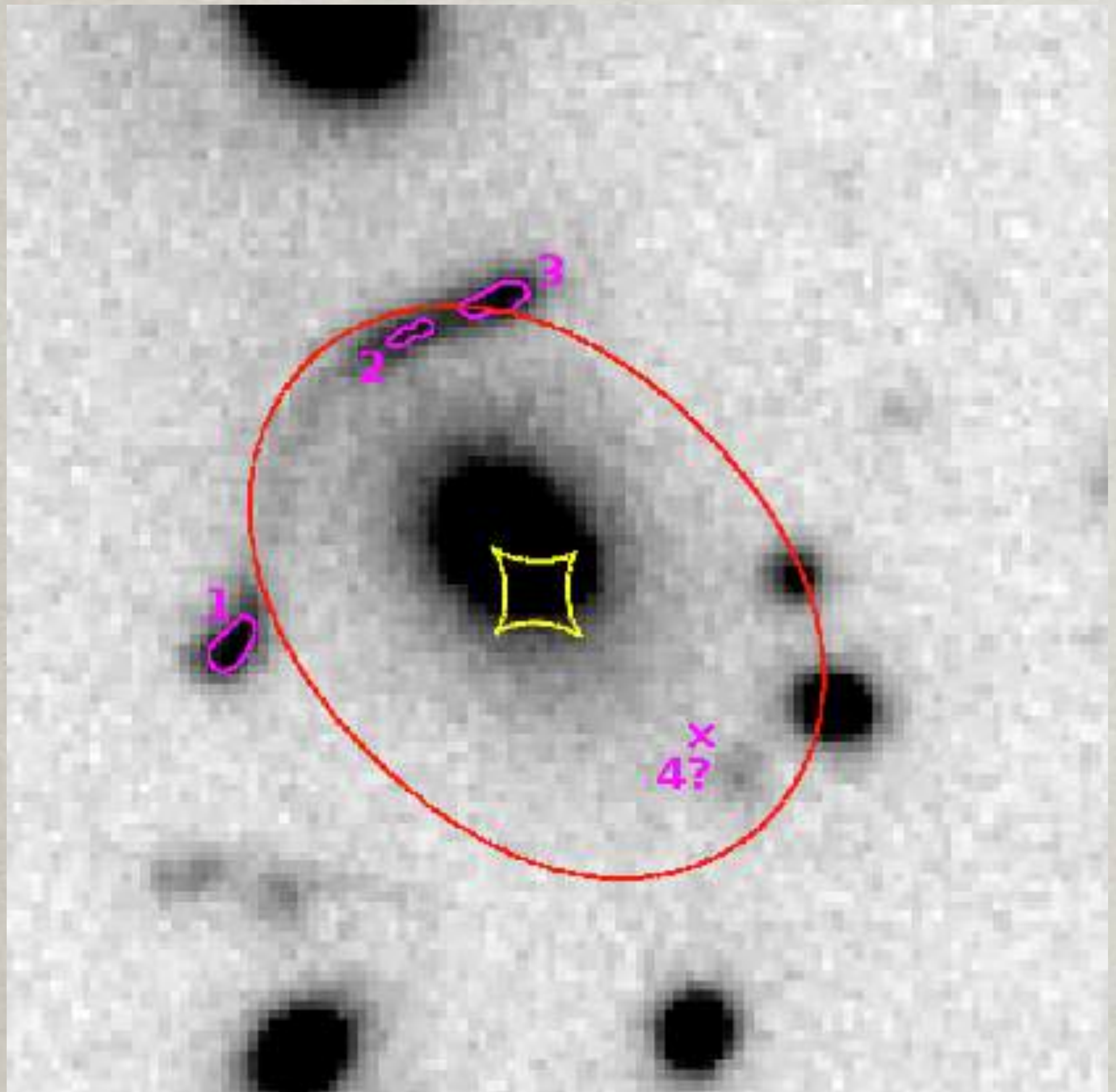

Use systems of multiple images to determine the lensing potential

$$\chi^2_{\mathrm{lente}} := \sum_i \left(\frac{\vec{\theta}_i^{\mathrm{obs}} - \vec{\theta}^{\mathrm{mod}}\left(\vec{\beta}, \vec{\Pi}\right)}{\sigma_i^{\mathrm{obs}}} \right)^2$$

Multiple image positions

Error on image positions

Methods: parametric (often "mass traces light"), free form

The more multiple images, the more constrains

Cluster x Galaxy scales

- Combination with independent mass constraints (e.g., x-ray, Sunyaev Zel'dovich, velocity dispersions) yields limits on cosmology or gravity

Inverse Modeling for system SOGRAS0041-0043

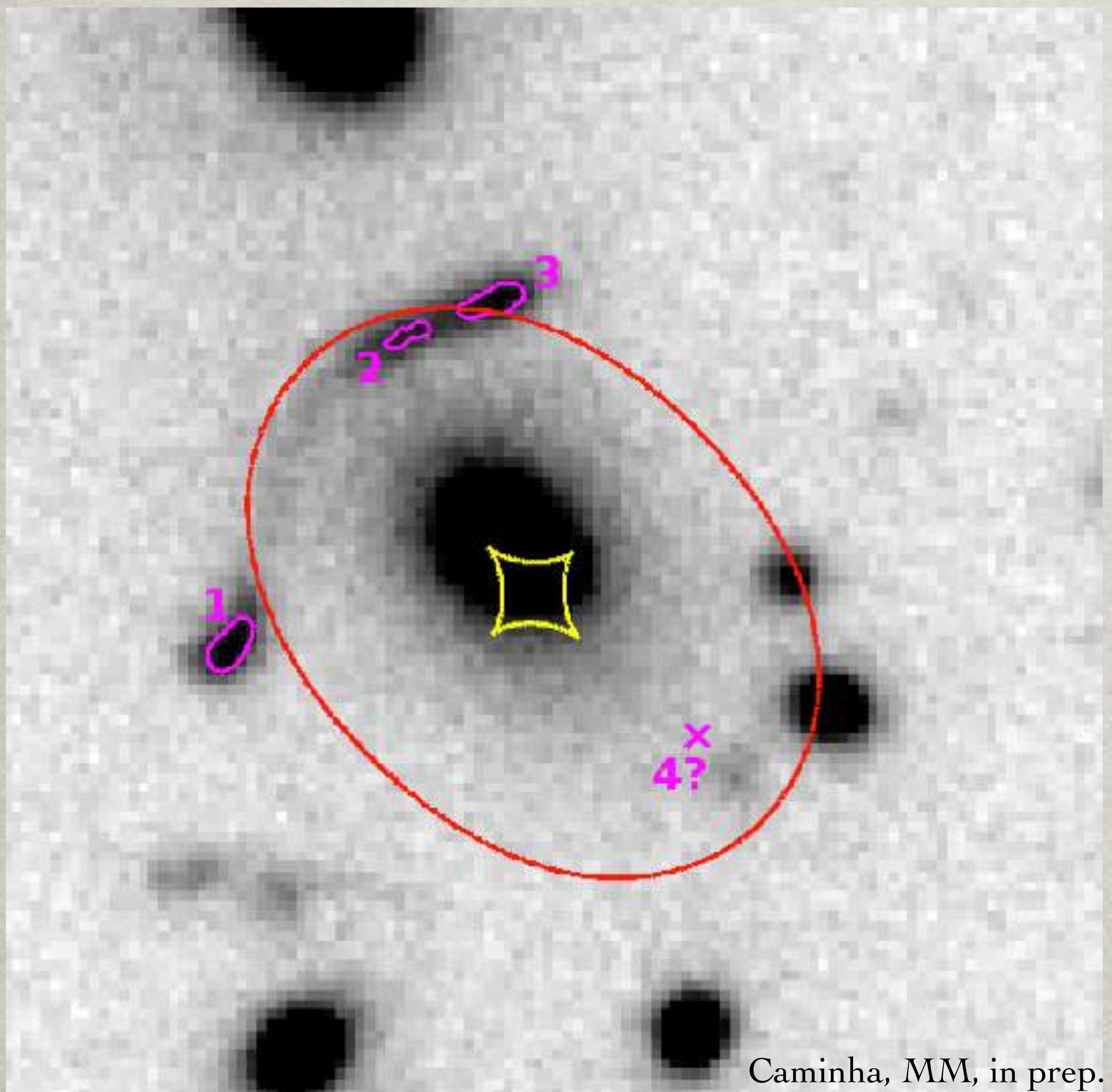

$$2.35^{+0.03}_{-0.14} \times 10^{14} M_{\odot}$$

Modelling with lenstool (Jullo, Kneib)

Fit 1: 3 images
Fit 2: 4 images

	Fit 1	Fit 2
$\sigma_v[km/s]$	622^{-11}_{-13}	642^{+3}_{-3}
$\theta_{or}[°]$	$135.2^{+0.7}_{-0.8}$	$135.2^{+1.5}_{-1.3}$
$x_{lente}['']$	$0.50^{+0.2}_{-0.2}$	$0.50^{+0.05}_{-0.06}$
$y_{lente}['']$	$-0.76^{+0.17}_{-0.15}$	$-0.86^{-0.06}_{-0.03}$
ε	—	$0.13^{+0.02}_{-0.03}$

~ 0.9" displacement between central galaxy and center of mass distribution (*Zitrin et al. 2012*)

Error estimate from simulations (Caminha et al. in prep.):

~ 8% bias in mass

~ 5% statistical errors

Modeling the full light distribution of the images

CS82SL01:36:39+00:08:18

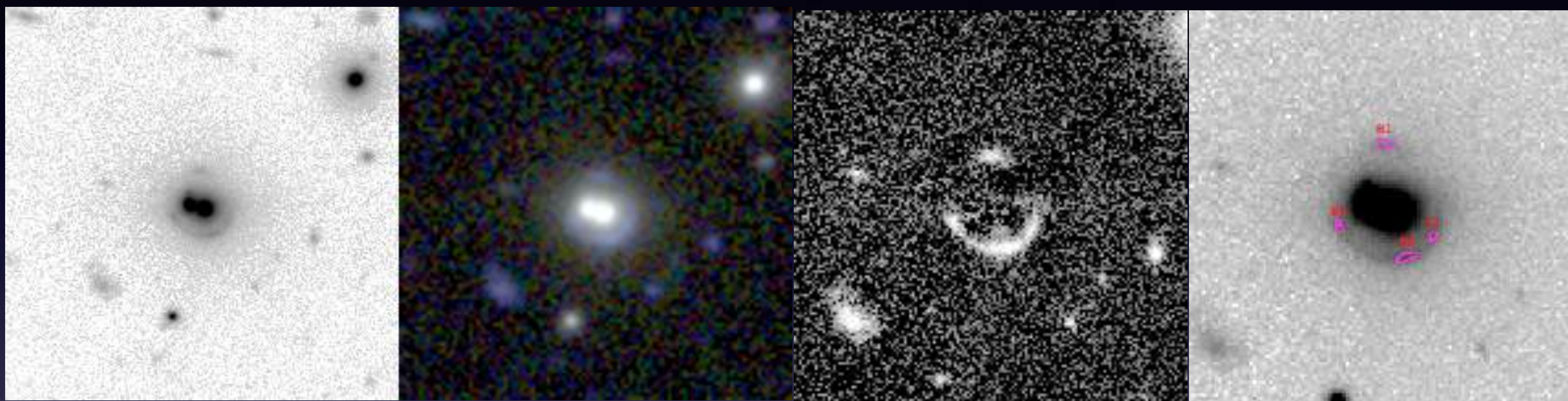

Anna Niemiec

- Instead of peak/multiple images, use the full information of the images
- Allows one to reconstruct source properties (often parametrically)
- Remove contamination from lens galaxy (with galfit) and mask other objects

Modeling the full light distribution of the images

CS82SL01:36:39+00:08:18

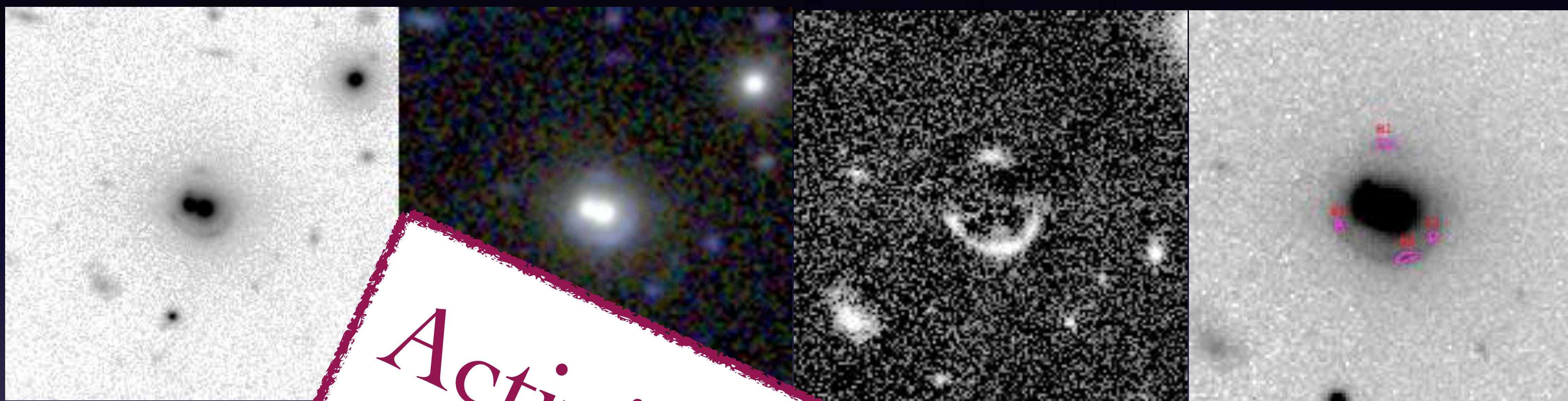

Anna Niemiec

Actividad Práctica

- Instead of pea… use the full information of the i…
- Allows one to reconstruct so… perties (often parametrically)
- Remove contamination from lens galaxy (with galfit) and mask other objects

Inverse modeling with extended sources

Example code: PyAutoLens

Parametric light distribution for lenses

$$I_{I'}(R,\theta) = \sum_{j=1}^{N} I_j \cdot \mathrm{Exp}\left(-\frac{R_i^2(x,y)}{2\sigma_i^2}\right)$$

$$R_i(x,y) = \sqrt{x'^2 + \left(\frac{y'}{q_i}\right)^2}$$

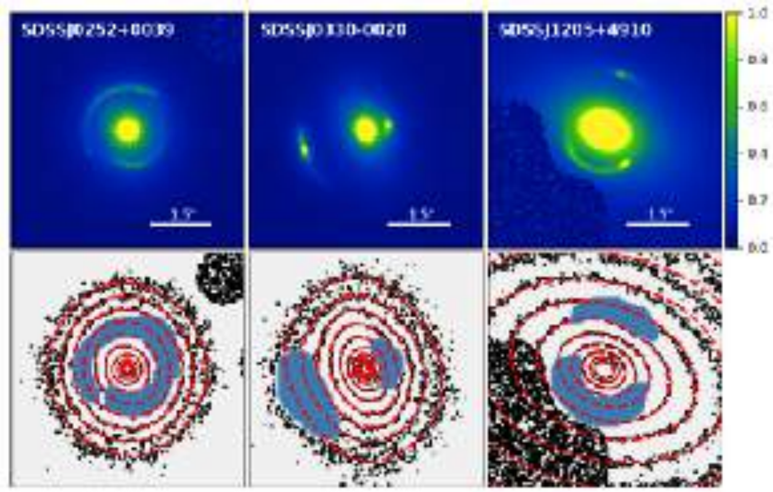

Elliptical Power-Law (EPL) projected mass density

$$k_\alpha(x,y) = \frac{\Sigma(\xi)}{\Sigma_{\mathrm{crit}}} = \frac{3-\alpha}{1+q}\left(\frac{b}{\xi}\right)^{\alpha-1}$$

External shear

$$\gamma_1 = \frac{1}{2}\left(\frac{\partial^2\psi}{\partial\theta_1^2} - \frac{\partial^2\psi}{\partial\theta_2^2}\right)$$

$$\gamma_2 = \frac{\partial^2\psi}{\partial\theta_1\partial\theta_2}$$

Total mass model is the sum of the two

MGE vs EPL on Lens light fitting on ground-based image modeling

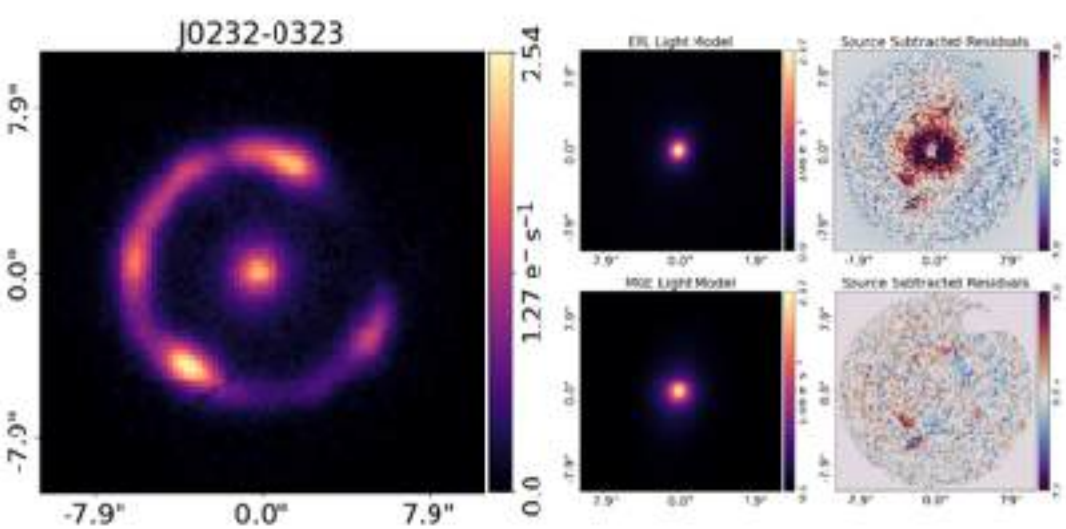

Voronoi adaptive pixelization for sources

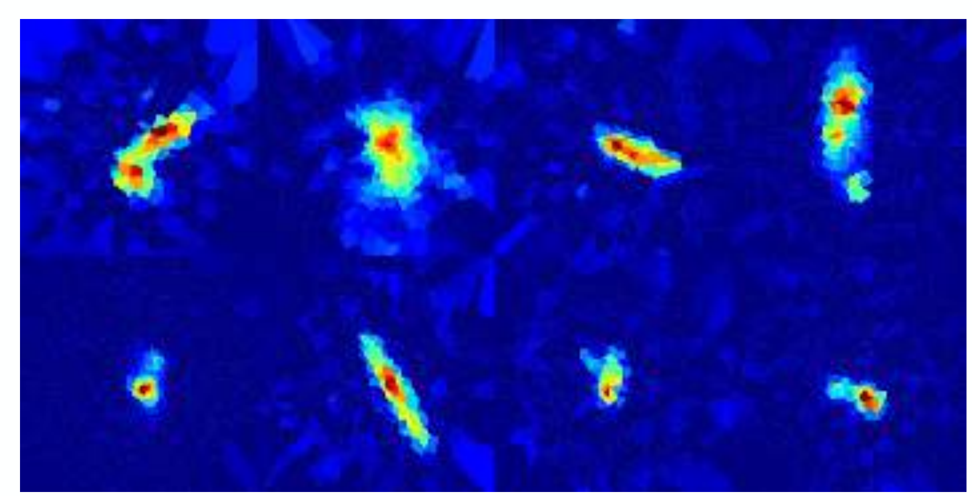

Galan+; *arxiv:***2012.02802**

Source Lens and Mass (SLaM) pipelines

with PyAutoLens

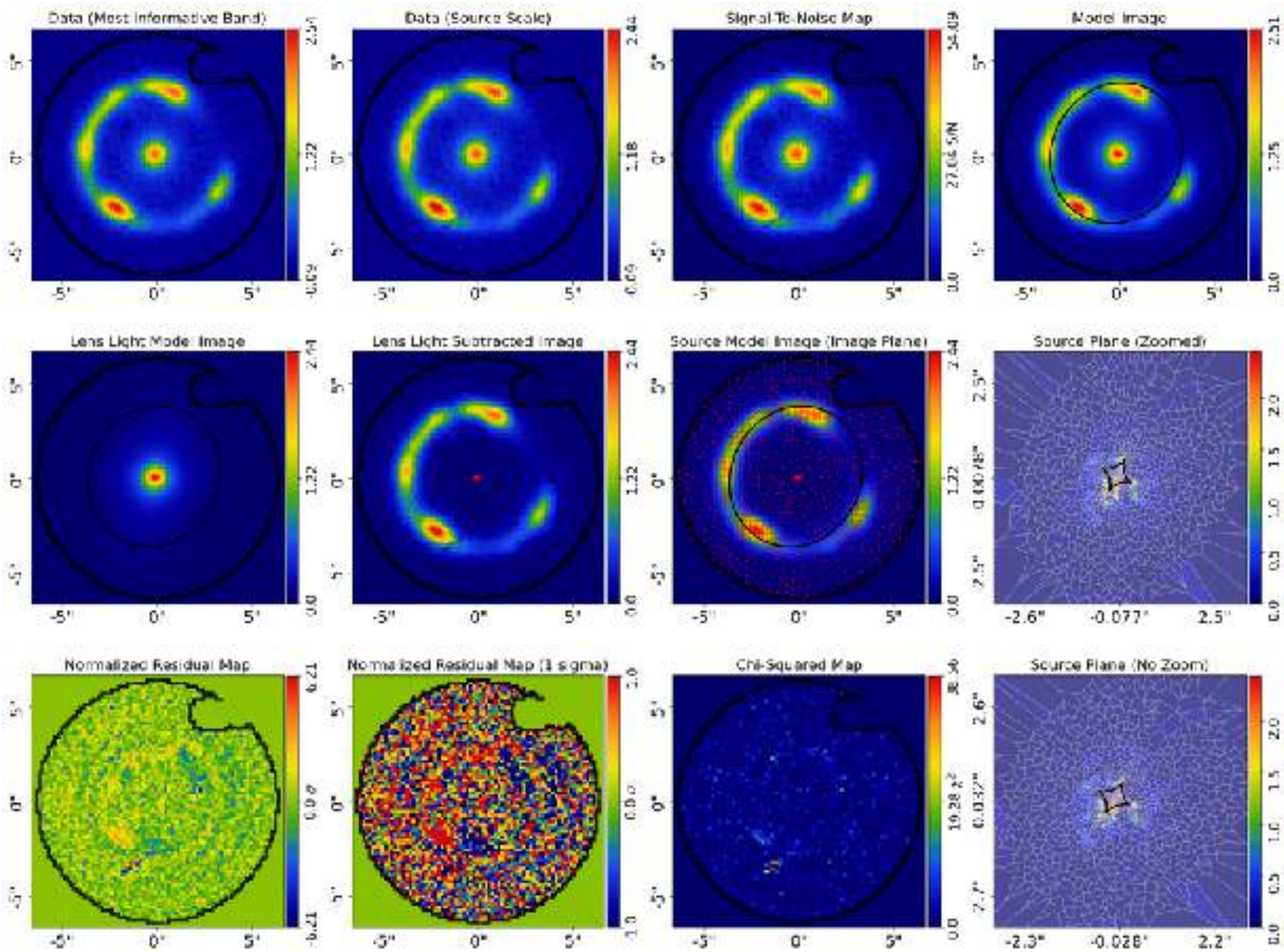

Session	Phase	Component	Model	Prior info
Source parametric	SP	Lens mass	SIE+Shear	-
		Lens light	MGE	-
		Source light	MGE	-
Source Inversion	SI1	Lens mass	SIE+Shear	SP
		Lens light	MGE	SP
		Source light	MPR	-
	SI2	Lens mass	SIE+Shear	SI1
		Lens light	MGE	SP
		Source light	BPR	-
Light Parametric	LP	Lens mass	SIE+Shear	SI1
		Lens light	MGE	SP
		Source light	BPR	SI2
Mass Total	MT	Lens mass	EPL+Shear	SI1
		Lens light	MGE	SP
		Source light	BPR	SI2

Other codes: lenstronomy, GLAMER, GIGA-Lens, caustics…

GIGA-Lens: a gradient-informed, GPU-accelerated Bayesian framework for modeling strong lensing systems, implemented in TensorFlow and JAX

Regimes and Challenges

- Galaxy cluster scale
  - Complex mass models, but many families of multiple images
  - HST Data: Frontier Fields, CLASH, RELICS, etc.
  - + Massive spectroscopic follow-up (IFU/MUSE)
  - Cosmology from single systems + high-z sources
  - Limited to very massive lenses and few systems
  - Promising for particle DM properties!
- Galaxy scale systems
  - Simple mass modes, but few constraints
  - Also HST imaging, but few IFU data (e.g. Gemini/NIFS)
  - Promising for Modified Gravity!
- Statistics
  - Spin-off from cosmological surveys:

    $\mathcal{O}(10^{1\text{-}2}) \rightarrow \mathcal{O}(10^{3\text{-}5})$
  - Need to find these systems!
    - Automated arc finders
  - Understand selection function.
    - Use simulations
  - Need to automate analyses!
- Challenge: Systematics
  - Use simulations ➔ end-to-end approach
  - Test modeling at the data level. Independent tests: predictions x SN!
  - Improve models from data: LSS/los, IFU, etc.

Cúmulos de galaxias

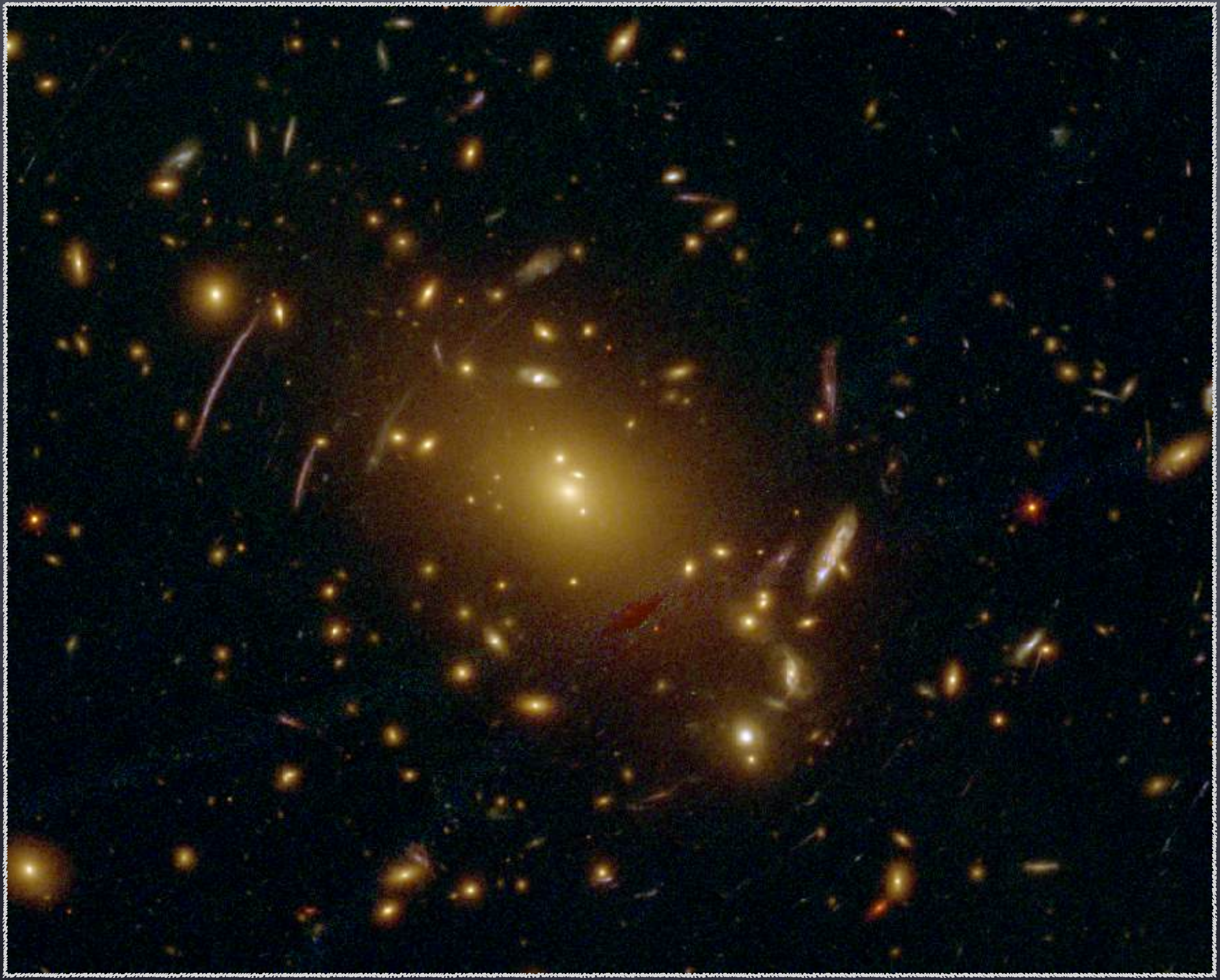

THE *HST* FRONTIER FIELDS

THE DEEPEST DATA EVER OBTAINED FOR LENSING GALAXY CLUSTERS !!!

Abell 2744 - z = 0.308
Fully observed

Atek et al. 2014a, ApJ, 786, 60 ; Laporte et al. 2014, A&A, 562, 8; Zitrin et al. 2014, ApJ, 793, 12; Ishigaki et al. 2015, ApJ, 799, 12; Atek et al. 2015, ApJ, 800, 18; Jauzac et al. 2015, MNRAS, 452, 437 ; Wang et al., ApJ, 811, 29

MACS J0416 - z = 0.396
Fully observed

Jauzac et al. 2014, MNRAS, 443, 1549; Lam et al. 2014, ApJ, 797, 98; Jauzac et al. 2015, MNRAS, 446 4132; Grillo et al. 2015, ApJ, 800, 38 ; Harvey et al. 2016, MNRAS, 458, 660 ; Caminha et al., 2016, arXiv1607.0346

MACS J1149 - z = 0.543
Fully observed
Kelly et al. 2015, *Science, 347, 1123* ; Sharon & Johnson 2015, *ApJ, 800, 26* ; Oguri 2015, *MNRAS, 449, 86* ; Diego et al. 2016, MNRAS, 459, 344 ; Jauzac et al. 2016, MNRAS, 457, 2029 ; Treu et al. 2016, ApJ, 817, 60 ; Grillo et al. 2016, ApJ, 822, 78

Abell S1063 - z = 0.348
Fully observed
Diego et al. 2016, MNRAS 459, 3447

MACS J0717 - z = 0.545
Fully observed
Diego et al. 2015, MNRAS, 451, 3920 ; Limousin et al. 2016, A&A, 588, 99; Kawamata et al. 2016, ApJ, 819, 14

Abell 370 - z = 0.375
ACS to go

¿Cómo se arma un modelo de cúmulos de galaxias?

- Modelos paramétricos: distribución de masa compuesta de
  - Uno o más halos de materia oscura para el cúmulo
  - Un halo para cada galáxia con relaciones empíricas de escaleo (exponente, radio de corte, etc.) $M = M_c(L/L_\star)^\gamma$
- Datos: posiciones de las imágenes múltiples (más parámetros: posiciones de las fuentes), o distribución de brillo superficial
- Hoy: datos de HST para los cúmulos más masivos, $\mathscr{O}(10)$ sistemas + JWST
- Futuro/actualidad: Euclid, Roman + ULTRASET, CSST, CASTOR
- Software: LensPerfect, LensTool, GLAFIC, Gravlens, Glee, HERCULENS…

Cúmulo de galaxias El Gordo (ACT-CL J0102-4915, SPT-CL J0102-4915) observado con el JWST

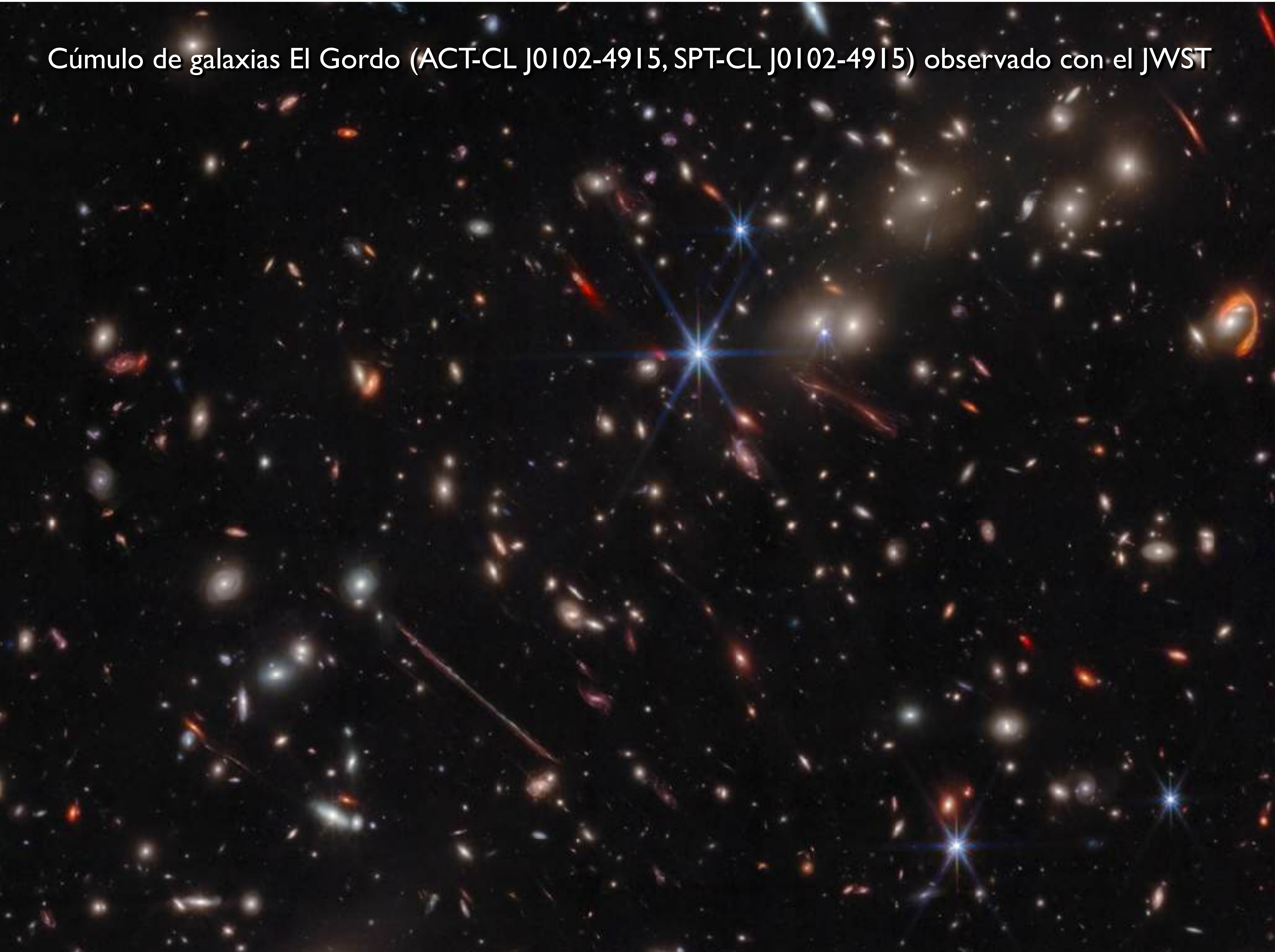

A&A, 689, A304 (2024)
https://doi.org/10.1051/0004-6361/202449876

Astronomy & Astrophysics

El Gordo needs El Anzuelo: Probing the structure of cluster members with multi-band extended arcs in JWST data

A. Galan[1,2,★], G. B. Caminha[1,2], J. Knollmüller[1,3,4], J. Roth[5,2,6], and S. H. Suyu[1,2]

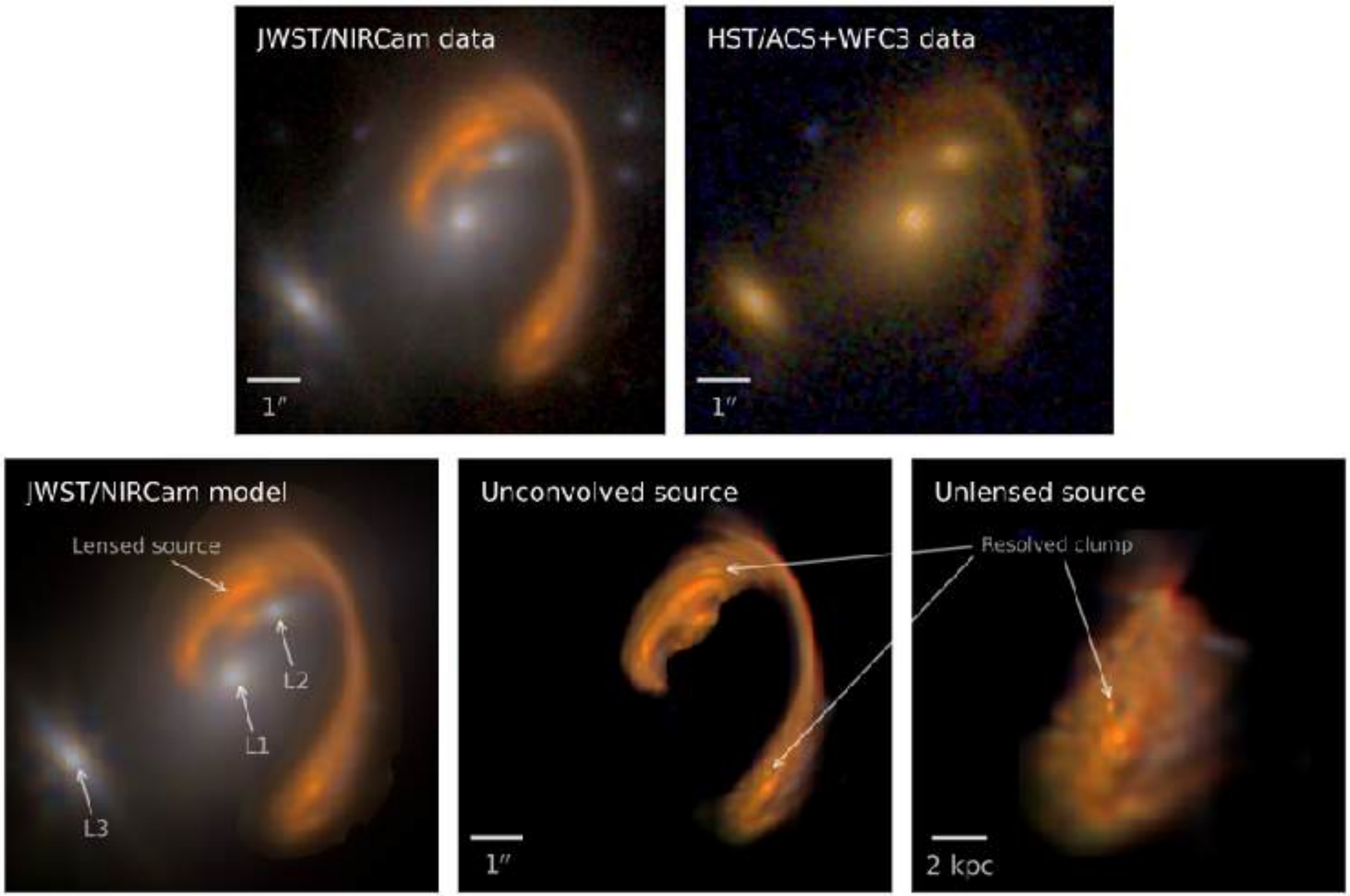

Reconstrucción de la fuente usando el modelo de lente

A massive compact quiescent galaxy at z = 2 with a complete Einstein ring in JWST imaging

Pieter van Dokkum[1], Gabriel Brammer[2,3], Bingjie Wang[4], Joel Leja[4,5], Charlie Conroy[6]

[1]*Department of Astronomy, Yale University, New Haven, CT 06511, USA*

[2]*Cosmic Dawn Center (DAWN), Denmark*

[3]*Niels Bohr Institute, University of Copenhagen, Jagtvej 128, DK-2200 Copenhagen N, Denmark*

[4]*Department of Astronomy & Astrophysics, The Pennsylvania State University, University Park, PA 16802, USA*

[5]*Institute for Computational & Data Sciences, The Pennsylvania State University, University Park, PA 16802, USA*

[6]*Harvard-Smithsonian Center for Astrophysics, 60 Garden Street, Cambridge, MA, USA*

One of the surprising results from HST was the discovery that many of the most massive galaxies at $z \sim 2$ are very compact, having half-light radii of only $1-2$ kpc. The interpretation is that massive galaxies formed inside-out, with their cores largely in place by $z \sim 2$ and approximately half of their present-day mass added later through minor mergers. Here we present a compact, massive, quiescent galaxy at $z_{\rm phot} = 1.94^{+0.13}_{-0.17}$ with a complete Einstein ring. The ring was found in the JWST COSMOS-Web survey and is produced by a background galaxy at $z_{\rm phot} = 2.98^{+0.42}_{-0.47}$. Its $1.54''$ diameter provides a direct measurement of the mass of the "pristine" core of a massive galaxy, observed before the mixing and dilution of its stellar population during the 10 Gyr of galaxy evolution between $z = 2$ and $z = 0$. We find a mass of $M_{\rm lens} = 6.5^{+3.7}_{-1.5} \times 10^{11}$ M$_\odot$ within a radius of 6.6 kpc. The stellar mass within the same radius is $M_{\rm stars} = 1.1^{+0.2}_{-0.3} \times 10^{11}$ M$_\odot$ for a Chabrier initial mass function (IMF), and the fiducial dark matter mass is $M_{\rm dm} = 2.6^{+1.6}_{-0.7} \times 10^{11}$ M$_\odot$. Additional mass is needed to explain the lensing results, either in the form of a higher-than-expected dark matter density or a bottom-heavy IMF.

The galaxy and its ring were identified in JWST NIRCam observations in the context of the COSMOS-Web project,[1] a public wide-area survey using the F115W, F150W, F277W, ous red concentrations. The lensed galaxy likely has a red center and a blue disk, with parts of the disk producing the ring. The diameter of the center of the ring is $1.54'' \pm 0.02''$. JWST-ER1 joins a large number of known Einstein rings,[3,4] although most are not complete. Like other strong lensing configurations Einstein rings can be used to reconstruct high resolution images of lensed background galaxies, using ray tracing techniques.[5] However, the unique value of Einstein rings is what they tell us about the lenses themselves: given the redshifts of the lens and source, they provide a model-independent measurement of the enclosed mass within the radius of the ring.[6]

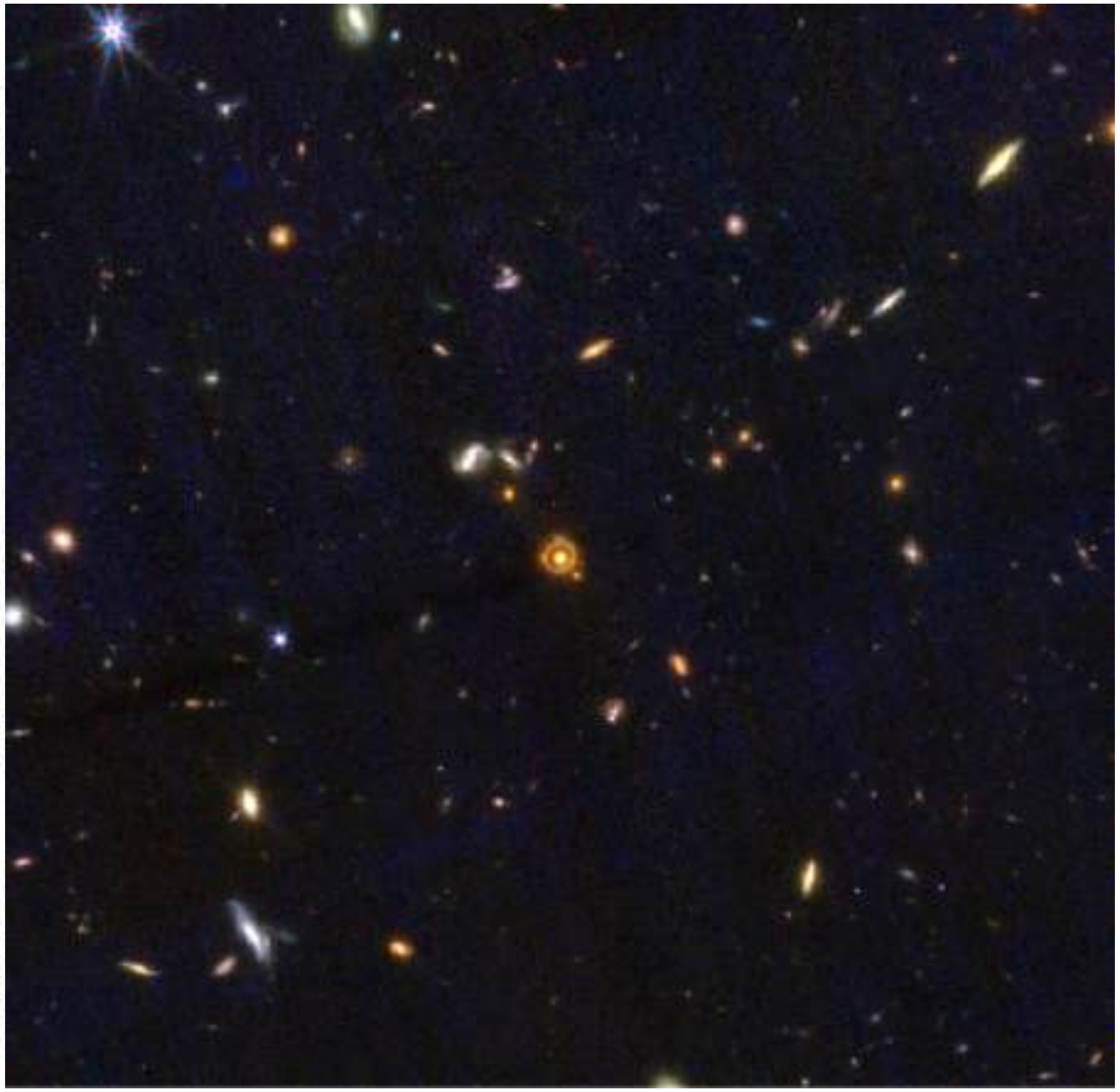

Dark Energy from Families of Multiple Images

Galaxy Cluster Scale
Cosmological Constraints and more

$$\vec{\theta} = \vec{\beta} + \frac{2}{c^2} \frac{D_{LS}}{D_{OS} D_{OL}} \nabla_\theta \psi \left(\vec{\theta} \right)$$

Families of images with sources at different *redshifts*

☑ constraints on cosmology, in addition to the matter distribution

The ratio of angular diameter distances for 2 (or more) images with sources at different redshifts defines a ratio of families

$$\Xi(z_l, z_{s1}, z_{s2}; \Omega_M, \Omega_X, w_X) = \frac{D(z_l, z_{s1})}{D(0, z_{s1})} \frac{D(0, z_{s2})}{D(z_l, z_{s2})}$$

☑ Jullo et al. 2010, Science: example of competitive limits in cosmological parameters fom the Abell 1689 system

☑ **8** families of sources with z = 1.15 to 4.86

☑ Caminha et al. 2016: RXC J2248.7-4431 (Abell S1063), 17 sources, 47 images

☑ Magaña, Motta, Cárdenas, Verdugo, Jullo, 2015: Dark Energy models

Reminder: Angular Diameter Distance

In the wCDM model $p = w\rho$

$$H^2(a) = H_0^2\left[\Omega_r a^{-4} + \Omega_M a^{-3} + \Omega_k a^{-2} + \Omega_{DE} a^{-3(1+w)}\right]$$

In the flat case

$$D_A\left(z_1, z_2\right) = \frac{\left(1+z_2\right)^{-1}}{H_0}\int_{z_1}^{z_2} \frac{dz'}{\sqrt{\Omega_M (1+z')^3 + \left(1-\Omega_M\right)\left(1+z'\right)^{3(1+w)}}}$$

$$D_{LS} = D_A(z_L, z_S)$$

Cosmological Constraints

Caminha et al., 2016

Frontier Field Cluster AS1063 (aka RXJ2248)

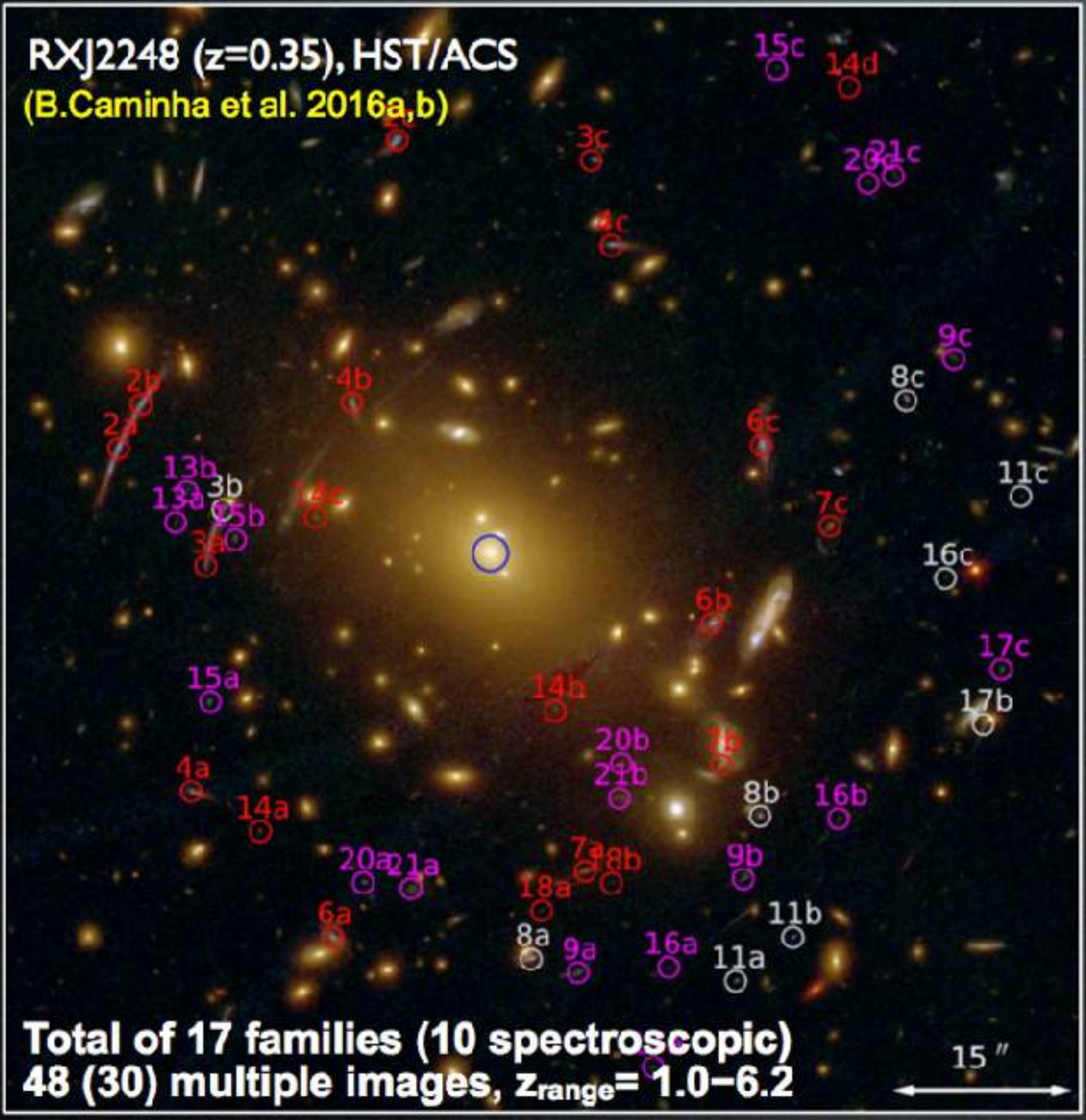

MUSE SV programme + GO (PI: K.Caputi)
(Karman et al. 2015)
(W.Karman et al. 2016, arXiv/160601471)

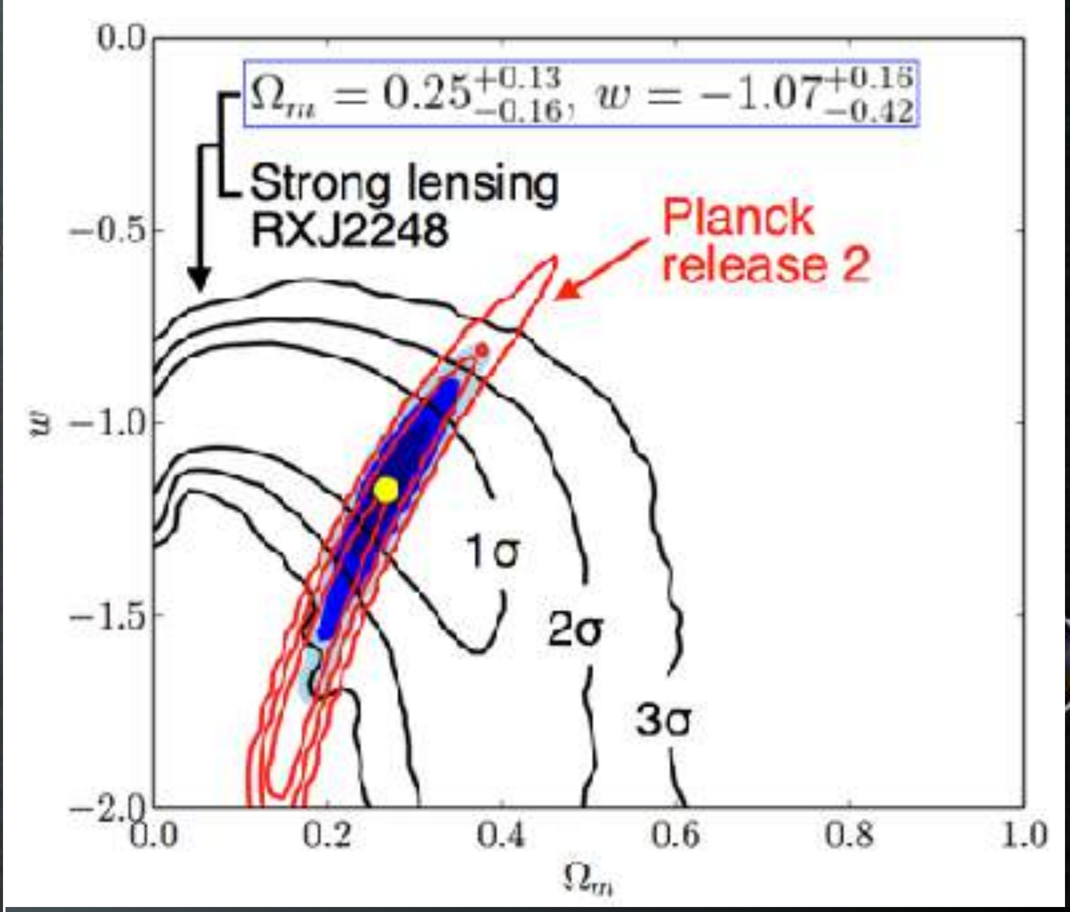

1 arcmin² FoV
2.6 Å resolution (4800-9300 Å)
0.2 arcsec/pxl
Exp. = 5 hrs

New constraints from Abell S1063

- **Doubling the number of families of multiple images**
- **Comparison and combination with other observables**

Bom, MM, Caminha, Vitenti, Penna-Lima (2022, in prep.)

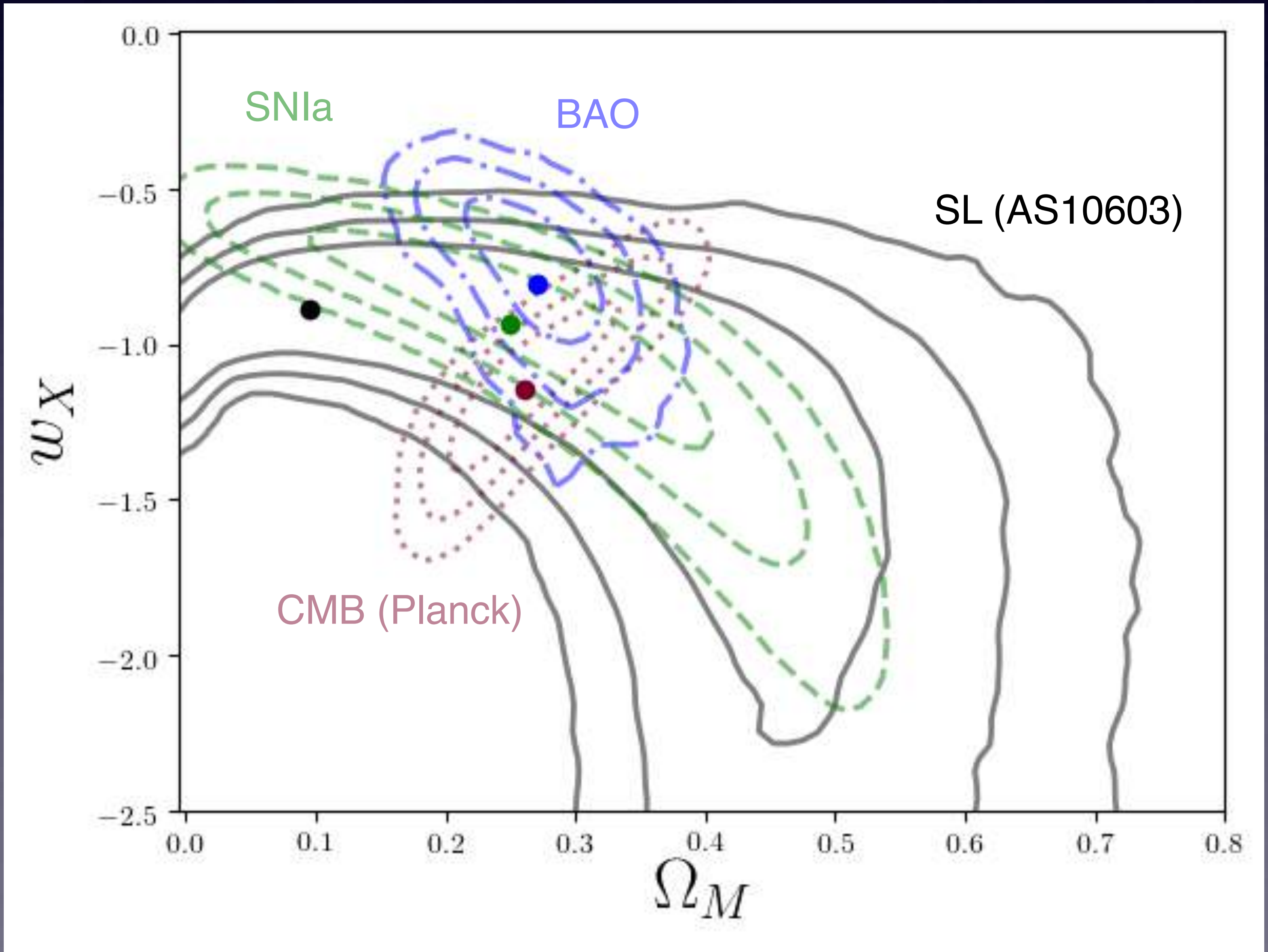

Limits from Strong Lensing only:

$$\Omega_M = 0.422^{+0.062}_{-0.274}$$

$$w = -0.911^{+0.030}_{-1.356}$$

Single system!

Improvement by combining with SL over each probe alone:

Probe	$\Delta\sigma_w$	$\Delta\sigma_{\Omega_M}$	ΔA_σ
SNIa	27%	23 %	31 %
BAO	29%	17%	28 %
CMB	44%	37%	36 %

The Astrophysical Journal, 850:49 (24pp), 2017 November 20 https://doi.org/10.3847/1538-4357/aa9575

Microlensing of Extremely Magnified Stars near Caustics of Galaxy Clusters

Tejaswi Venumadhav[1], Liang Dai[1,4], and Jordi Miralda-Escudé[2,3]
[1] Institute for Advanced Study, 1 Einstein Drive, Princeton, NJ 08540, USA
[2] Institució Catalana de Recerca i Estudis Avançats, Barcelona, Catalonia, Spain
[3] Institut de Ciències del Cosmos, Universitat de Barcelona IEEC-UB Barcelona E-08028, Catalonia, Spain
Received 2017 June 28; revised 2017 September 30; accepted 2017 October 19; published 2017 November 16

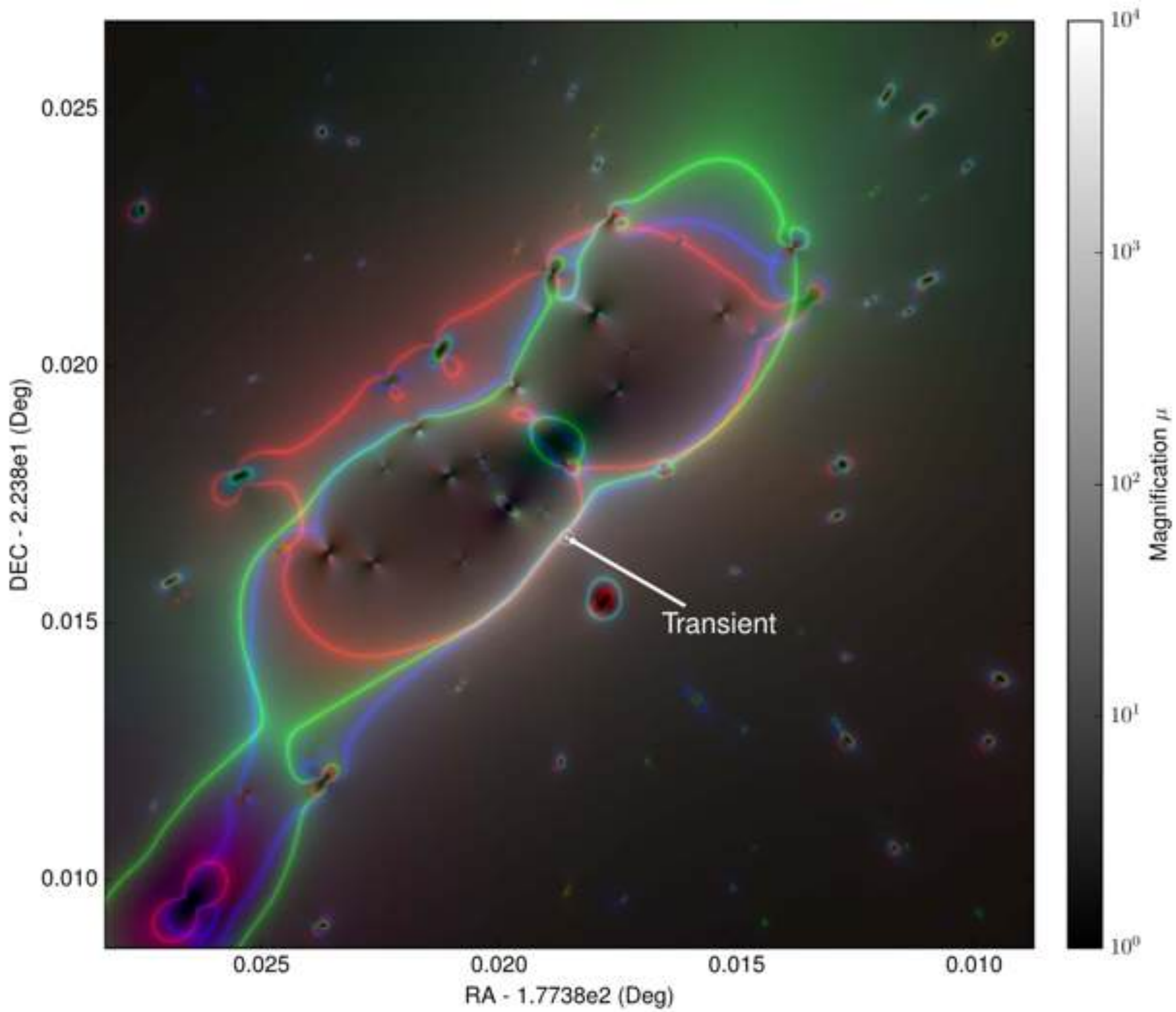

Article | Published: 02 April 2018

Extreme magnification of an individual star at redshift 1.5 by a galaxy-cluster lens

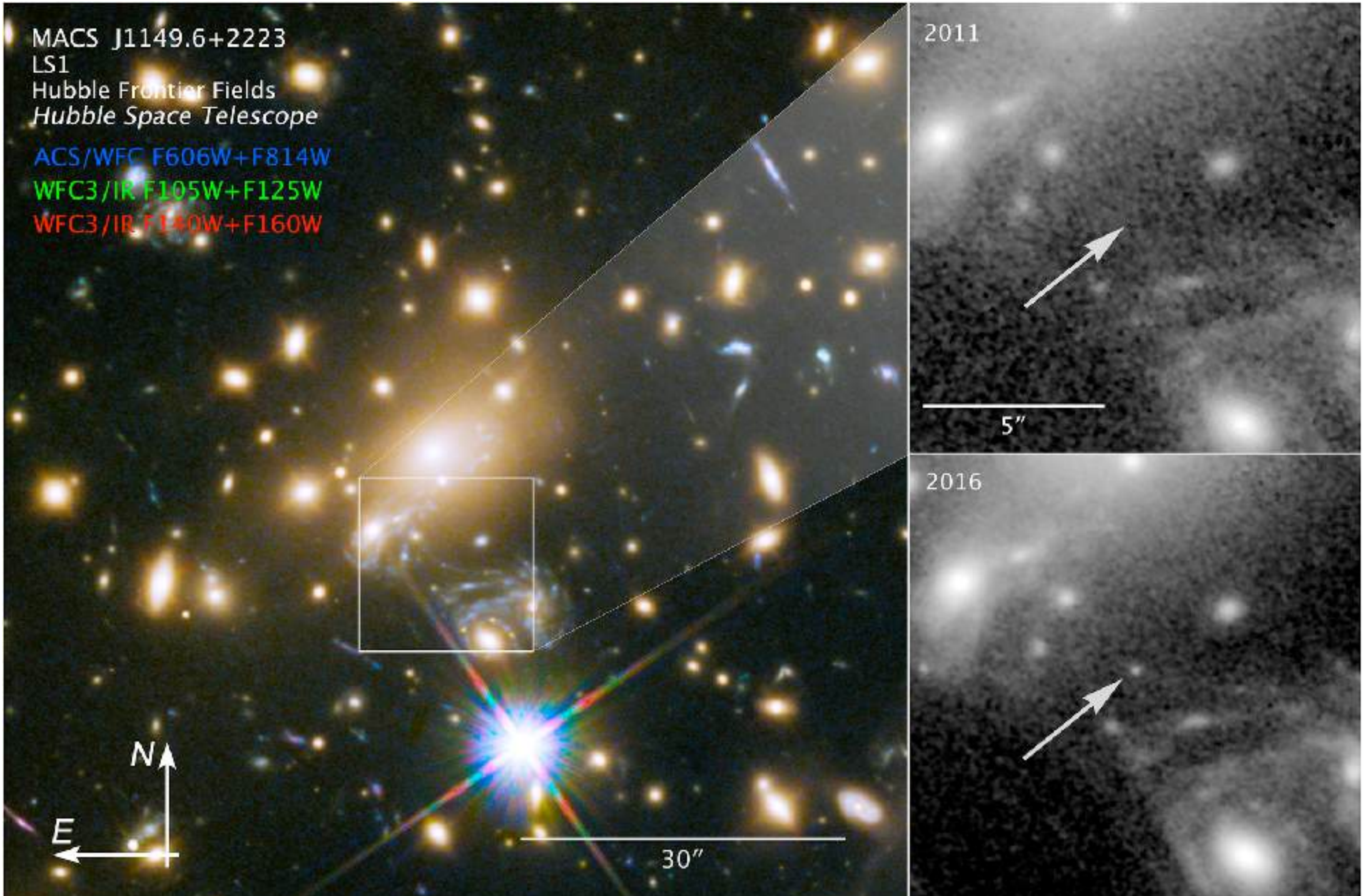

Article | Published: 30 March 2022

A highly magnified star at redshift 6.2

Brian Welch, Dan Coe, Jose M. Diego, Adi Zitrin, Erik Zackrisson, Paola Dimauro, Yolanda Jiménez-Teja, Patrick Kelly, Guillaume Mahler, Masamune Oguri, F. X. Timmes, Rogier Windhorst, Michael Florian, S. E. de Mink, Roberto J. Avila, Jay Anderson, Larry Bradley, Keren Sharon, Anton Vikaeus,

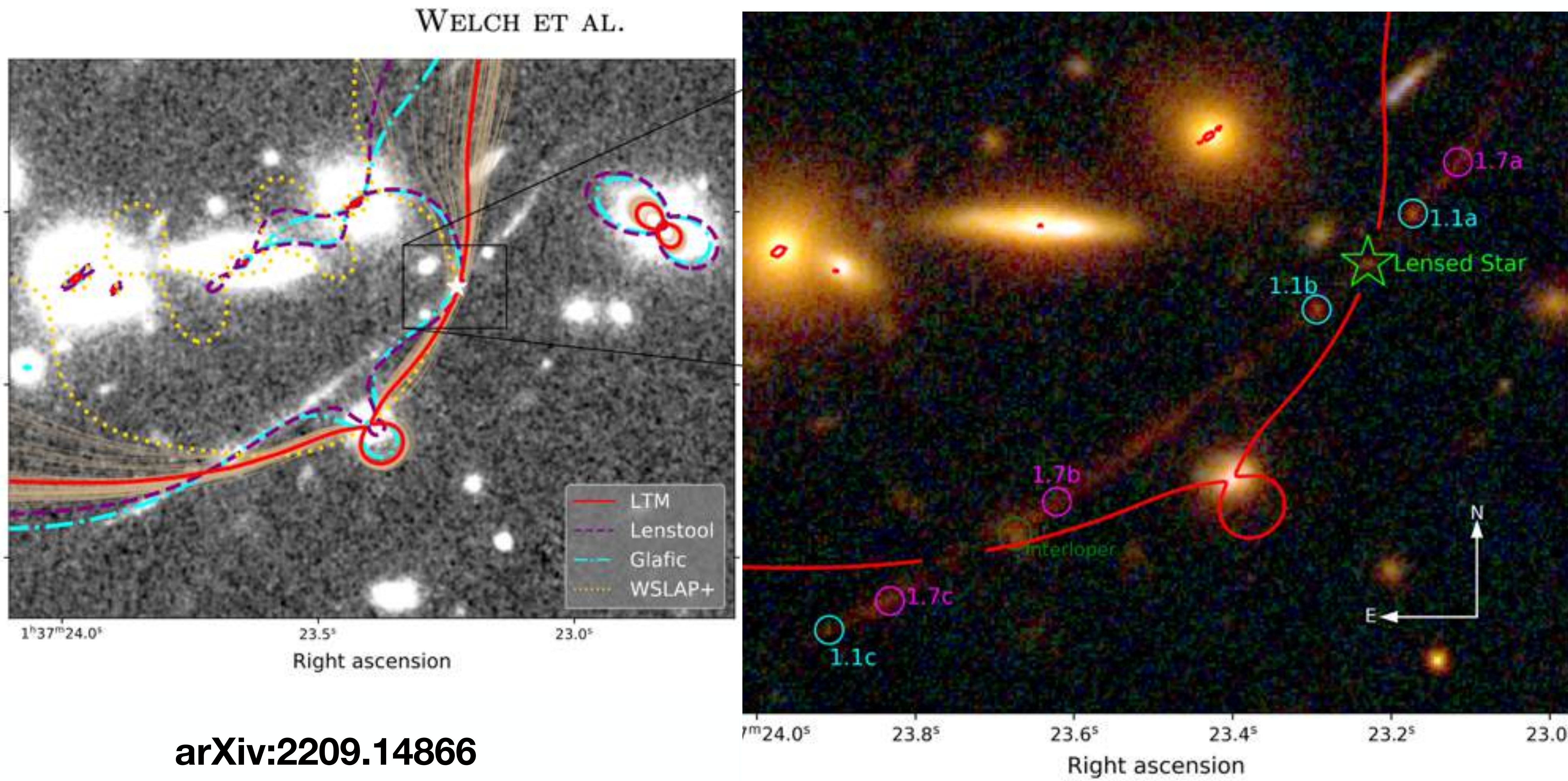

arXiv:2209.14866

Mililentes de Cuasares

- Patrón de magnificación
- Curvas de luz

Joachim Wambsganss
http://www.livingreviews.org/lrr-1998-12

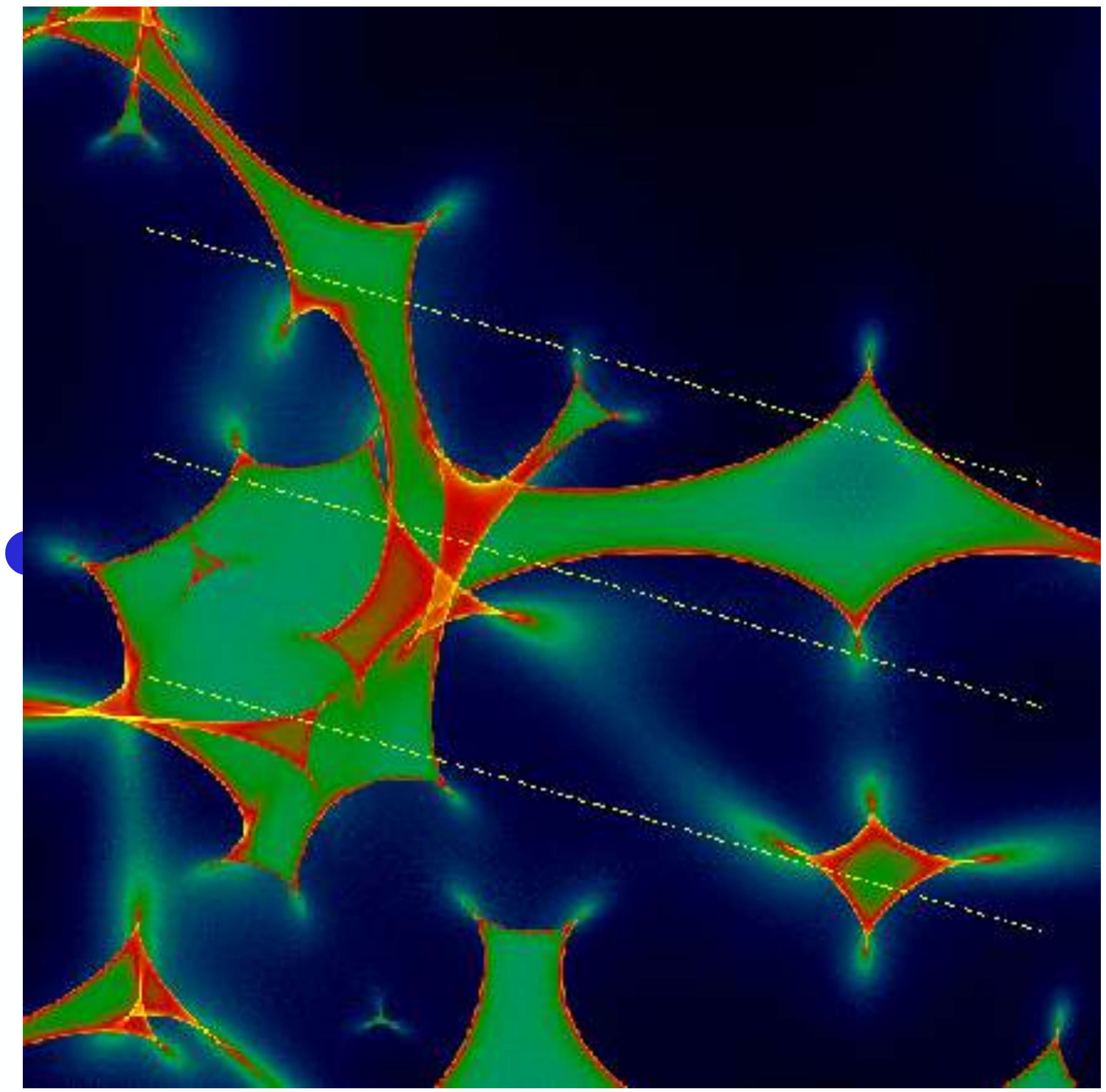

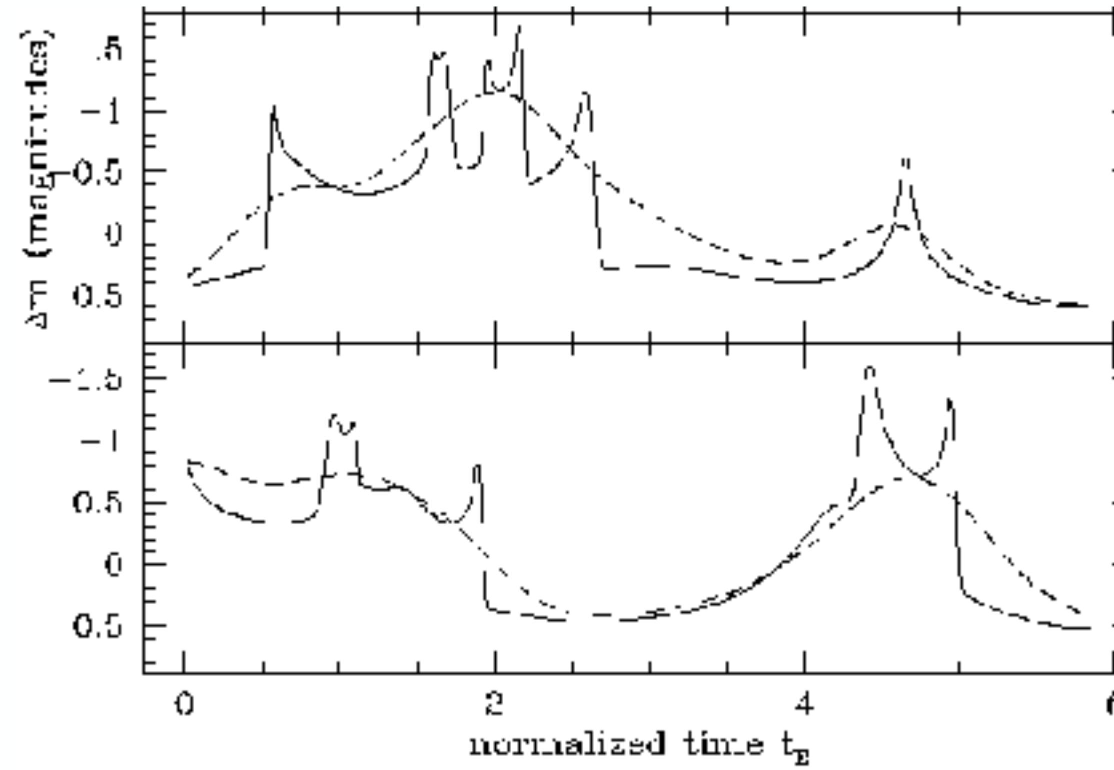

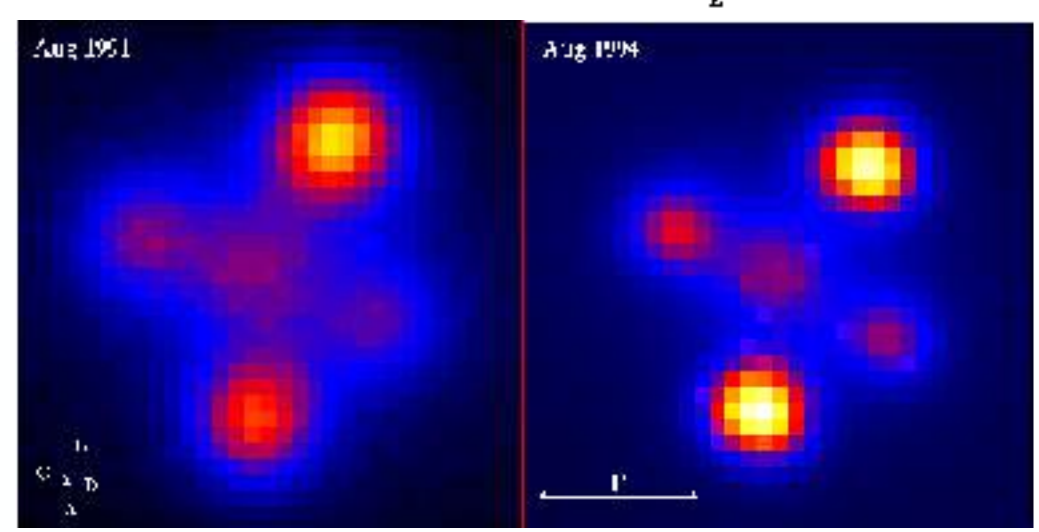

Review actual: arXiv:2312.00931

The Astrophysical Journal Letters, 853:L27 (5pp), 2018 February 1
https://doi.org/10.3847/2041-8213/aaa5fb

Probing Extragalactic Planets Using Quasar Microlensing

Xinyu Dai and Eduardo Guerras
Homer L. Dodge Department of Physics and Astronomy, University of Oklahoma, Norman, OK 73019, USA
Received 2017 November 16; revised 2017 December 28; accepted 2018 January 7; published 2018 February 2

Abstract

Previously, planets have been detected only in the Milky Way galaxy. Here, we show that quasar microlensing provides a means to probe extragalactic planets in the lens galaxy, by studying the microlensing properties of emission close to the event horizon of the supermassive black hole of the background quasar, using the current generation telescopes. We show that a population of unbound planets between stars with masses ranging from Moon to Jupiter masses is needed to explain the frequent Fe Kα line energy shifts observed in the gravitationally lensed quasar RXJ 1131–1231 at a lens redshift of $z = 0.295$ or 3.8 billion lt-yr away. We constrain the planet mass-fraction to be larger than 0.0001 of the halo mass, which is equivalent to 2000 objects ranging from Moon to Jupiter mass per main-sequence star.

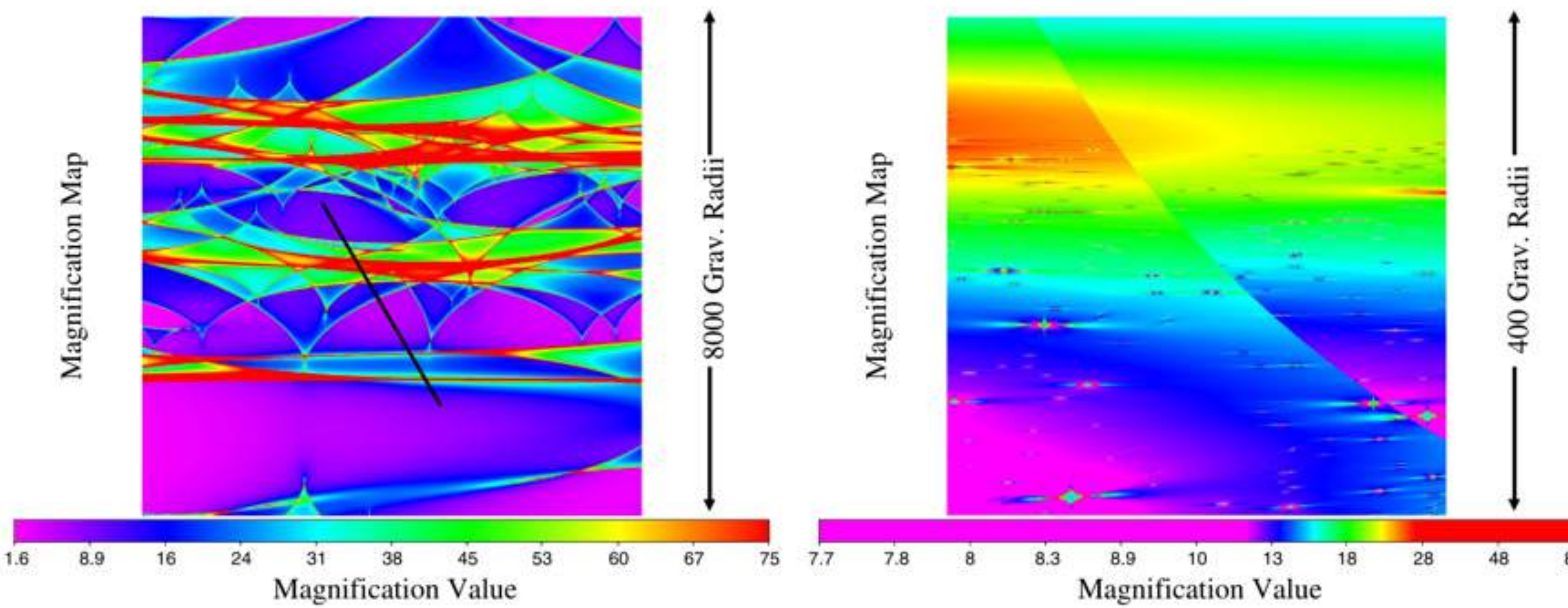

Time Delays and Cosmology

Desfasaje temporal gravitacional

Metrica perturbada

$$ds^2 = \left(1 + \frac{2\phi}{c^2}\right) c^2 dt^2 - \left(1 - \frac{2\phi}{c^2}\right) d\sigma^2$$

Localmente euclidiano próximo a la lente

Geodésica radial

$$t_S - t_0 = \frac{1}{c} \int_{r_O}^{r_S} \left(1 - \frac{2\phi(r)}{c^2}\right) dr$$

Desfasaje temporal gravitacional

$$\delta t_{grav} = -\frac{2}{c^3} \int_{r_O}^{r_S} \phi(r) dr = -\frac{2}{c^3} \psi$$

Desvio temporal geométrico

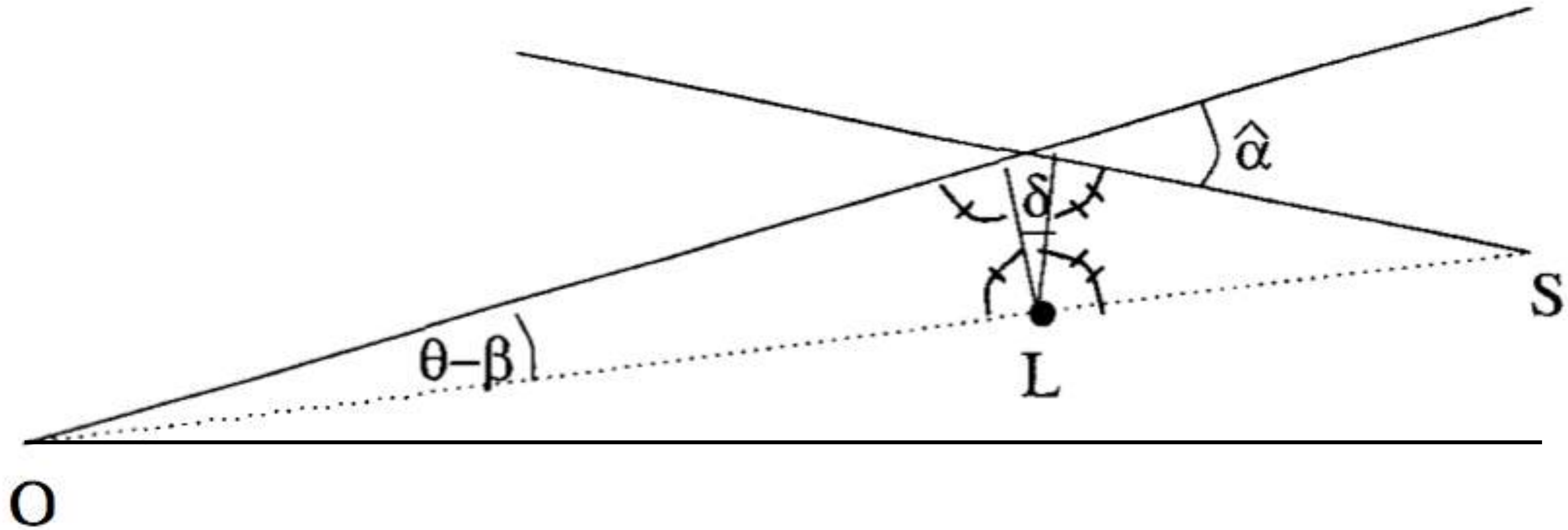

$$\delta L = \frac{D_{OS} D_{OL}}{2 D_{LS}} (\vec{\theta} - \vec{\beta})^2$$

$$\delta t_{\rm geom} = \delta L / c = \frac{D_{OS} D_{OL}}{2c D_{LS}} (\vec{\theta} - \vec{\beta})^2$$

Obs.: Deducción rigurosa en Petters, Levine, Wambsganss

Desvio temporal total

Desvio total en el referencial de la lente

$$\delta t_L = \delta t_{\rm geom} + \delta t_{\rm grav}$$

$$\delta t_{\rm geom} = \delta L/c = \frac{D_{OS}D_{OL}}{2cD_{LS}}(\vec{\theta} - \vec{\beta})^2$$

$$\delta t_{grav} = -\frac{2}{c^3}\psi$$ pero $$\Psi \equiv \frac{2}{c^2}\frac{D_{\rm LS}}{D_{\rm OS}D_{\rm OL}}\psi$$

De forma que

$$\boxed{\delta t_L = \frac{D_{OS}D_{OL}}{cD_{LS}}\left(\frac{1}{2}(\vec{\theta} - \vec{\beta})^2 - \Psi\right)}$$

Desvio temporal total

Efecto Doppler

$$\delta_{t_O}/\delta_{t_L} = a_O/a_L = (1+z_L)$$

$$\delta t_L = \frac{D_{OS}D_{OL}}{cD_{LS}}\left(\frac{1}{2}(\vec{\theta}-\vec{\beta})^2 - \Psi\right)$$

$$\boxed{\delta t = (1+z_L)\frac{D_{OS}D_{OL}}{cD_{LS}}\left(\frac{1}{2}(\vec{\theta}-\vec{\beta})^2 - \Psi\right)}$$

$\vec{\nabla}_\theta(\delta t) = 0 \Rightarrow$ Ecuación de la lente!

Obs.: Deducción rigurosa en Petters, Levine, Wambsganss

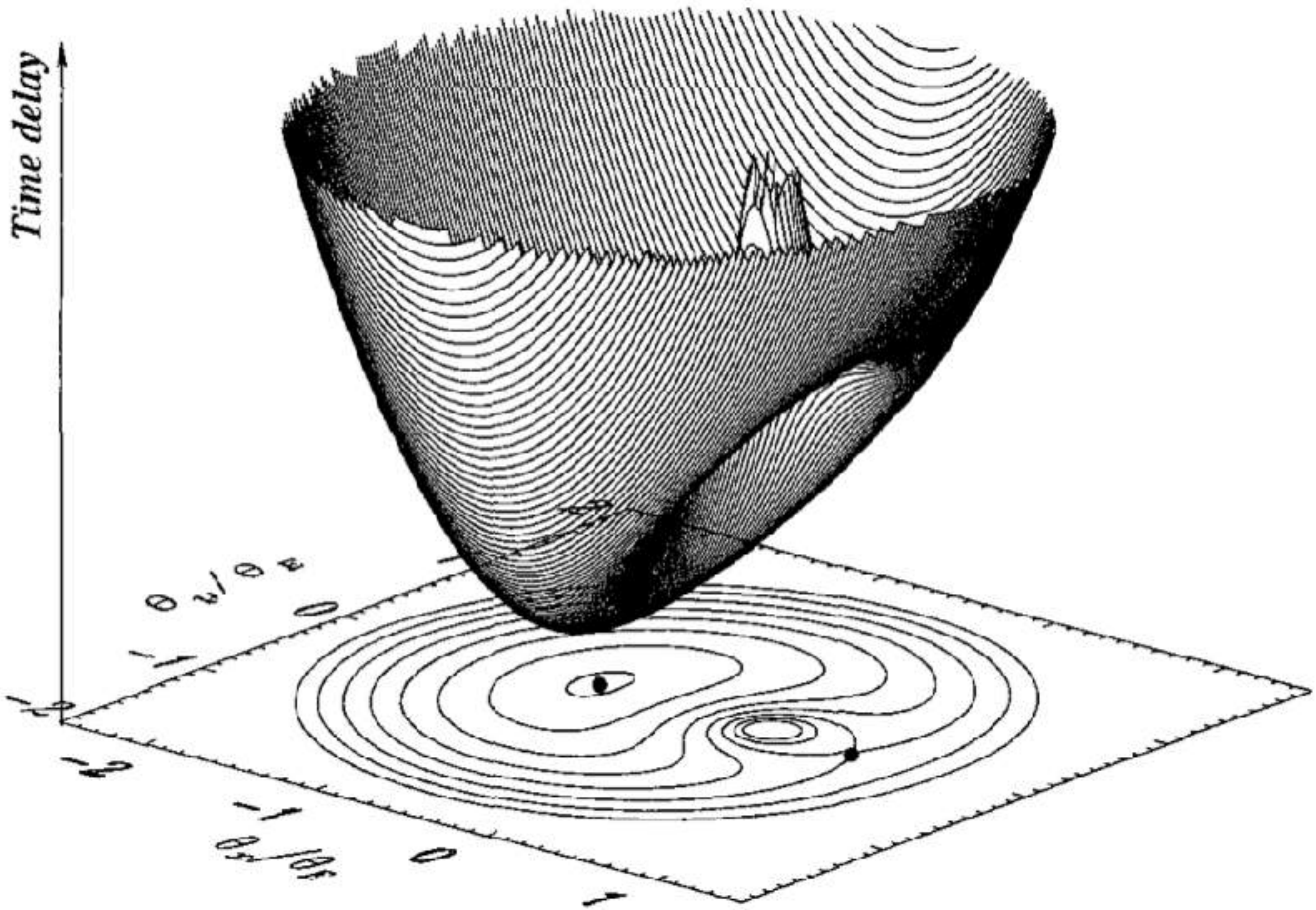
Time delay
θ_2/θ_E
θ_1/θ_E
-2
-1
0
1

Desfasaje temporal y Jacobiana de la transformación

Es fácil ver que $$\frac{\partial^2 \delta t}{\partial\theta_i \partial\theta_j} \propto \left(\frac{\partial\vec{\beta}}{\partial\vec{\theta}}\right)_{ij} = \delta_{ij} - \frac{\partial^2 \Psi}{\partial\theta_i \partial\theta_j}$$

La curvatura de la función $\delta t(\theta)$ define la paridad de las imágenes

Cuanto menor la curvatura de δt, mayor la magnificación

Segunda derivada se anula -> magnificación infinita:
Fusión de máximos y puntos de ensilladura (curvas críticas)

Teorema de Burke

Las imágenes se forman a los pares (salvo si hay singularidades) y con distintas paridades)

THE ASTROPHYSICAL JOURNAL, 244:L1, 1981 February 15

MULTIPLE GRAVITATIONAL IMAGING BY DISTRIBUTED MASSES[1]

WILLIAM L. BURKE
Lick Observatory, Boards of Studies in Astronomy and Astrophysics and in Physics, University of California, Santa Cruz, CA 95064
Received 1980 September 26; accepted 1980 November 5

ABSTRACT

A transparent galaxy, not necessarily spherical, acting as a gravitational lens produces an odd number of images.

Subject headings: galaxies: general — gravitation — quasars

In a recent *Letter* (Dyer and Roeder 1980) it was shown that a transparent spherical galaxy of finite mass acting as a gravitational lens produces an odd number of images. The result is in fact true for arbitrary mass distributions as long as the bending (roughly m/r) remains bounded as r goes to infinity. This covers all realizable cases, since larger masses would be within their own event horizons.

A proof of this stronger result is easy. Parametrize the rays leaving the source by their impact parameters (u, v), measured in some plane near the deflector and transverse to the rays. See Figure 1. You may think of this plane as the celestial sphere. The action of the gravitational lens bends a ray. Let us look at the intersection of this bent ray with another transverse plane, this one passing through the receiver. We can measure the bending by the direction cosines (s, w) between two lines: one from the source to the point (u, v) in the deflector plane, and one from that point to the point where the actual ray hits the receiver plane. By a transparent deflector we mean one for which all the rays hitting the first plane also hit the second. This excludes solid objects and black holes.

[1] *Lick Observatory Bulletin*, No. 848.

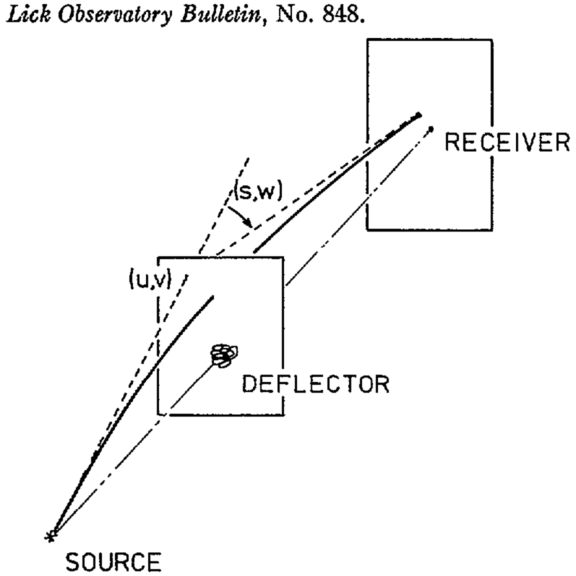

FIG. 1

The action of the gravitational lens is specified by giving the bendings (s, w) as functions of the impact parameters (u, v). Such functions can be represented by a vector field on the (u, v)-plane with components (s, w). A ray with impact parameters (u, v) will reach the receiver only for specific bendings (s, w). This condition can also be represented as a vector field. The gravitational lens will form an image of the source at the receiver whenever these two vector fields are equal.

Subtract these two vector fields. Our problem is to study the zeros of this difference vector field. Since the bending is assumed bounded, for large impact parameter the difference vector field is dominated by the requirement that it takes a large bend for the ray to reach us. For large impact parameter the difference vector field is mainly radial. The zeros of a vector field on the plane are constrained by the Poincaré-Hopf index theorem (see Guillemin and Pollack 1974), which assigns an index to a region by counting the net rotation of the vector field around the boundary of the region. The index of a region is the sum of the indices around the zeros. Simple zeros of a vector field are either sources, sinks, or saddle points. Sources and sinks have index $+1$ and correspond to direct images, while saddle points have index -1 and correspond to inverted images (as in Dyer and Roeder's 1980 Fig. 2). The sum of the indices of the zeros for our difference vector field must be $+1$ because of the behavior at large impact parameter. Thus if there are only simple images, there must be an odd number of them, with one more direct image than inverted images.

Because this is a topological argument the transverse planes need not be flat, the bendings can be measured by angles, tangents, or whatever, and the straight lines need only be straight in some coordinate chart. The (u, v)-plane can be thought of as the celestial sphere of the source or, since rays are reversible, as the celestial sphere of the receiver.

This research was done at the Aspen Center for Physics, and their hospitality and the partial support of the National Science Foundation are gratefully acknowledged.

REFERENCES

Dyer, C. C., and Roeder, R. C. 1980, *Ap. J.* (*Letters*), **238**, L67.
Guillemin, V., and Pollack, A. 1974, *Differential Topology* (Englewood Cliffs, N.J.: Prentice-Hall).

Desfasaje Temporal Relativo

$$\Delta t_{ij} = \frac{D_\Delta}{c}\left(\frac{1}{2}(\vec{\theta}_i - \vec{\beta})^2 - \Psi(\theta_i) - \frac{1}{2}(\vec{\theta}_j - \vec{\beta})^2 + \Psi(\theta_j)\right)$$

Onde $D_\Delta = (1+z_L)\frac{D_{OS}D_{OL}}{D_{LS}}$

"time delay distance"

modelado inverso
(imágenes múltiples)

Principal dependencia cosmológica: $\propto H_0^{-1}$

Curvas de luz de cuasares

Desfasaje temporal entre imágenes

$$\Delta t_{ij} = \delta t\left(\vec{\theta}_i, \vec{\beta}\right) - \delta t\left(\vec{\theta}_j, \vec{\beta}\right)$$

$$= (1+z_L)\frac{D_{OS}D_{OL}}{cD_{LS}}\left(\frac{1}{2}(\vec{\theta}_i - \vec{\beta})^2 - \Psi(\theta_i) - \frac{1}{2}(\vec{\theta}_j - \vec{\beta})^2 + \Psi(\theta_j)\right)$$

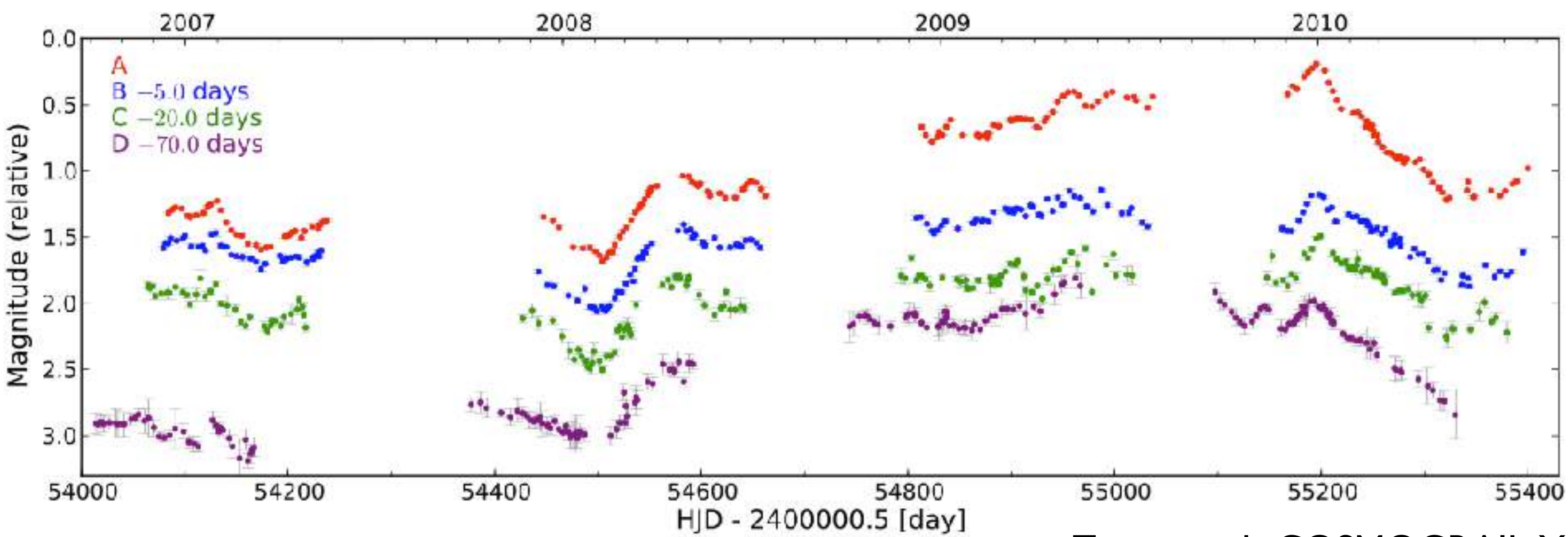

Tewes et al.: COSMOGRAIL XI

Ejemplo: RX J1131−1231

- COSMOGRAIL: the COSmological MOnitoring of GRAvItational Lenses
- Curvas de luz + modelo de la lente (+"todo")

$$\kappa_{\rm pl}(\theta_1,\theta_2) = \frac{3-\gamma'}{2}\left(\frac{\theta_{\rm E}}{\sqrt{q\theta_1^2+\theta_2^2/q}}\right)^{\gamma'-1}$$

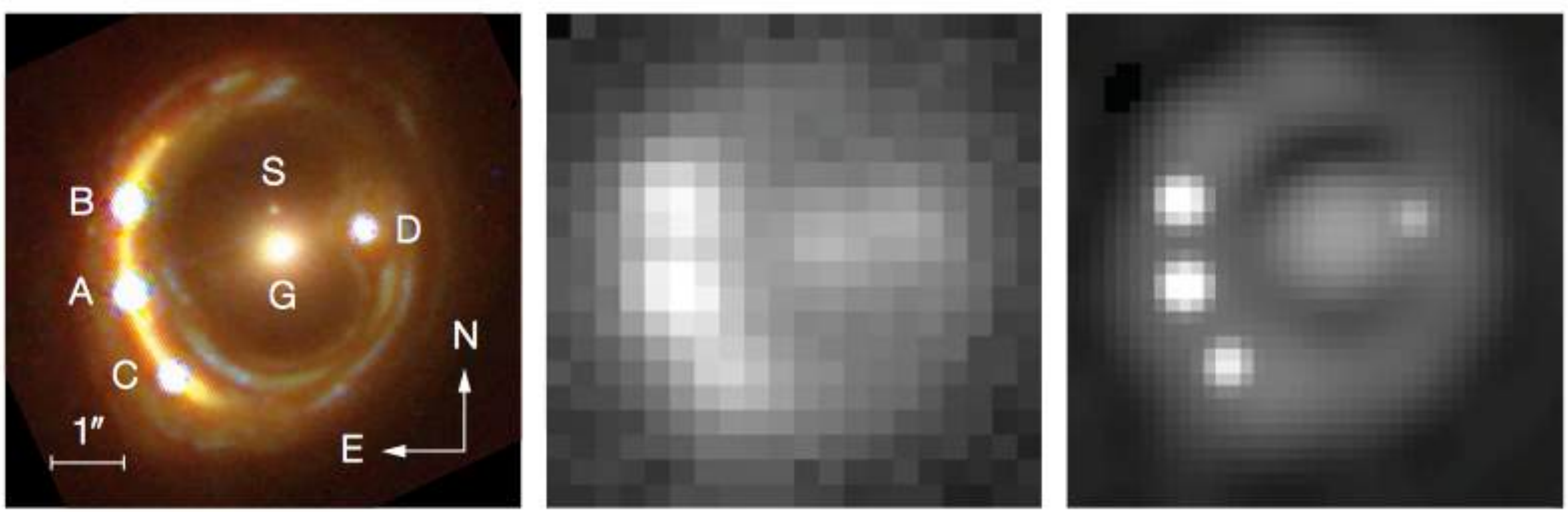

Hubble Space Telescope

Swiss Leonhard Euler Telescope

Euler deconvolved

Modeling of RX J1131−1231

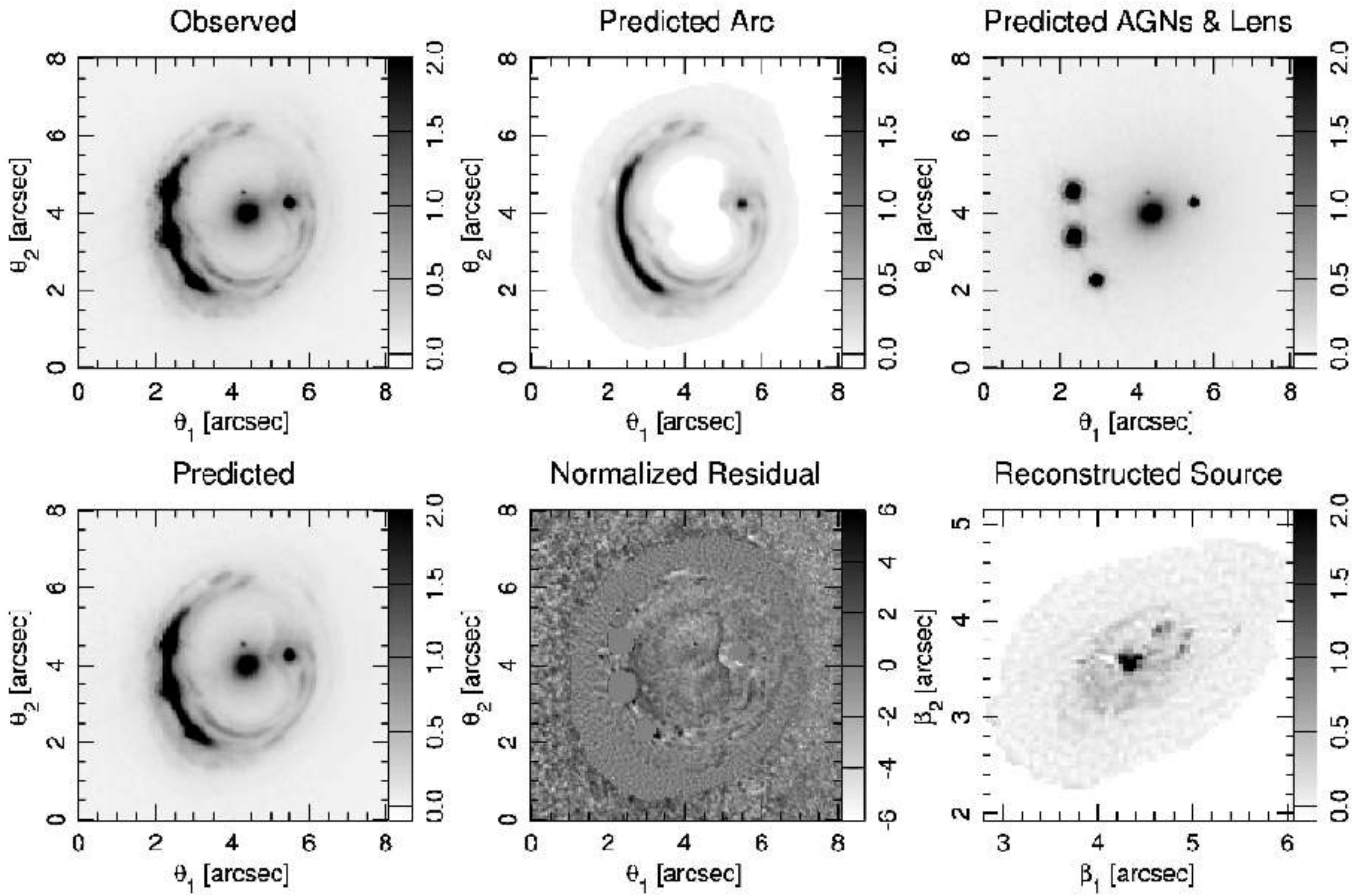

Curva de Luz de RX J1131−1231

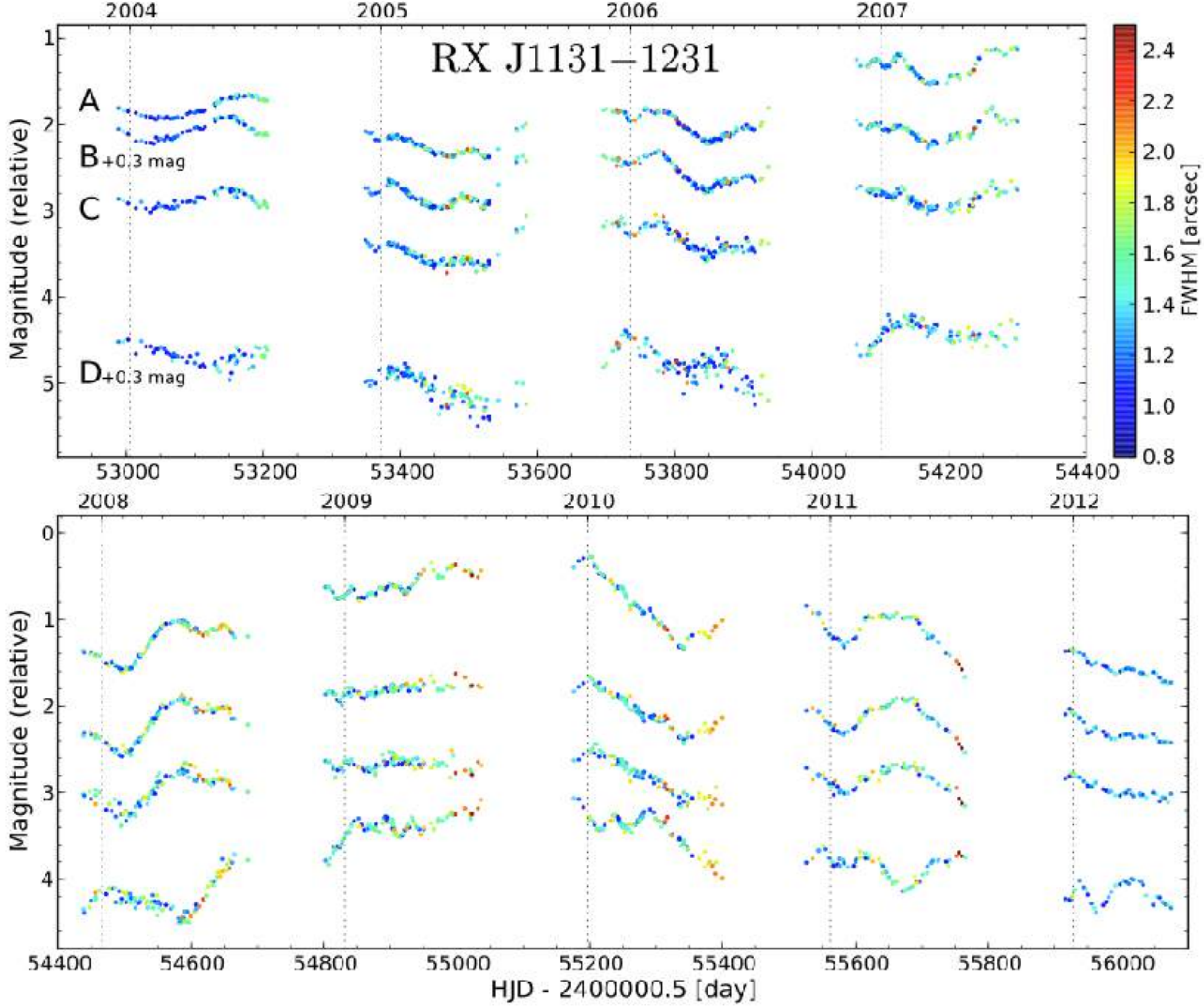

Tewes et al., COSMOGRAIL

TDCOSMO 2025: Cosmological constraints from strong lensing time delays

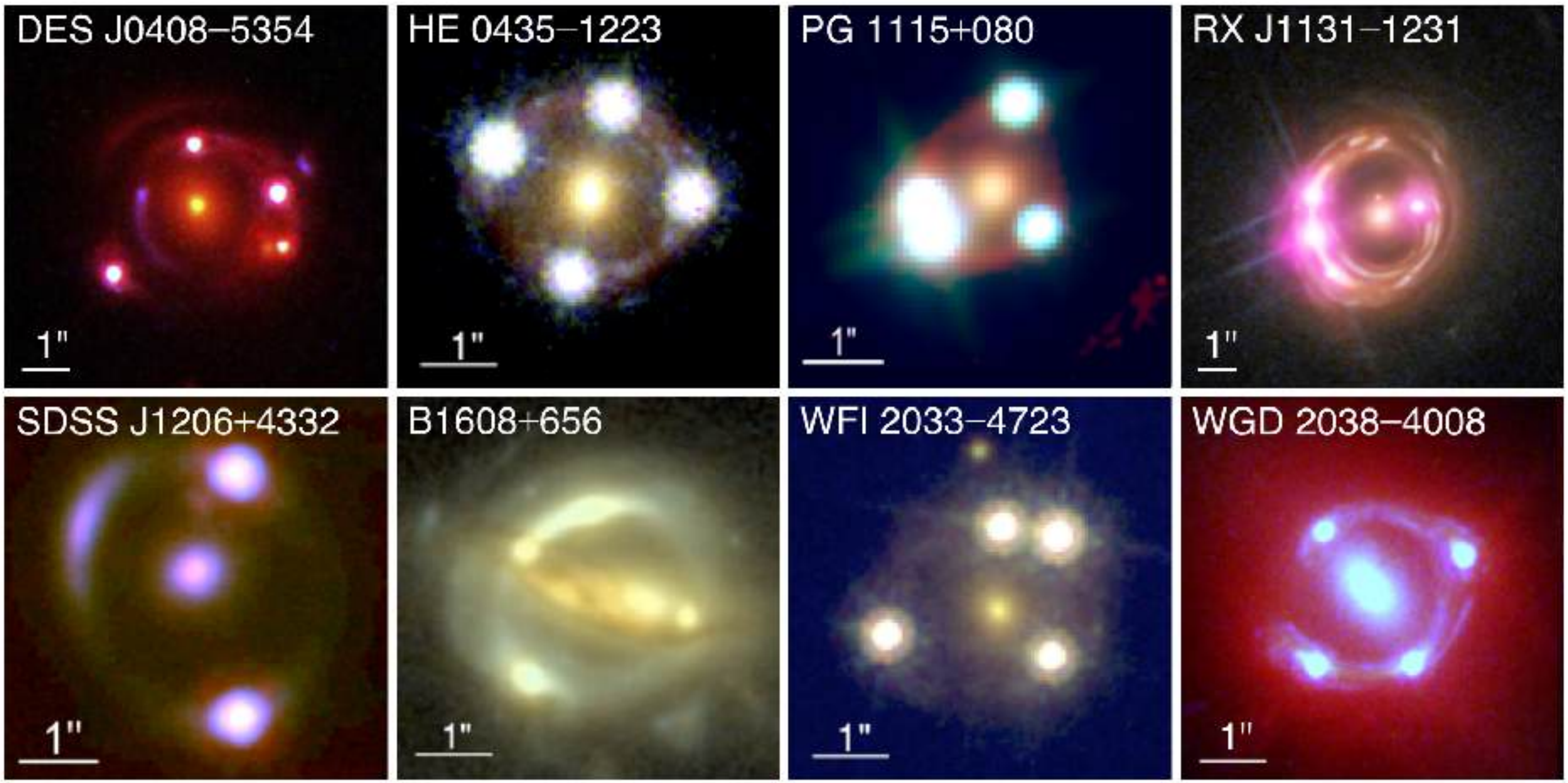

arXiv:2506.03023

TDCOSMO 2025: Cosmological constraints from strong lensing time delays

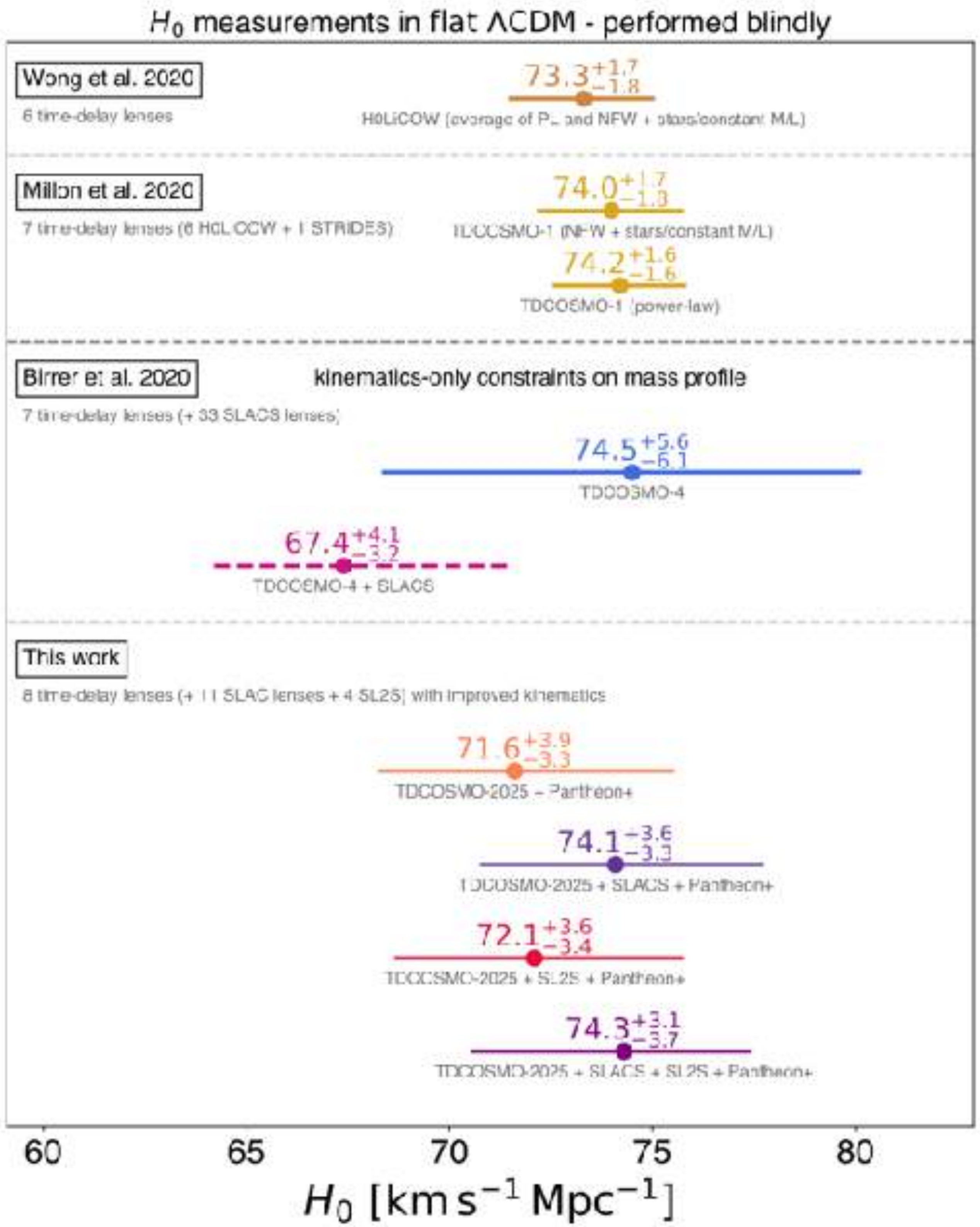

arXiv:2506.03023

TDCOSMO 2025: Cosmological constraints from strong lensing time delays

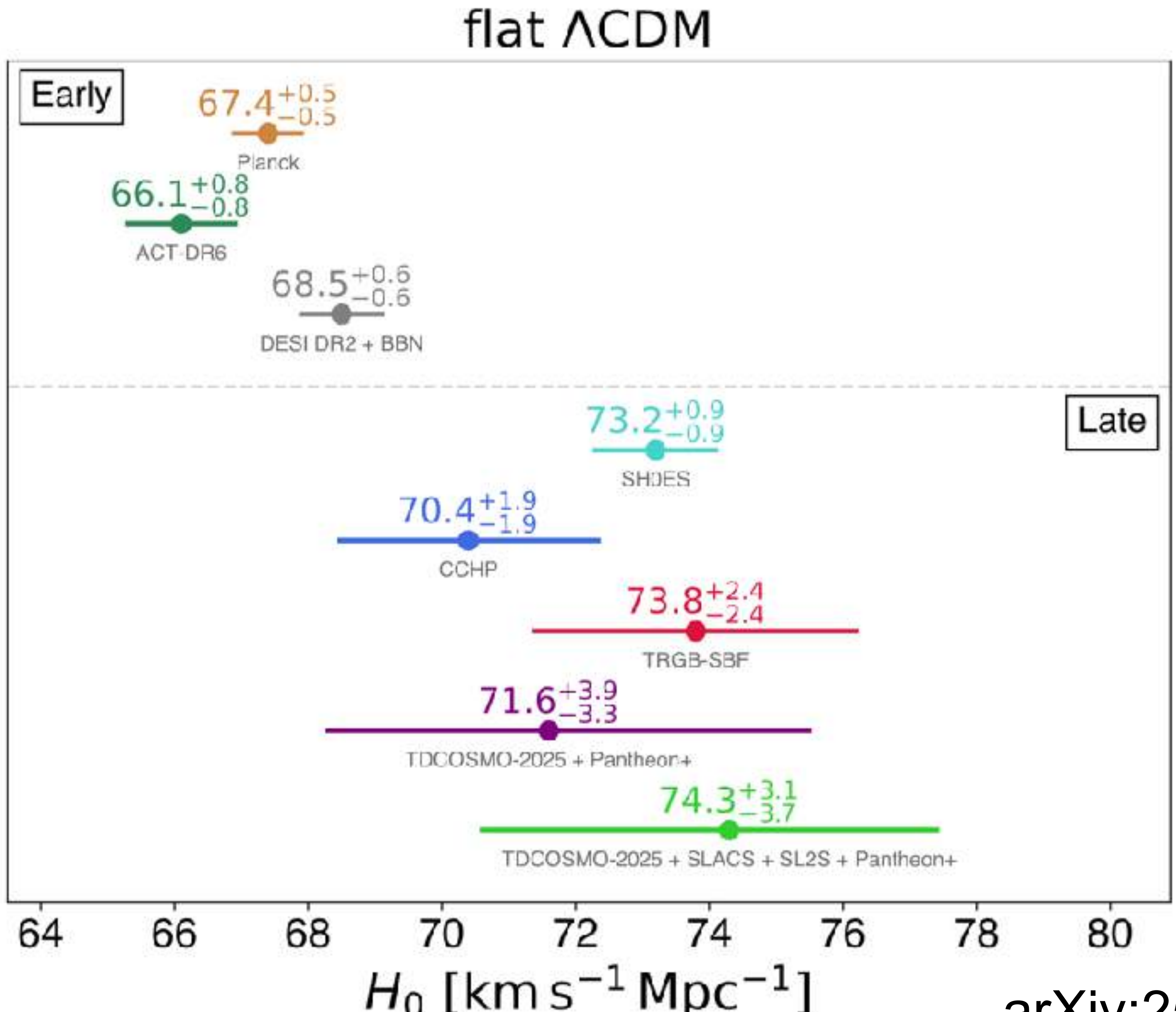

arXiv:2506.03023

Strongly lensed supernovae

- ¿Por qué no usar transientes para medir los desfasajes temporales, en lugar de las complejas curvas de variabilidad de QSO?
- ¡Usar supernovas!
- Menos de 10 conocidas hasta ahora, en su mayoría en cúmulos

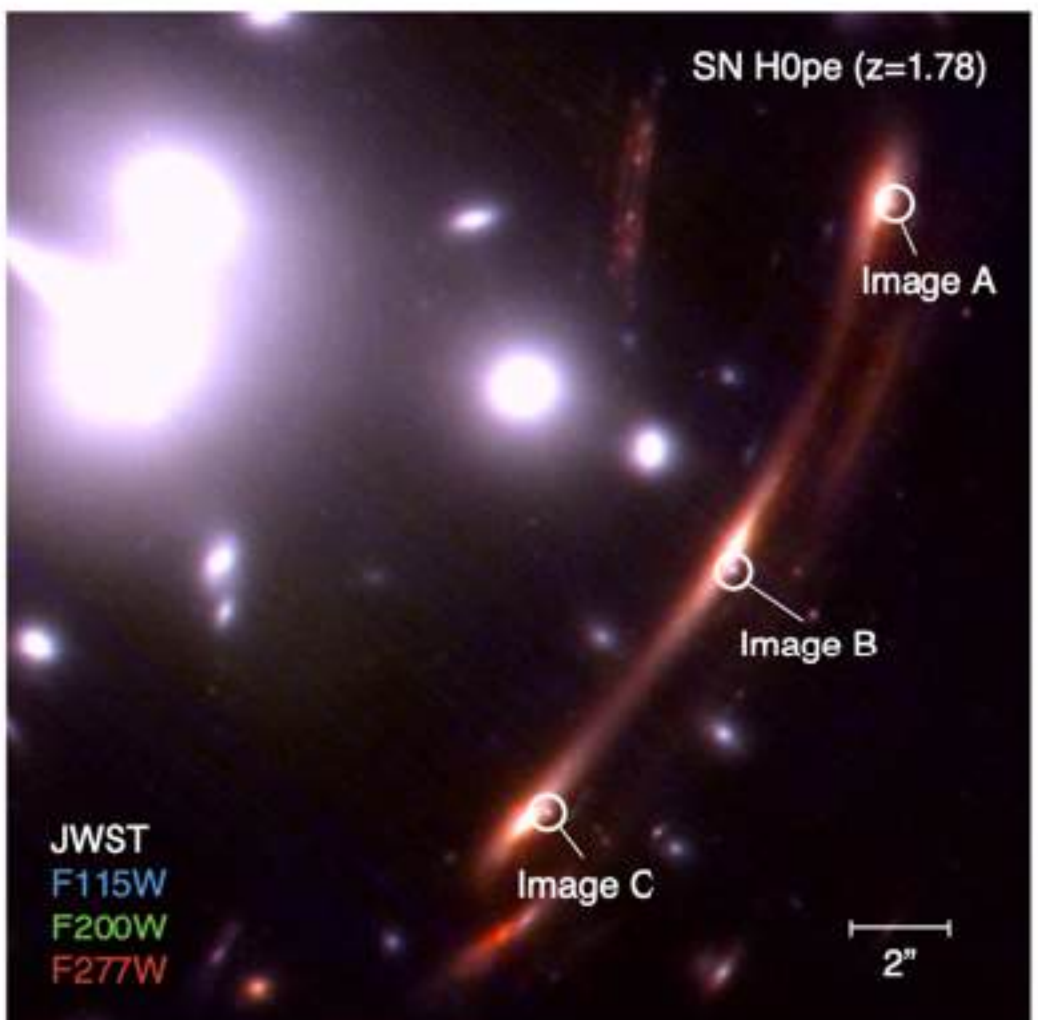

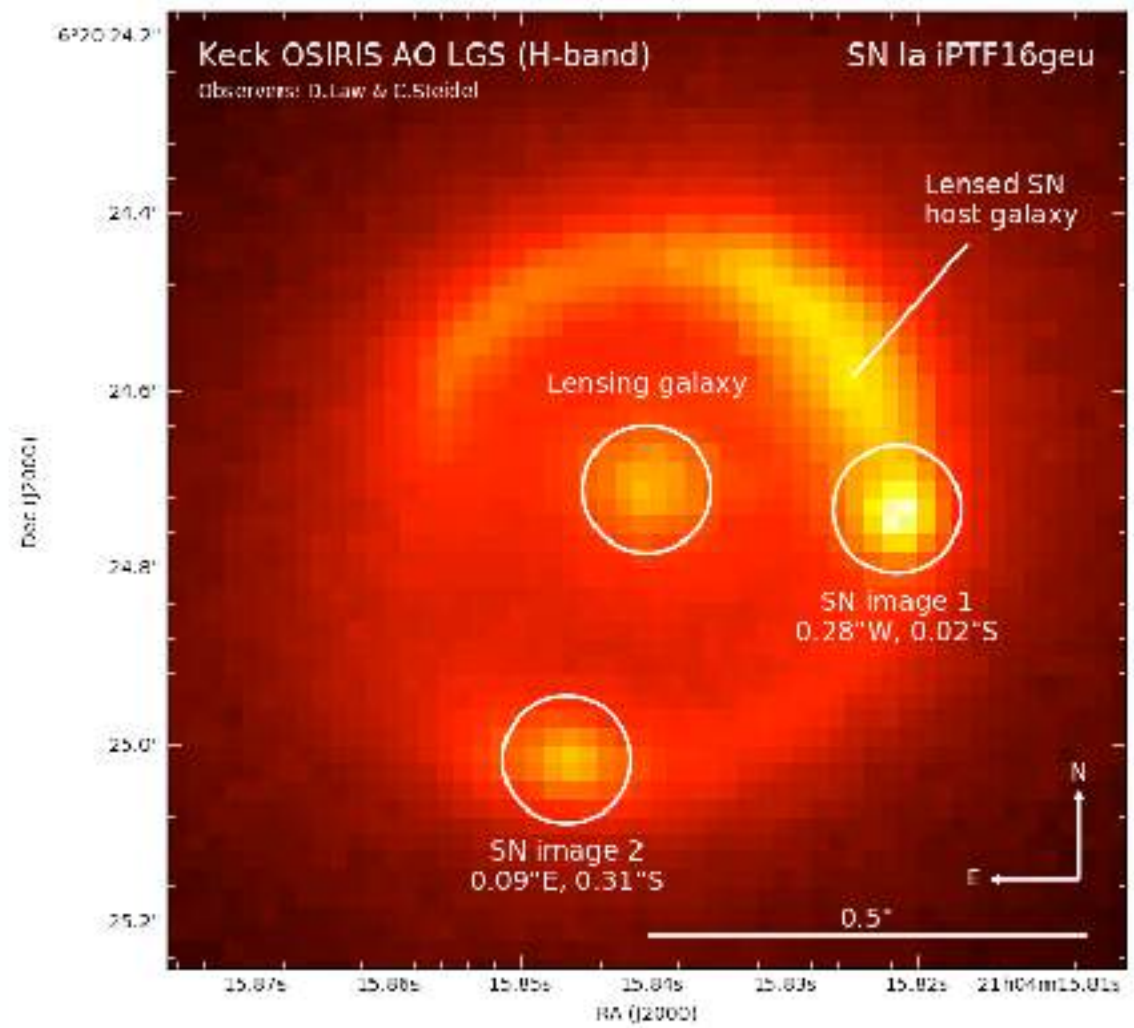

Goobar et al., The discovery of the multiply-imaged lensed Type Ia supernova iPTF16geu, arXiv:1611.00014

Lensing of Supernovae

- Power of Standard candles + time-delays + Strong Lensing Modeling
- Emerging field
- MMA sources…
- Expected LSST anual discovery rates:
  - 50 SNIa

(3/4 doubles, 1/4 quads)
golden sample: 13
[Arendse++, arXiv:2312.04621]

  - 120 Core-collapse

[Wojtak++ arXiv:1903.07687]

- Need to find these systems in real time!

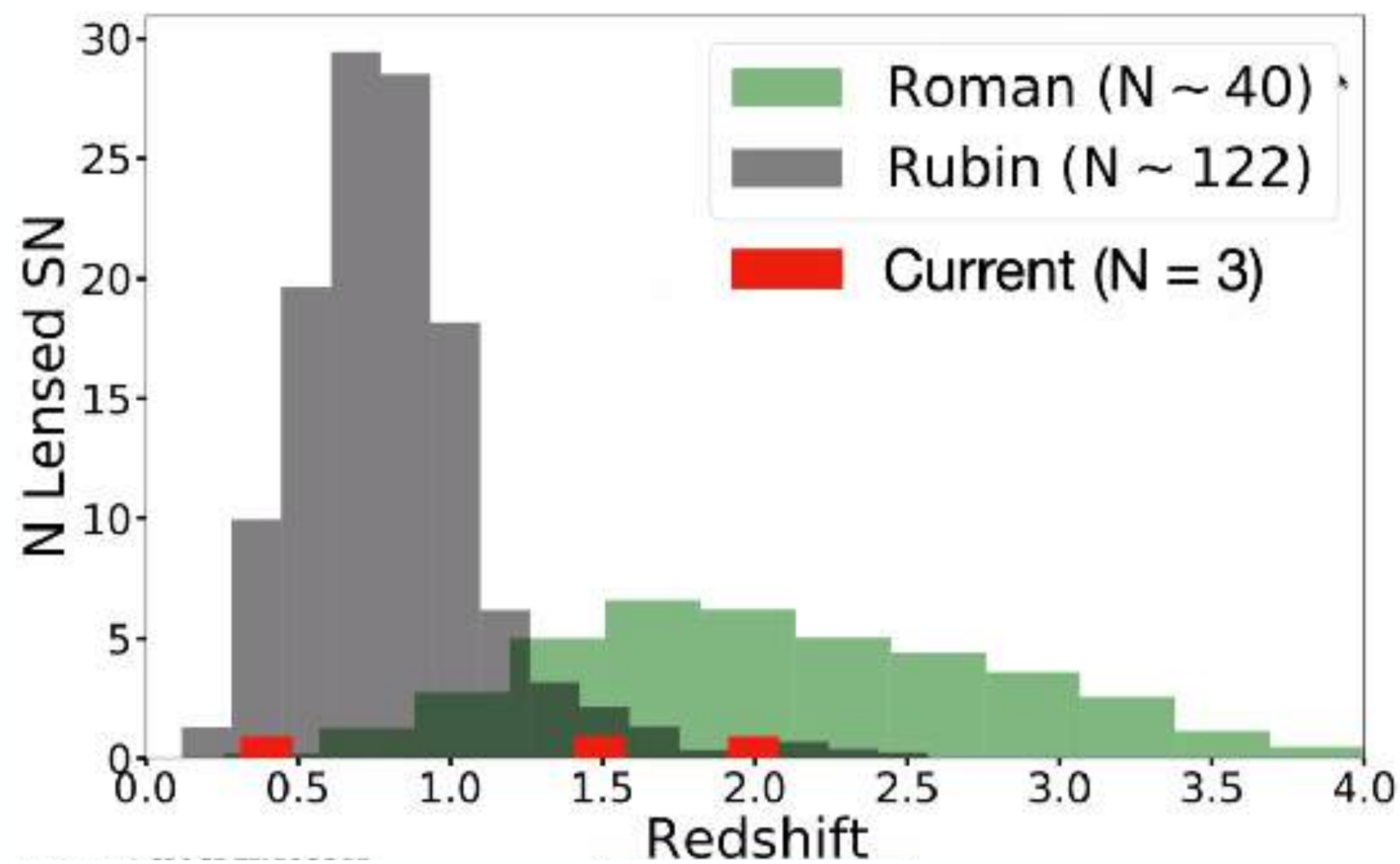

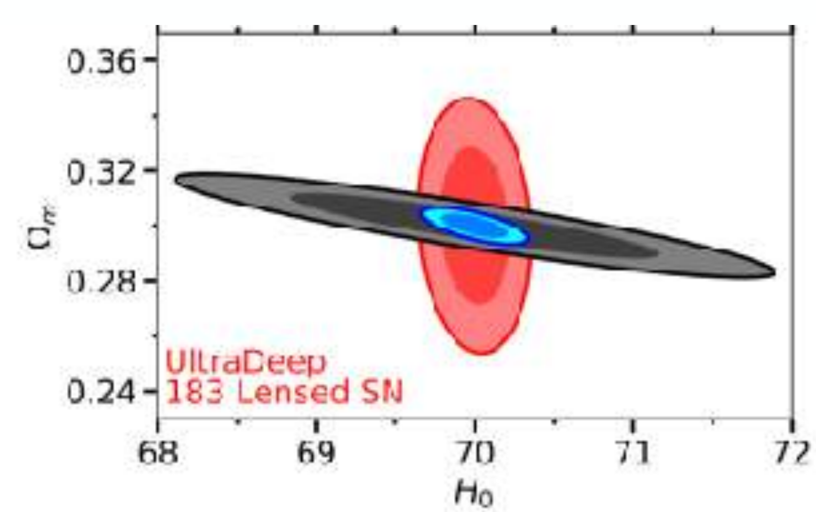

arXiv:2010.12399

João França

Predicting Time-delays

- From the SL modeling, one can predict PDFs for the time-delays between images

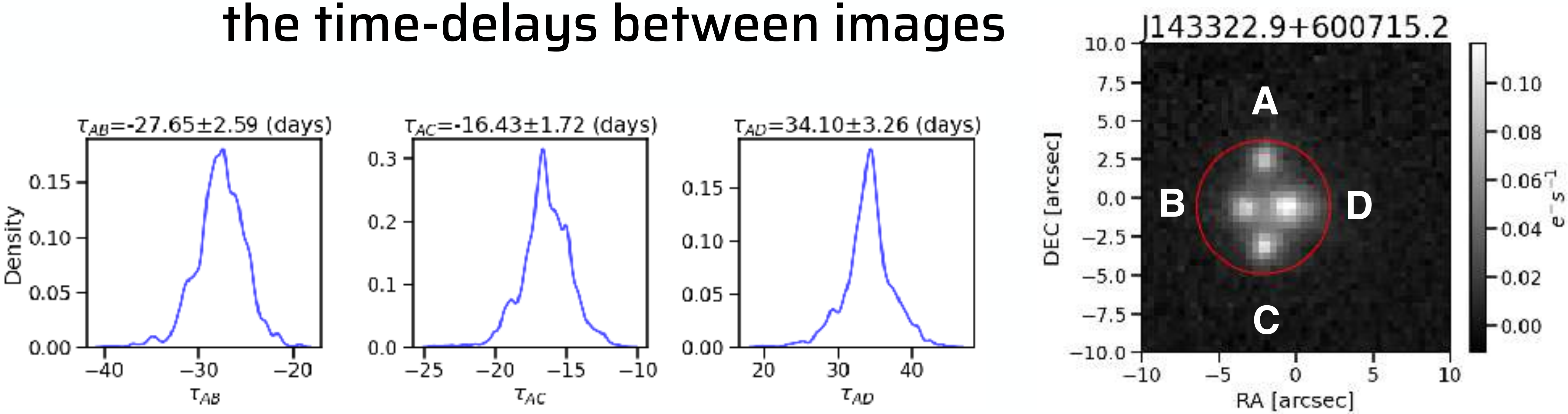

- Match direction and observed time-delays (even with no EM signal!)
- Look up tables to identify the visible and invisible lensed sources
- Distinct signal, the simplest being a repeating transient
- GW: Localization region is usually much larger than optical, but strong lenses are rare!
- Detailed modeling, precise time delay: improve localization (even for dark sirens!)
- Other possibly repeating signals: GRB, FRB…

Strong Lensing and Scientific Method

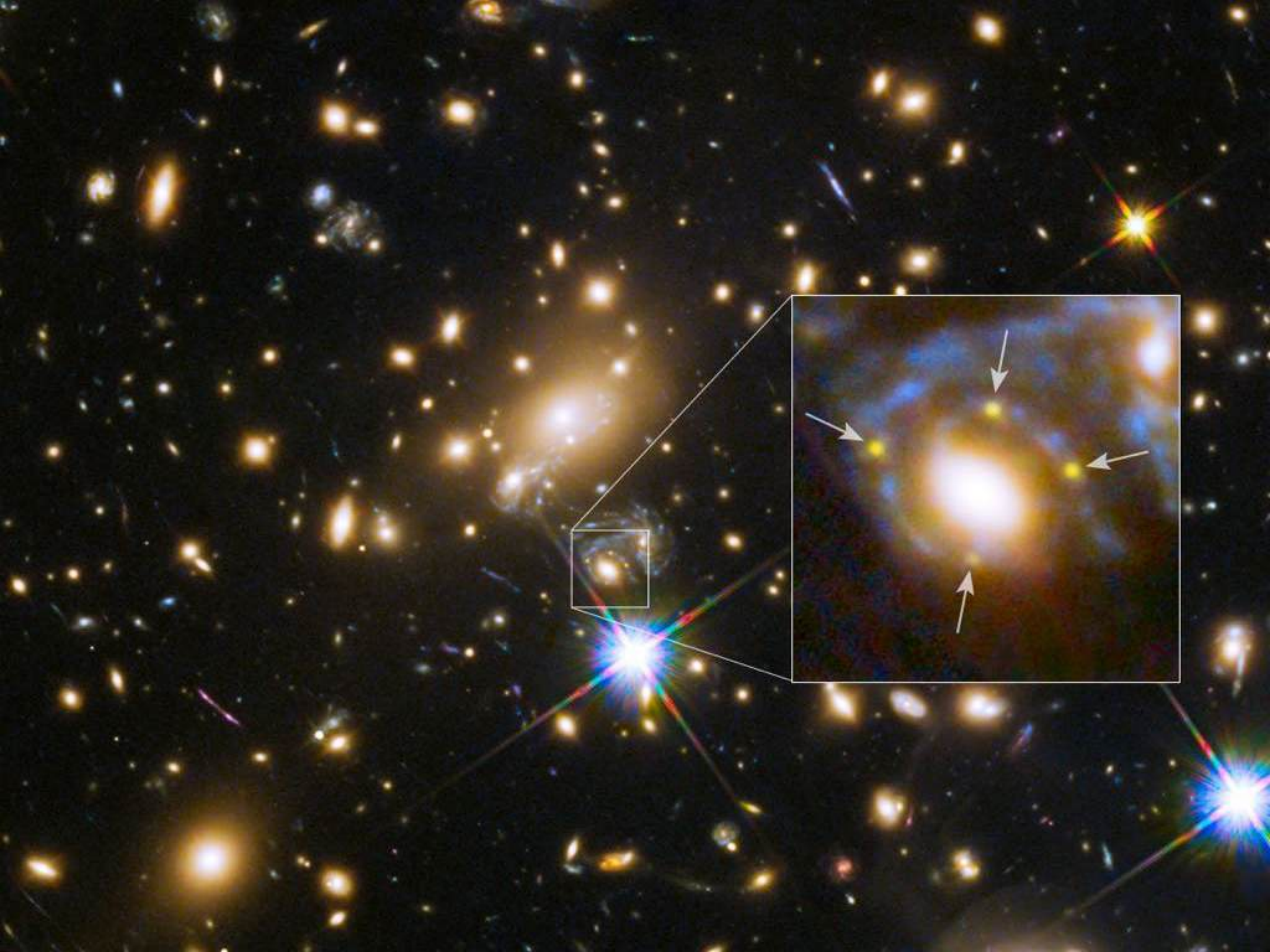

Supernova in MACS J1149.6+2223

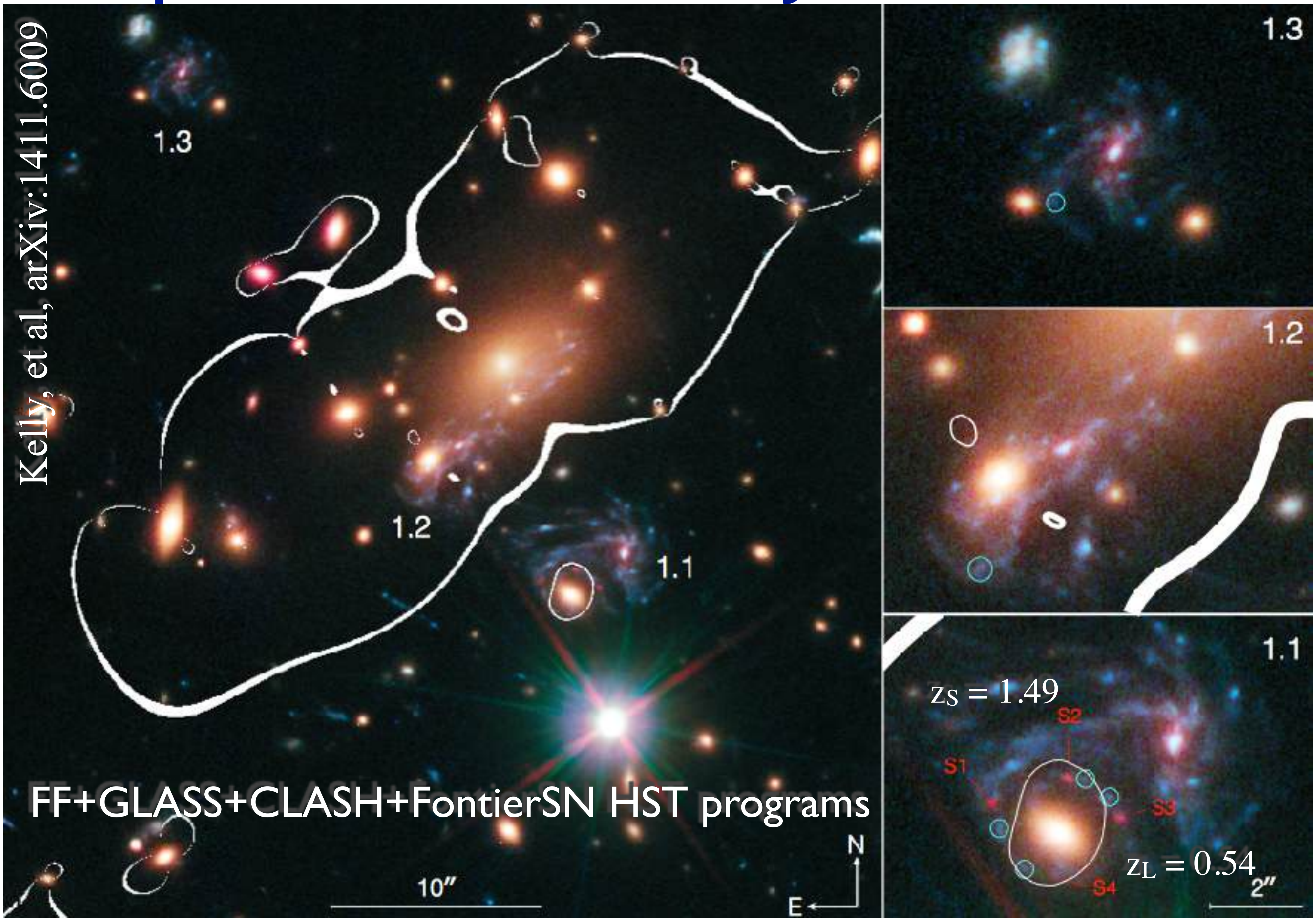

Multiple images by a galaxy cluster member + overall cluster potential

Can be modeled with many degrees of freedom

Modeling
Strong Lensing Clusters

- Use positions of multiple images/arcs
  - possibly: surface light distribution, relative fluxes
- Use positions and properties of the cluster galaxies
- Free parameters: 2D mass distribution!
- Parametric approach:
  - Dark matter halos: mass, shapes, number
  - Scaling relations for light - mass
- Can derive a lot of information
- But does it make sense?

Supernova em MACS J1149.6+2223

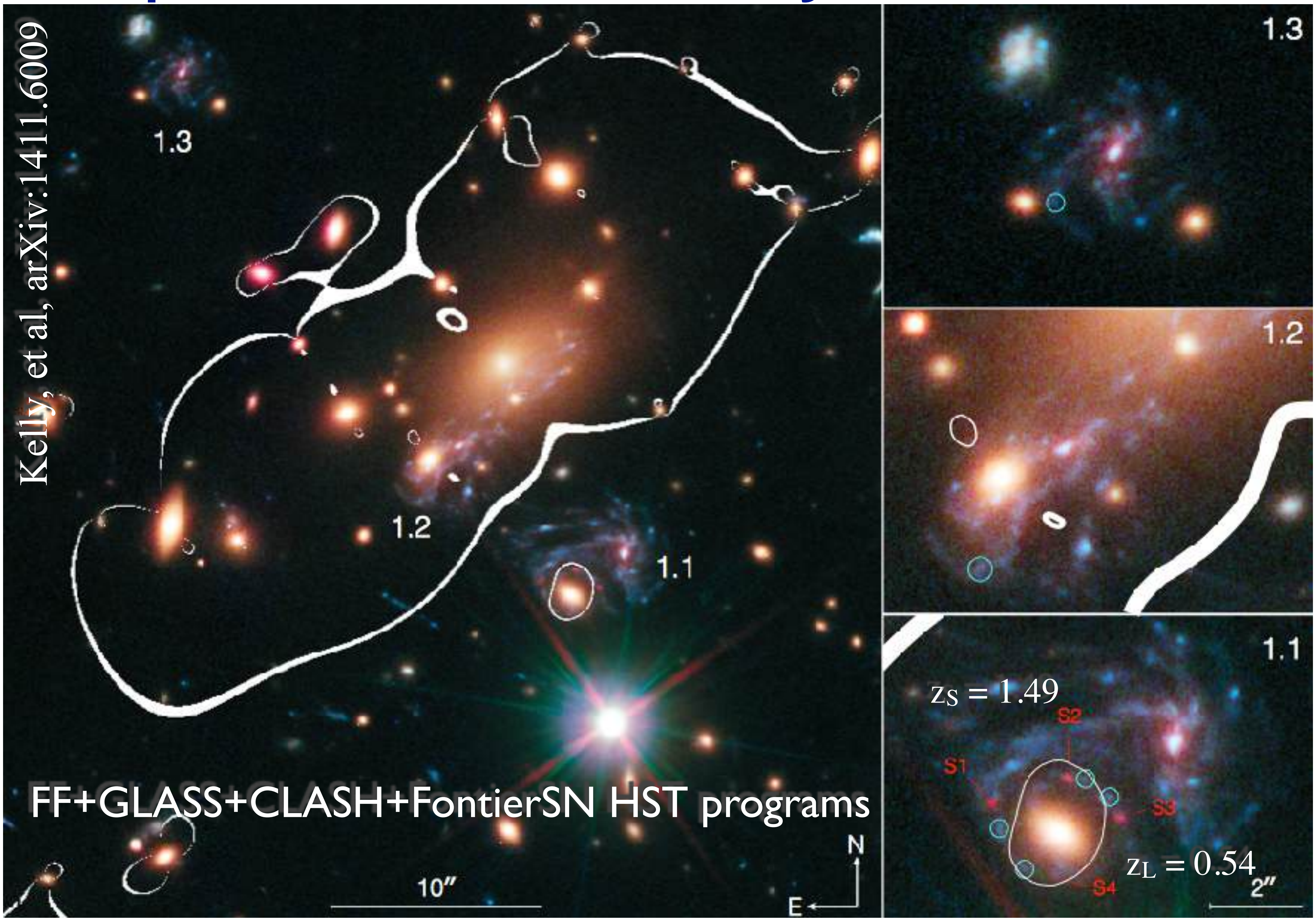

Use prediction for the appearance of multiple images to test the model

When Refsdal meets Popper!

THE STORY OF SUPERNOVA 'REFSDAL' TOLD BY MUSE*

C. GRILLO[1], W. KARMAN[2], S. H. SUYU[3], P. ROSATI[4], I. BALESTRA[5], A. MERCURIO[6], M. LOMBARDI[7], T. TREU[8], G. B. CAMINHA[4], A. HALKOLA, S. A. RODNEY[9,10,11], R. GAVAZZI[12], K. I. CAPUTI[2]

Draft version March 7, 2016

ABSTRACT

We present Multi Unit Spectroscopic Explorer (MUSE) observations in the core of the Hubble Frontier Fields (HFF) galaxy cluster MACS J1149.5+2223, where the first magnified and spatially-resolved multiple images of supernova (SN) 'Refsdal' at redshift 1.489 were detected. Thanks to a Director's Discretionary Time program with the Very Large Telescope and the extraordinary efficiency of MUSE, we measure 117 secure redshifts with just 4.8 hours of total integration time on a single 1 arcmin^2 target pointing. We spectroscopically confirm 68 galaxy cluster members, with redshift values ranging from 0.5272 to 0.5660, and 18 multiple images belonging to 7 background, lensed sources distributed in redshifts between 1.240 and 3.703. Starting from the combination of our catalog with those obtained from extensive spectroscopic and photometric campaigns using the *Hubble Space Telescope*, we select a sample of 300 (164 spectroscopic and 136 photometric) cluster members, within approximately 500 kpc from the brightest cluster galaxy, and a set of 88 reliable multiple images associated to 10 different background source galaxies and 18 distinct knots in the spiral galaxy hosting SN 'Refsdal'. We exploit this valuable information to build 6 detailed strong lensing models, the best of which reproduces the observed positions of the multiple images with a root-mean-square offset of only 0.26″. We use these models to quantify the statistical and systematic errors on the predicted values of magnification and time delay of the next emerging image of SN 'Refsdal'. We find that its peak luminosity should occur between March and June 2016, and should be approximately 20% fainter than the dimmest (S4) of the previously detected images but above the detection limit of the planned *HST*/WFC3 follow-up. We present our two-dimensional reconstruction of the cluster mass density distribution and of the SN 'Refsdal' host galaxy surface brightness distribution. We outline the roadmap towards even better strong lensing models with a synergetic MUSE and *HST* effort.

Subject headings: gravitational lensing – galaxies: clusters: general – galaxies: clusters: individuals: MACS J1149.5+2223 – Dark matter

"REFSDAL" MEETS POPPER: COMPARING PREDICTIONS OF THE RE-APPEARANCE OF THE MULTIPLY IMAGED SUPERNOVA BEHIND MACSJ1149.5+2223

T. Treu[1,28], G. Brammer[2], J. M. Diego[3], C. Grillo[4], P. L. Kelly[5], M. Oguri[6,7,8]
K. Sharon[12], A. Zitrin[13,29] Show full author list

Published 2016 January 20 • © 2016. The American Astronomical Society. All righ
The Astrophysical Journal, Volume 817, Number 1

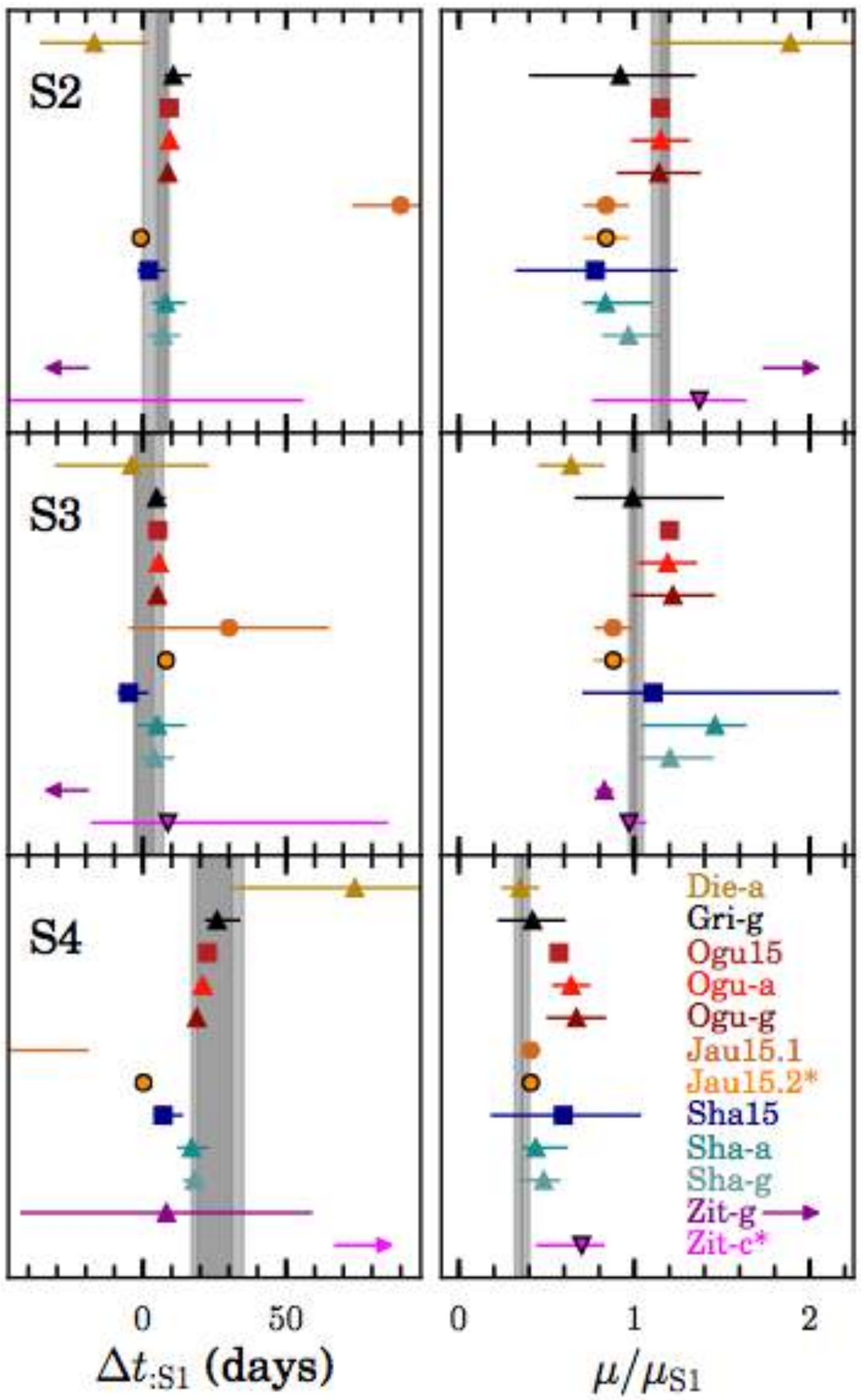

A free-form prediction for the reappearance of supernova Refsdal in the Hubble Frontier Fields cluster MACSJ1149.5+2223

Jose M. Diego,[1★] Tom Broadhurst,[2,3] Cuncheng Chen,[4] Jeremy Lim,[4] Adi Zitrin,[5†] Brian Chan,[4] Dan Coe,[6] Holland C. Ford,[6] Daniel Lam[4] and Wei Zheng[6]

[1]IFCA, Instituto de Física de Cantabria (UC-CSIC), Av. de Los Castros s/n, E-39005 Santander, Spain
[2]Fisika Teorikoa, Zientzia eta Teknologia Fakultatea, Euskal Herriko Unibertsitatea UPV/EHU, E-48080 Bilbao, Spain
[3]IKERBASQUE, Basque Foundation for Science, Alameda Urquijo 36-5, E-48008 Bilbao, Spain
[4]Department of Physics, The University of Hong Kong, 0000-0002-6535-5575, Pokfulam Road, Hong Kong
[5]Cahill Center for Astronomy and Astrophysics, California Institute of Technology, MS 249-17, Pasadena, CA 91125, USA
[6]Department of Physics and Astronomy, Johns Hopkins University, Baltimore, MD 21218, USA

THE STORY OF SUPERNOVA 'REFSDAL' TOLD BY MUSE*

C. Grillo[1], W. Karman[2], S. H. Suyu[3], P. Rosati[4], I. Balestra[5], A. Mercurio[6], M. Lombardi[7], T. Treu[8], G. B. Caminha[4], A. Halkola, S. A. Rodney[9,10,11], R. Gavazzi[12], K. I. Caputi[2]

Draft version March 7, 2016

Monthly Notices of the ROYAL ASTRONOMICAL SOCIETY
MNRAS 457, 2029–2042 (2016) doi:10.1093/mnras/stw069

Hubble Frontier Fields: predictions for the return of SN Refsdal with the MUSE and GMOS spectrographs

M. Jauzac,[1,2,3★] J. Richard,[4] M. Limousin,[5] K. Knowles,[3] G. Mahler,[4] G. P. Smith,[6] J.-P. Kneib,[5,7] E. Jullo,[5] P. Natarajan,[8] H. Ebeling,[9] H. Atek,[8] B. Clément,[4] D. Eckert,[10] E. Egami,[11] R. Massey[1,2] and M. Rexroth[7]

of MACS J0416.1−2403 and Abell 2744. In light of the discovery of the first resolved quadruply lensed supernova, SN Refsdal, in one of the multiply imaged galaxies identified in MACS J1149, we use our revised mass model to investigate the time delays and predict the rise of the next image between 2015 November and 2016 January.

Supernova em MACS J1149.6+2223

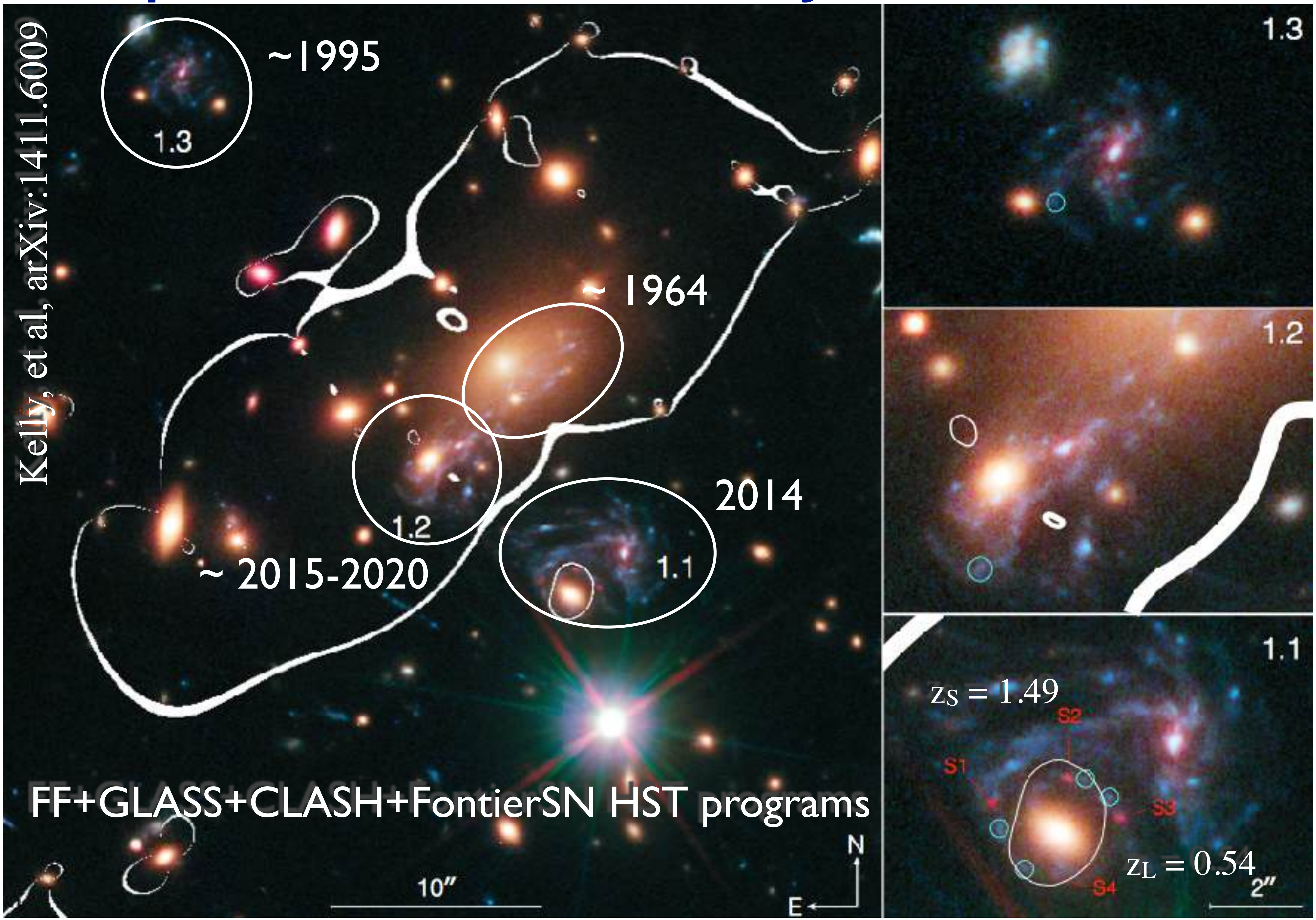

DEJA VU ALL OVER AGAIN: THE REAPPEARANCE OF SUPERNOVA REFSDAL

P. L. Kelly[1], S. A. Rodney[2], T. Treu[3,3], L.-G. Strolger[4], R. J. Foley[5,6], S. W. Jha[7], J. Selsing[8], G. Brammer[4], M. Bradač[9], S. B. Cenko[10,11] Show full author list

Published 2016 February 24 •

The Astrophysical Journal Letters, Volume 819, Number 1

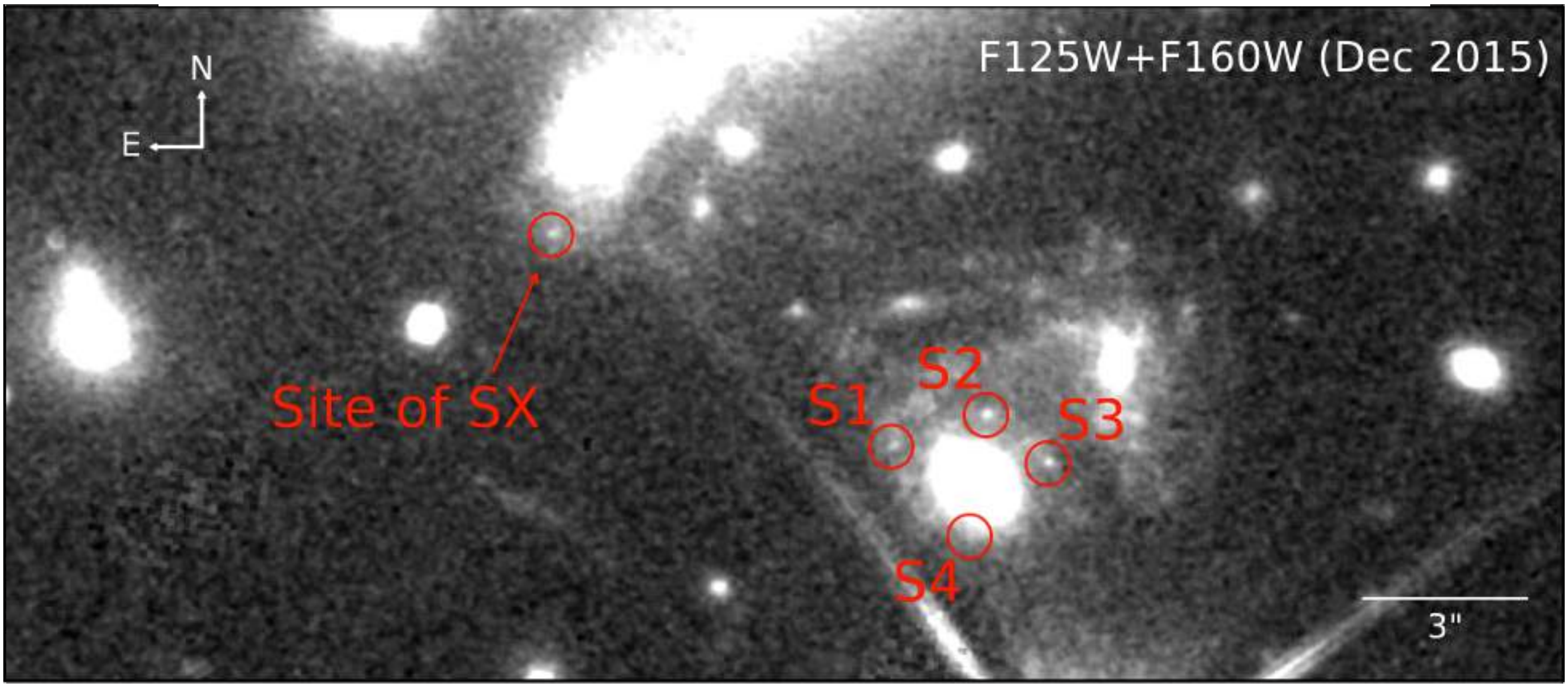

DEJA VU ALL OVER AGAIN: THE REAPPEARANCE OF SUPERNOVA REFSDAL

P. L. Kelly[1], S. A. Rodney[2], T. Treu[3,3], L.-G. Strolger[4], R. J. Foley[5,6], S. W. Jha[7], J. Selsing[8], G. Brammer[4], M. Bradač[9], S. B. Cenko[10,11] Show full author list

Published 2016 February 24 •

The Astrophysical Journal Letters, Volume 819, Number 1

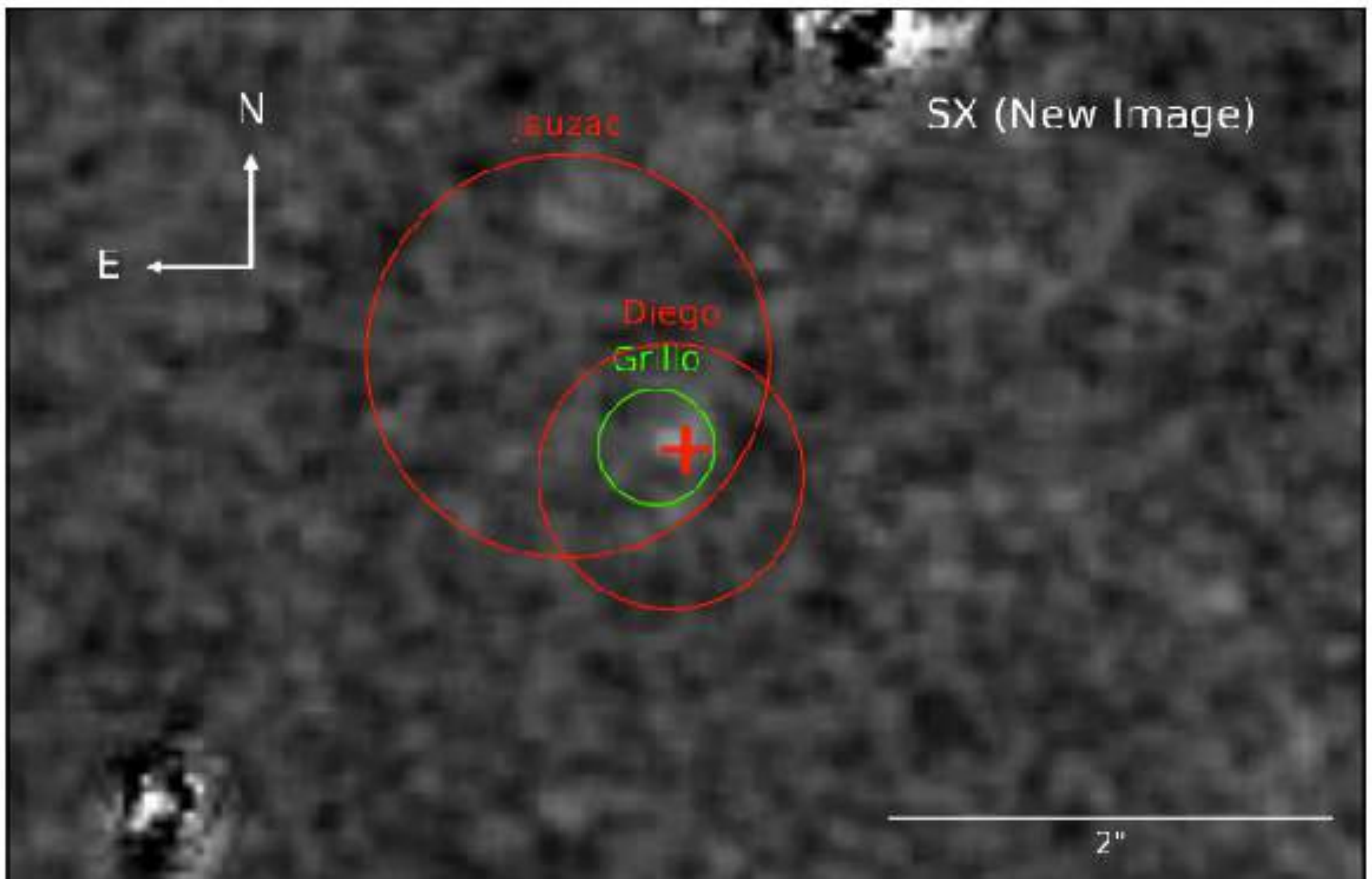

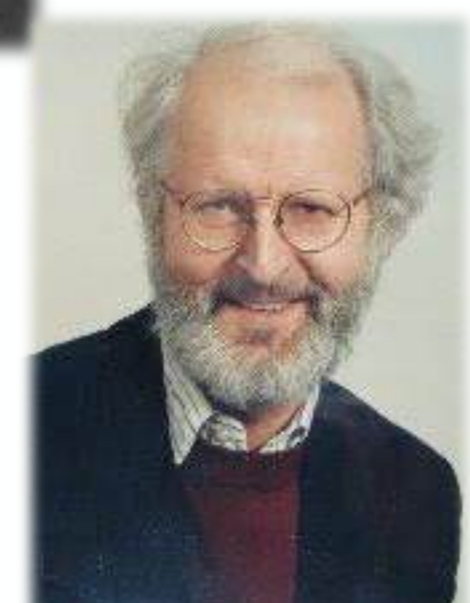

Past, present and **future**

Homogeneous Strong Lensing Samples (arcs)

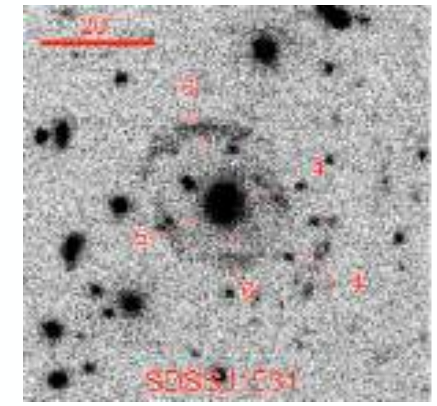

- 1986-2016: $\mathcal{O}(10^2)$ systems
  - $\mathcal{O}(10^2)$ deg^2 surveys: CFHTLS/SL2S, SOGRAS, CS82
  - Spectroscopy + HST: SLACS, BELLS
- 2016-2024: $\mathcal{O}(10^3)$ systems
  - $\mathcal{O}(10^3)$ deg^2 surveys: KiDS, RCSLens, DES, HSC, DELVE
  - Spectroscopy: SDSS/SILO, SWELLS, SL4TM
  - automated arcfinding

DARK ENERGY SURVEY

- > 2024: $\mathcal{O}(10^4 - 10^5)$ systems
  - Rubin/LSST, EUCLID, Roman/WFIRST
  - Rubin: ~ 100 strongly lensed supernovae!
  - DESI, Subaru PFS/SUMIRE, 4MOST

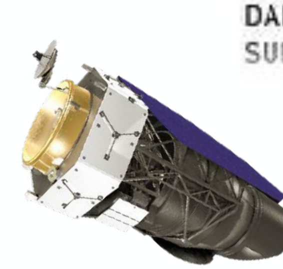

LSST: 1/2 sky per night, **10^{10}** galaxies! (+DDF+**TD**)

- arcfinding codes
- **automated analyses (ML, everywhere, lots to do)**

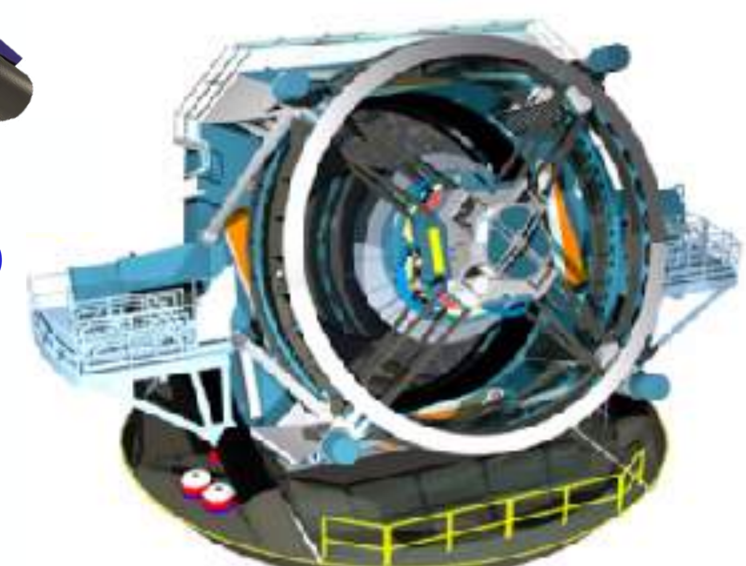

Telescópio Vera Rubin y su LSST

Estado del arte de la astronomía por imágenes con *seeing* natural

- Observatorio completamente nuevo en Cerro Pachón, Chile (con Gemini y SOAR)
- Gran apertura, luminosidad y campo de visión: espejo primario de 8.4 m, nuevo diseño óptico *f* /1.2
- Cámara de 10 *sq-deg* en 3.2 Gpx (mayor cámara del mundo)
- **CCDs gruesas (sensible al rojo) y de lectura rápida** (2s!)
- Habilidad de exposiciones cortas, totalmente automatizado
- Instrumento **ideal y único para relevamientos**
- **No solo el próximo paso: nueva dimensión temporal!**
- 1 millón de alertas por noche!
- Início del *survey* con la cámara completa: 2025
- Contribución *in-kind* del IATE/AOC/UNC: membresía en LSST!

Transformational Strong Lensing Science with Rubin

- Strong Lensing of Transients (extragalactic)
  - ~ 400 SGLSNe
  - ~ 10.000 strong lenses: watchlist for lensed transients (GW, GRB, FRB...)
- Microlensing (stelar)
  - unprecedented combination of sky coverage, depth and cadence (microlensing all over the sky!)
  - overlap with Roman in the bulge

Strongly lensed transients

- In addition to all strong lensing science: time delays
  - Directly sensitive to H_0 ! + cosmography
  - SNIa: power of Standard candles + time-delays + Strong Lensing Modeling
- How to find the first SGLSNe in Rubin?
  - It will take time to build up imaging for SL searches
  - Assemble a watchlist with *current imaging* data and *known candidates*!
- Also:
  - Multi-messenger Strong lensing (also with no EM emission!)
  - Train and validate ML models with real data
  - Use compilation for science!

Lensing of Supernovae

- Power of Standard candles + time-delays + Strong Lensing Modeling
- Before LSST: ZTF
  - not enough resolution to identify the images
  - enough to localize the system
  - if multiple SN in same region (simultaneously or not): SGLSN candidate!
- Need a look-up table for SL systems
  - even for single SN match
  - confirmation: consistency of time delays!
- Prepare for LSST:
  - Build up a sample before pixel data is available, before arc finders can be run, before modeling is run, and before data goes public

베르

Last Stand Before Rubin: LaStBeRu

- A semi-automated infrastructure for the aggregation of SL systems, cross matches, and generation of cut-outs
- v2.0: > 30k SL candidates, > 150k images, > 5k spectra
- prepare for LSST Strong Lensing science
- Ongoing work:
    - visual inspection: vetting + tagging (zooniverse)
    - massive modeling + time delay predictions (new)
- Watch list + sample for ML appliactions
- Look-up table (cross match with variability)
- Carry out precursor follow-ups (e.g. SOAR, Gemini)

SLSC

LSST DESC
Dark Energy Science Collaboration

The last stand before LSST: A collection of Strong Lensing Systems with Ground Based Images from Wide-Field Surveys

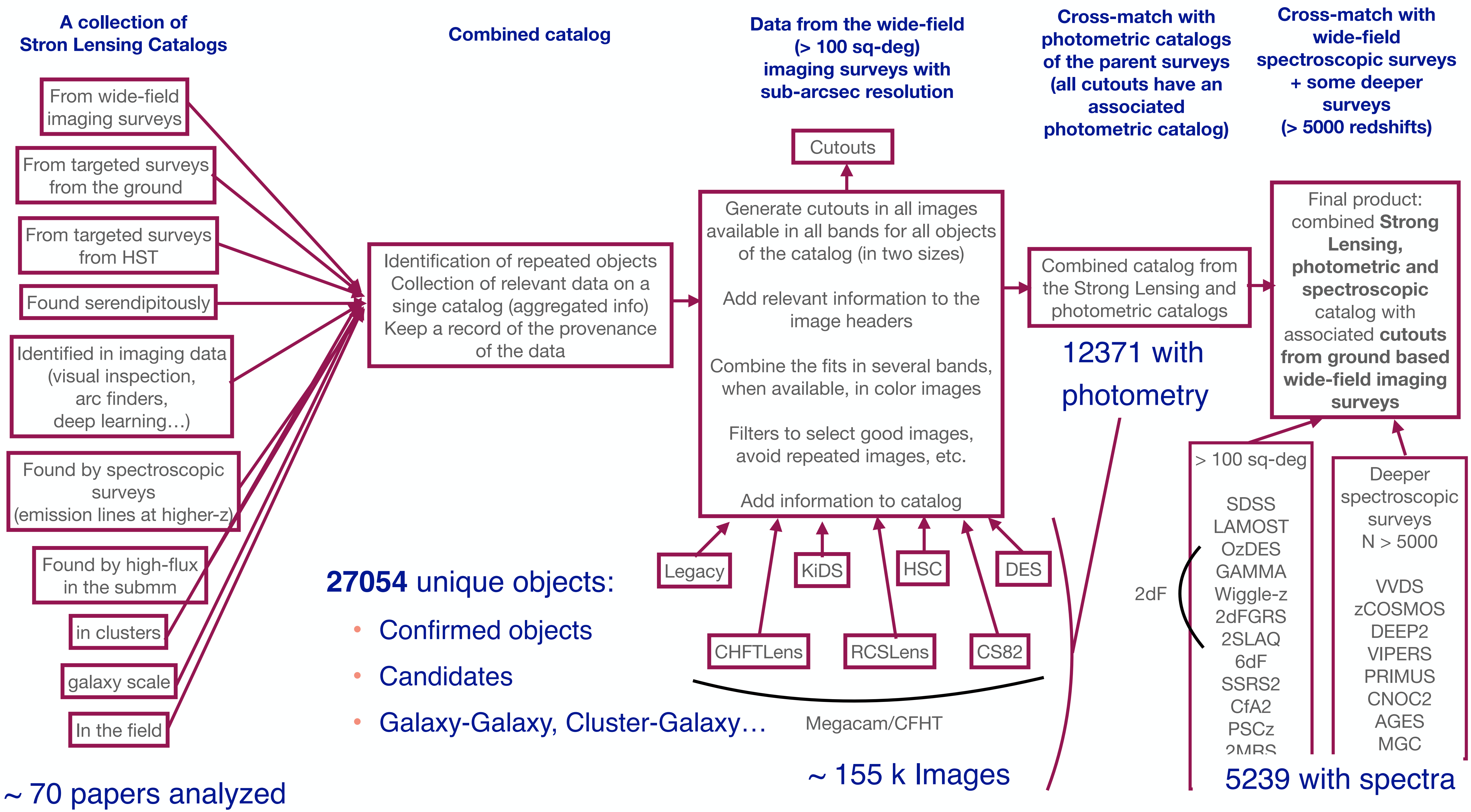

The last stand before LSST: A collection of Strong Lensing Systems with Ground Based Images from Wide-Field Surveys

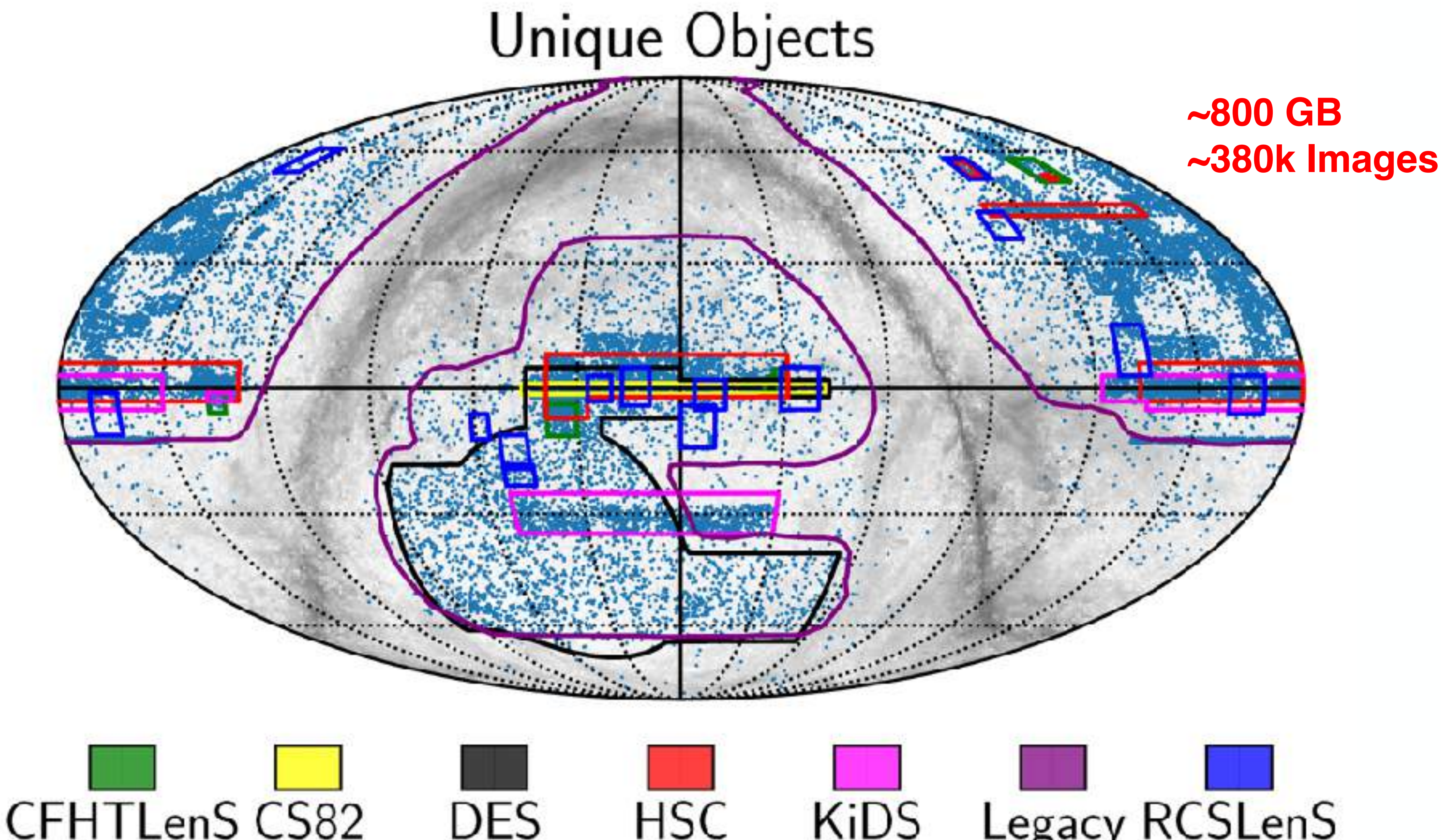

slcomp

Some systems….

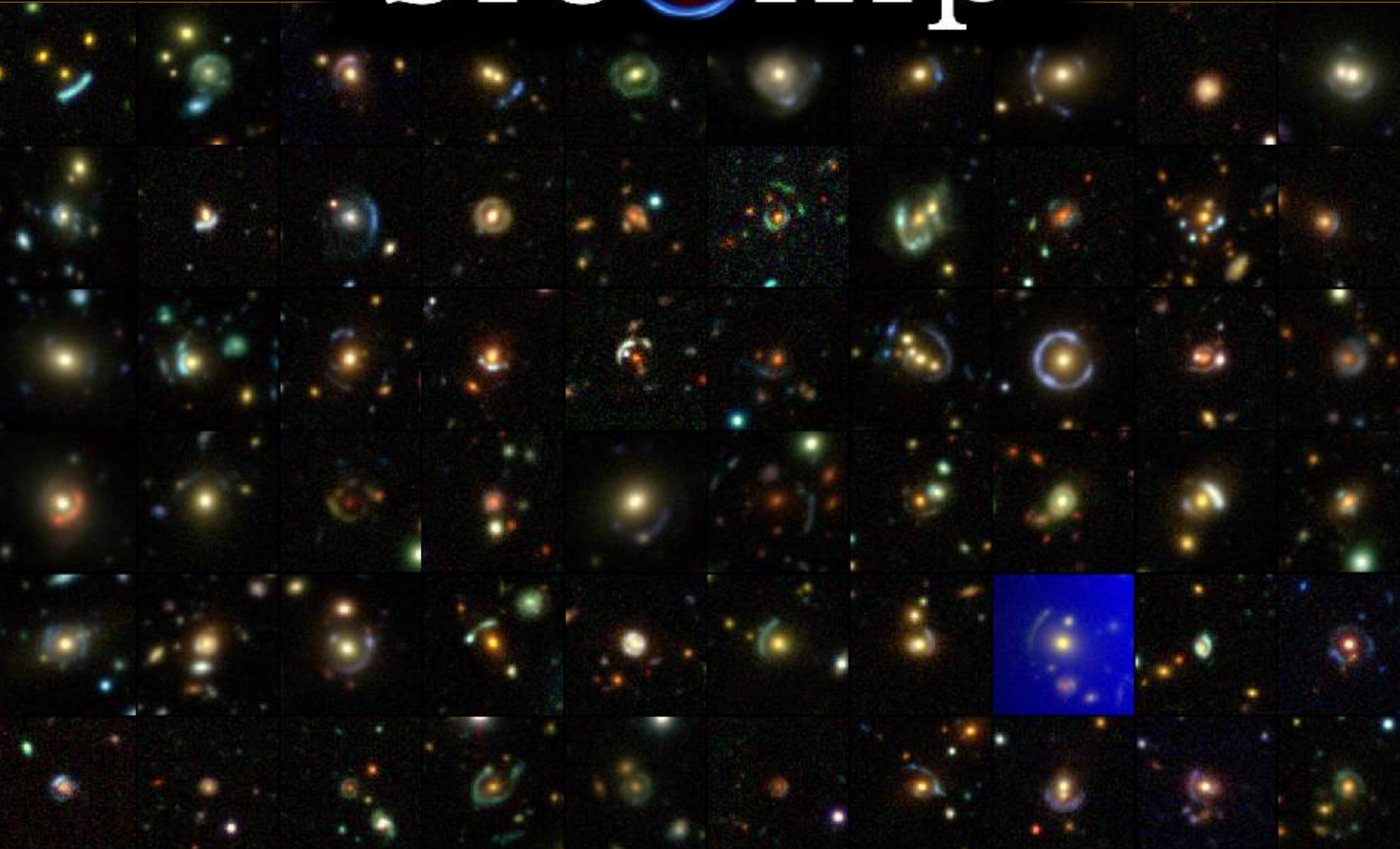

slcomp

- slcomp: a semi-automated infrastructure for the aggregation of SL systems, cross matches, and generation of cut-outs
- current version: Last Stand Before Rubin

LaStBeRu

- ongoing work:
  - visual inspection: vetting + tagging (zooniverse, ML appliactions - SLImageNet)
  - massive modelling + time delay predictions (new)

베르

LaStBeRu

Groovy, cool, or otherwise something good or favored